

High-density hard-core model on \mathbb{Z}^2 and norm equations in ring $\mathbb{Z}[\sqrt[6]{-1}]$

A. Mazel¹, I. Stuhl², Y. Suhov^{2,3}

Abstract

We study the Gibbs statistics of high-density hard-core configurations on a unit square lattice \mathbb{Z}^2 , for a general Euclidean exclusion distance D . As a by-product, we solve the disk-packing problem on \mathbb{Z}^2 for disks of diameter D . To this end we exploit connections between the structure of the ground states and the algebraic number theory. Here the key point is an analysis of solutions to norm equations in the ring $\mathbb{Z}[\sqrt[6]{-1}]$. We use Delaunay triangulations to describe the *ground state* configurations in terms of *M-triangles*, i.e., non-obtuse \mathbb{Z}^2 -triangles of a minimal area with the side-lengths $\geq D$. Further, we identify \mathbb{Z}^2 -triangles and elements of $\mathbb{Z}[\sqrt[6]{-1}]$; this yields a convenient classification of values D^2 and the corresponding periodic ground states.

First, there is a *finite* class (Class S) formed by values D^2 generating *sliding*, a phenomenon leading to countable families of periodic ground states. Following an idea from [28], we identify all D^2 with sliding. Each of the remaining classes is proven to be *infinite*; they are characterized by uniqueness or non-uniqueness of a minimal triangle for a given D^2 , up to \mathbb{Z}^2 -congruencies. For values of D^2 with uniqueness (Class A) we describe the periodic ground states as admissible sublattices in \mathbb{Z}^2 of maximum density. By using the *Pirogov-Sinai* theory [42], [44], it allows us to identify the *extreme Gibbs measures* (pure phases) for large values of fugacity and describe symmetries between them. For this purpose we establish a non-trivial *Peierls bound* based on an appropriate definition of a *contour*. This yields a complete diagram for the phase coexistence at large fugacities.

Furthermore, we analyze the values D^2 with non-uniqueness. For some D^2 all M-triangles are \mathbb{R}^2 -congruent but not \mathbb{Z}^2 -congruent (Class B0). For other values of D^2 there exist non- \mathbb{R}^2 -congruent M-triangles, with different collections of side-lengths (Class B1). Moreover, there are values D^2 for which both cases occur (Class B2). The large-fugacity phase diagram for Classes B0, B1, B2 is determined by *dominant* ground states.

Thus, for all classes but Class S, we show the non-uniqueness of Gibbs measures and hence, establish the existence of a phase transition. Algebraically, all classes A, B0-B2 are described in terms of *cosets* in $\mathbb{Z}[\sqrt[6]{-1}]$ by the group of units.

2010 *Mathematics Subject Classification*: primary 60A10, 60B05, 60C05, 60J20, secondary 68P20, 68P30, 94A17

Key words and phrases: square lattice, hard-core exclusion distance, admissible hard-core configuration, Gibbs measure, high density, dense-packing, periodic ground state, phase transition, contour representation of the partition function, Peierls bound, dominance, Pirogov-Sinai theory, Zahradnik's argument, norm equation, quadratic integer ring, coset by the unit group, leading solution

¹ AMC Health, New York, NY, USA; ² Math Department, Penn State University, PA, USA; ³ DPMMS, University of Cambridge and St John's College, Cambridge, UK.

1 The hard-core model on \mathbb{Z}^2 . Gibbs measures

1.1 Introduction. A summary of the main results.

High-density hard-core (HC) configurations in a continuous space or on a discrete structure (lattices, (random) graphs, etc.) are important in a number of theoretical and applied areas, which includes Mathematical and Theoretical Physics, Computer/Information Sciences, Theoretical Biology etc. The problem is to study the statistical mechanics of configurations formed by non-overlapping hard spheres of a given dimension and diameter (or exclusion distance) D . A survey of different aspects of the hard-core model and its applications can be found, e.g., in [8], [40], [41], [4], [29], [27].

High-density hard-core models are intrinsically related to the sphere-packing problem. In this regard, one can mention the Thue theorem in \mathbb{R}^2 , the Kepler conjecture in \mathbb{R}^3 and recent results in \mathbb{R}^8 , \mathbb{R}^{24} . Cf. [15, 23, 22, 47, 9]. Randomized hard-core configurations are interesting as they may describe a non-ideal situation where dense-packing can be occasionally frustrated. The corresponding mathematical model is provided by Gibbs probability measures in a high density/large fugacity regime. In a continuous space \mathbb{R}^d , the analysis of such measures for $d \geq 2$ is a well-known challenging open problem.

We do not think that a discrete version of the model in a high-density/large-fugacity regime is an appropriate approximation for the continuous model. It turns out that a discrete HC model has a variety of properties which cannot be expected in the continuous case. Nevertheless, discrete models are interesting, and in some aspects more challenging than the continuous ones. In particular, discrete models depend heavily on the choice of the underlying lattice and the exclusion distance.

On a unit cubic lattice \mathbb{Z}^d , initial results for the HC model have been obtained in 1966-8 by Dobrushin (and in a part by Suhov); cf. [13, 45]. Namely, non-uniqueness of a Gibbs measure was established for large fugacities for $D = \sqrt{2}$. A detailed study of the high-density/large-fugacity hard-core model in a unit triangular lattice \mathbb{A}_2 and a unit honeycomb graph \mathbb{H}_2 for a general D is presented in [32]. In [33] a number of results have been established about the HC model on a unit cubic lattice \mathbb{Z}^3 for $D^2 = 2, 3, 4, 5, 6, 8, 9, 10, 11, 12, 2\ell^2, \ell \in \mathbb{N}$ in the large fugacity regime. Short expositions of these results are provided in [34] and [35].

H-C models on two-dimensional lattices gained a growing popularity in the recent Physics literature: see [1], [2], [10], [16], [25], [26], [36], [37], [46] and references therein. Most of these papers specify the model as k -NN exclusion, indicating that a particle excludes all 1-st to k -th nearest-neighboring sites (all in the planar Euclidean metric). The value D used to specify the model in the current paper is the Euclidean distance to the $(k + 1)$ -st nearest-neighbors. Depending on the lattice type and the value of D , one expects different forms of phase transitions when the particle density/fugacity/chemical potential in the system varies. Simulations and analytical techniques have been applied to make predictions for critical points and types of the related phase transitions for some initial values of k . For HC models on \mathbb{Z}^2 we refer to [16], [36], [37], on \mathbb{A}_2 to [1], [25], and on \mathbb{H}_2 to [10], [46]. However, a rigorous analysis of criticality and related phase transitions remains an open (and challenging) mathematical problem.

In the present paper we focus on random HC configurations in \mathbb{Z}^2 distributed according to a Gibbs measure in a large-fugacity regime. The HC exclusion distance D is imposed in

the Euclidean metric ρ on \mathbb{R}^2 . After the work [13] the further progress has been blocked, in particular, because of the so-called *sliding* phenomenon in dense-packing configurations first observed by Dobrushin for the value $D = 2$. See Figure 1. Here sliding means that

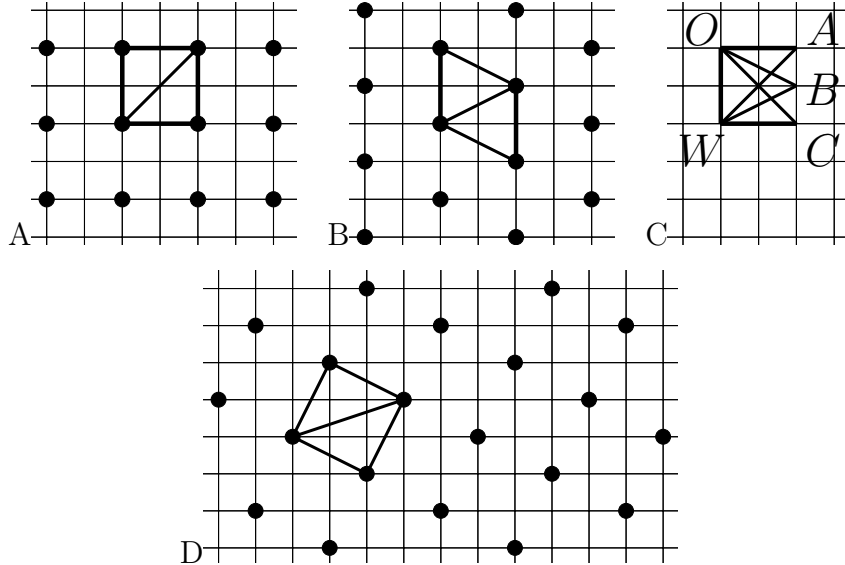


Figure 1: Frames A and B show sliding in \mathbb{Z}^2 for $D = 2$: a 1D array of occupied sites can be \mathbb{Z}^2 -shifted without violating the exclusion distance and decreasing the density. Frame C shows competing fundamental triangles OAW , OBW and OCW , which generates sliding. Note arising trapezes $OABW$ and $OBCW$ and rectangle $OACW$. In contrast, frame D shows the absence of sliding for the next attainable exclusion distance $D = \sqrt{5}$.

the model exhibits a continuum of dense-packing configurations which can be mapped into each other by \mathbb{Z}^2 -shifts of one dimensional arrays of occupied sites. This particular case of sliding has been recently analyzed in [21], where the existence of a columnar order has been established. In the current paper it is shown that the sliding is a rare phenomenon, and there exist only 39 values of D with sliding. The behavior of the model in the high-fugacity regime for the 38 cases of sliding different from $D = 2$ remains an open question and in this paper we focus on non-sliding cases of D . Our main results can be described as follows.

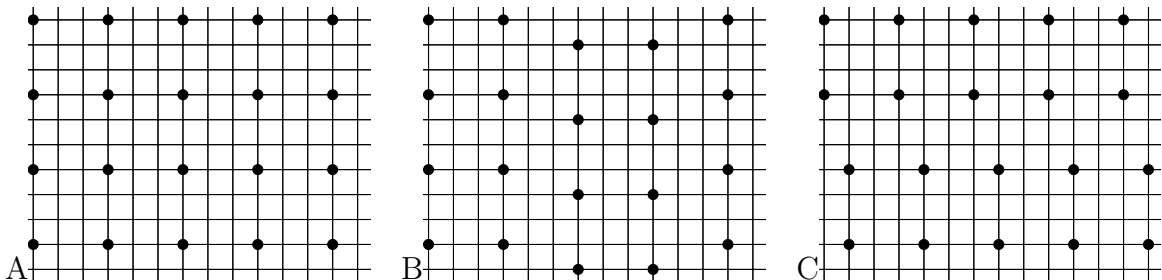


Figure 2: The hard-core model in \mathbb{Z}^2 may have lattice (A) and non-lattice (B) periodic ground states as well as non-periodic ground states (C) of maximal density (shown for the exclusion distance $D = 3$, with sliding). Non-periodic ground states are not interesting in our context (as follows from a general result by Dobrushin-Shlosman [14]). For a non-sliding D the non-lattice periodic ground states are ruled out by one of our results (see Lemma I in Section 2.3).

- (i) For any non-sliding value of D we prove that all periodic ground states come from optimal (i.e., max-dense) admissible *sub-lattices* constructed from a minimum-area *fundamental parallelogram* (FP). The latter is determined via a minimizer in a specific discrete optimization problem; see Eqn (2.1) in Section 2.1.
- (ii) For the values of D of Class A, where the max-dense sub-lattice is unique up to \mathbb{Z}^2 -symmetries (in the sense defined later), we use the Pirogov-Sinai theory [42, 44] (complemented by Zahradnik [49] and Dobrushin-Shlosman [14]) and give a complete description of the extreme Gibbs measures for large fugacities. See Theorem 1 in Section 2.3. In particular, in Class A the large-fugacity extreme Gibbs measures occur in collections of cardinality mS . Here $m = 1$ for $D = 1, \sqrt{2}$; for $D > \sqrt{2}$, $m = 2$ or 4 , depending on whether the optimal FP is composed of isosceles or non-isosceles *fundamental triangles* (FTs). (The factor m is related to the aforementioned \mathbb{Z}^2 -symmetries occurring in each of these cases.) Here $S = S(D)$ stands for the area of the optimal FP (i.e., twice the area of an optimal FT). (See Figures 3, 4.) In this approach, sliding is treated as a specific form of non-uniqueness in the minimization problem Eqn (2.1).

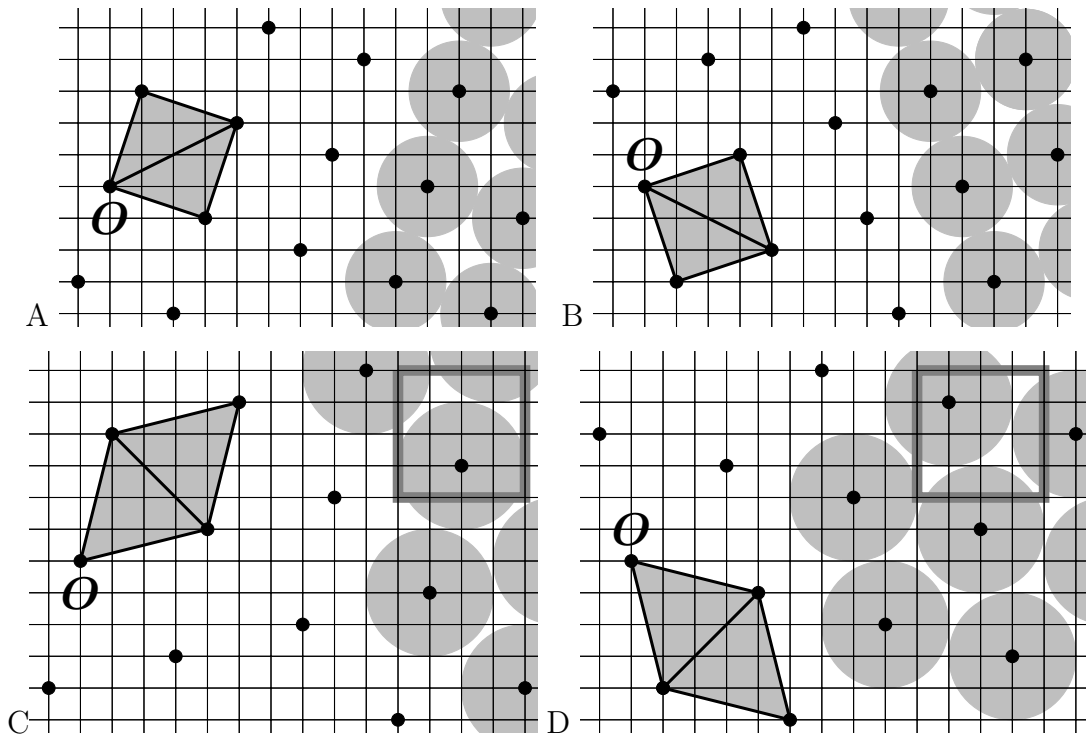


Figure 3: Counting the extreme Gibbs measures for exclusion distances $D = \sqrt{10}$ (A, B) and $D = 4, \sqrt{17}$ (C, D), of Class A. The minimal area of the fundamental parallelograms (light-gray) is $S = 10$ and $S = 15$, and the fundamental triangles are isosceles, with side-lengths and $\sqrt{10}, \sqrt{10}, \sqrt{20}$ and $\sqrt{17}, \sqrt{17}, \sqrt{18}$, respectively. In each case, there are two max-dense sub-lattices obtained from each other by \mathbb{Z}^2 -symmetries: $\pm\frac{\pi}{2}$ -rotations or reflections. Each sub-lattice contributes 10 and 15 periodic ground states obtained by \mathbb{Z}^2 -shifts along the fundamental parallelogram; this explains why the number of periodic ground states equals 20 for $D = \sqrt{10}$ and 30 for $D = 4$. Our Theorem 1 states that the number of extreme Gibbs measures for large fugacities is exactly 20 and 30, respectively. For $D = 4$, the 4×4 squares (dark gray) would lead to a non-optimal sub-lattice.

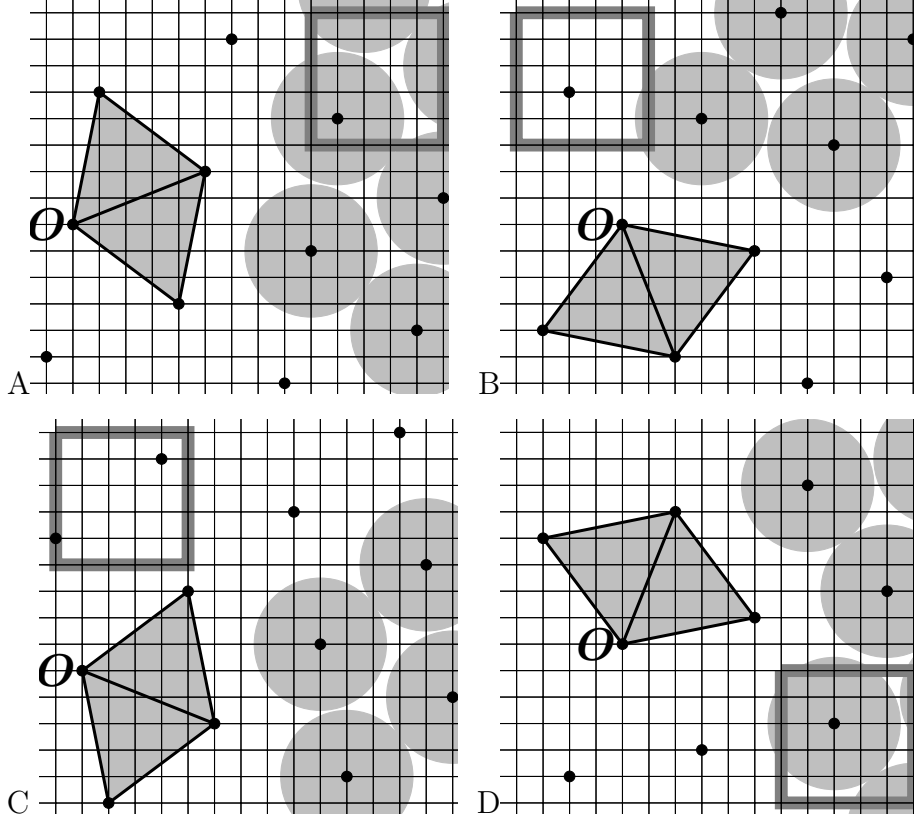


Figure 4: Counting the extreme Gibbs measures for exclusion distance $D = 5$ of Class A. The minimal area of the fundamental parallelograms (light-gray) is $S = 23$. The corresponding fundamental triangles are non-isosceles, with side-lengths 5 , $\sqrt{26}$ and $\sqrt{29}$. There are four max-dense sub-lattices A–C obtained from each other by \mathbb{Z}^2 -symmetries: $\pm\frac{\pi}{2}$ -rotations (A, B and C, D) or reflections (A, C and B, D). Each sub-lattice contribute 23 periodic ground states obtained by \mathbb{Z}^2 -shifts along the fundamental parallelogram; this explains why the number of periodic ground states for $D = 5$ equals $4S = 92$. Our Theorem 1 is that the number of extreme Gibbs measures for large fugacities is exactly 92. The 5×5 squares would lead to a (non-optimal) sub-lattice.

Observe that Figures 3 and 4 demonstrate partial touching or absence of touching of disks in ground states.

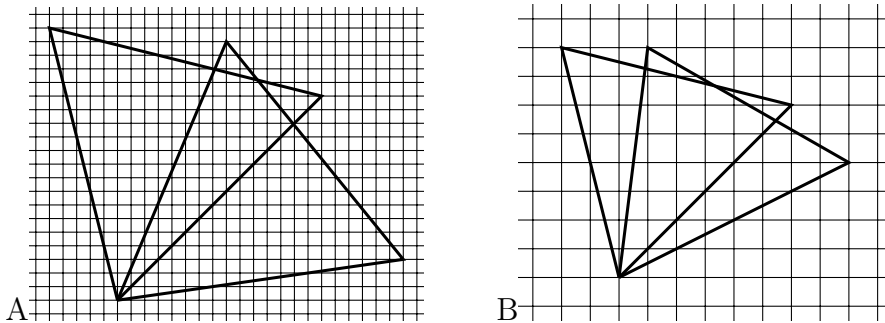


Figure 5: Examples of non-uniqueness of optimal fundamental triangles: $D^2 = 425$, $S = 375$ (Frame A) and $D^2 = 65$, $S = 60$ (Frame B). The optimal squared side lengths for the case $D^2 = 425$ are $425, 425, 450$, with two non-equivalent \mathbb{Z}^2 implementations, which falls in Class B0. The optimal squared side-lengths for $D^2 = 65$ are $65, 65, 80$ (right) and $68, 68, 72$ (left); both triangles admit a unique implementation up to \mathbb{Z}^2 -symmetries. This case belongs to Class B1, and to determine the number of extreme Gibbs measures one has to use the dominance formalism in full. Cf. Section 4.2.

- (iii) For the values of D with non-uniqueness but without sliding (Class B), we offer in our Theorem 2, Section 2.3, a less explicit result, that extreme high-density Gibbs measures come from a particular ‘dominant’/‘stable’ group (or groups) of optimal FPs. Cf. [6, 49]. An identification of a dominant group requires a separate analysis and is outside the scope of this paper. However, we provide a guidance in this direction, via the so-called *dominance analysis* based on counting *local excitations* of periodic ground states. Such a technique was introduced in [32] for the HC model in \mathbb{A}_2 .
- (iv) The uniqueness and non-uniqueness of an optimal FP and FT can be examined both analytically and numerically. We prove that uniqueness (Class A) occurs for countably many exclusion distances by constructing natural infinite sequences of D for which uniqueness of an optimal FP/FT is valid. The construction has a number-theoretical character and is based upon *norm equations* in the ring $\mathbb{Z}[\sqrt[6]{-1}]$. (A particular case here is the famous Pell equation.)
- (v) Next, we establish that Class B is also infinite. Moreover, we describe all possible patterns of non-uniqueness which can occur along natural infinite sequences of values of D . As before, it follows from the study of norm equations in $\mathbb{Z}[\sqrt[6]{-1}]$.
- (vi) For all non-sliding values of D we show the existence of a phase transition due to the non-uniqueness of extreme Gibbs measures [18].
- (vii) Finally, by developing the construction from paper [28], we identify all values D^2 with sliding. See Theorem S in Section 2.2.

Therefore, we provide a complete structure of the phase diagram of the HC model on \mathbb{Z}^2 for large values of fugacity and for all non-sliding exclusion distances. In a sense, it gives a full description of phenomena that can occur in this model in the high-fugacity regime and in the absence of sliding.

In [32] we obtained a number of similar results about the HC model on a unit triangular lattice \mathbb{A}_2 and the honeycomb graph \mathbb{H}_2 ; the comparisons between the two models will be instructive for understanding the present work and show lattice-dependence of the obtained results. We conduct such comparisons in Remarks 1.1–4.1 located at appropriate places throughout the text.

Remark 1.1. As was shown in [32], the periodic max-density HC configurations in \mathbb{A}_2 are produced from equilateral triangular sub-lattices and can be treated as direct analogs of a max-dense disk-packing in the Euclidean plane \mathbb{R}^2 . The situation in \mathbb{Z}^2 is more complex since the max-dense sub-lattices are formed by non-equilateral triangles. Furthermore, the max-dense sub-lattices for a given D are not necessarily congruent. Consequently, the results of group (i) (see above) require a technically involved proof. ▲

1.2 Hard-core Gibbs/DLR measures.

As was mentioned, the HC exclusion is imposed in the Euclidean metric ρ and is described via the HC exclusion distance $D > 0$ (aka the HC *diameter*). We will suppose that the value D is *attainable*, i.e., D^2 is a *Gaussian* number admitting the *Fermat representation*

$D^2 = m^2 + n^2$, where m and n are integers. Physically, attainability means that there exists a pair of sites $x, y \in \mathbb{Z}^2$ with $\rho(x, y) = D$.

For convenience, an initial list of attainable values of D is given in Table 1. The assumption of attainability is justified, since if $D_1 < D < D_2$ where $D_{1,2}$ are subsequent Gaussian numbers then the HC model with the exclusion distance D is reduced to that with distance D_2 .

1, 2, 4, 5, 8, 9, 10, 13, 16, 17, 18, 20, 25, 26, 29, 32, 34, 36, 37, 40, 41, 45, 49, 50, 52, 53, 58, 61, 64, 65, 68, 72, 73, 74, 80, 81, 82, 85, 89, 90, 97, 98, 100, 101, 104, 106, 109, 113, 116, 117, 121, 122, 125, 128, 130, 136, 137, 144, 145, 146, 148, 149, 153, 157, 160, 162, 164, 169, 170, 173, 178, 180, 181, 185, 193, 194, 196, 197, 200, 202, 205, 208, 212, 218, 221, 225, 226, 229, 232, 233, 234, 241, 242, 244, 245, 250, 256, 257, 260, 261, 265, 269, 272, 274, 277, 281, 288, 289, 290, 292, 293, 296, 298

Table 1: Gaussian numbers $D^2 \leq 300$.

We work with D -admissible configurations (D -ACs) in \mathbb{Z}^2 , represented by maps $\phi : \mathbb{Z}^2 \rightarrow \{0, 1\}$ such that $\rho(x, y) \geq D$ for every pair of distinct sites $x, y \in \mathbb{Z}^2$ with $\phi(x) = \phi(y) = 1$. A site x with $\phi(x) = 1$ is interpreted as occupied by a ‘particle’ while site y with $\phi(y) = 0$ as vacant. Particles are treated as disjoint open disks of diameter D with the centers placed at lattice sites. We write $x \in \phi$ if $\phi(x) = 1$ and identify ϕ with the subset in \mathbb{Z}^2 where $\phi(x) = 1$.

The collection $\mathcal{A} = \mathcal{A}(D)$ of D -ACs forms a closed subset in the Cartesian product $\mathcal{X} := \{0, 1\}^{\mathbb{Z}^2}$ in the Tychonov topology. The notion of an admissible configuration can be defined for any $\mathbb{V} \subset \mathbb{Z}^2$; accordingly, one can use the notation $\mathcal{A}(\mathbb{V}) = \mathcal{A}(D, \mathbb{V})$.

We analyze probability measures μ on $(\mathcal{X}, \mathfrak{B}(\mathcal{X}))$ sitting on \mathcal{A} (i.e., such that $\mu(\mathcal{A}) = \mu(\mathcal{X}) = 1$) where $\mathfrak{B}(\mathcal{X})$ is the Borel σ -algebra in \mathcal{X} . Let $\mathbb{V} \subset \mathbb{Z}^2$ be a finite set and $\phi \in \mathcal{A}$ a D -AC. We say that a finite configuration $\psi^{\mathbb{V}} \in \{0, 1\}^{\mathbb{V}}$ is (ϕ, \mathbb{V}) -compatible if the concatenated configuration $\psi^{\mathbb{V}} \vee (\phi \upharpoonright_{\mathbb{Z}^2 \setminus \mathbb{V}}) \in \mathcal{A}$ (which requires that $\psi^{\mathbb{V}} \in \mathcal{A}(\mathbb{V})$). Here and below, symbol \upharpoonright stands for the restriction. The set of (ϕ, \mathbb{V}) -compatible configurations is denoted by $\mathcal{A}(\mathbb{V} \parallel \phi)$.

Given $u > 0$, consider a probability measure $\mu_{\mathbb{V}}(\cdot \parallel \phi)$ on $\{0, 1\}^{\mathbb{V}}$ given by

$$\mu_{\mathbb{V}}(\psi^{\mathbb{V}} \parallel \phi) = \begin{cases} \frac{u^{\sharp(\psi^{\mathbb{V}})}}{\mathbf{Z}(\mathbb{V} \parallel \phi)}, & \text{if } \psi^{\mathbb{V}} \in \mathcal{A}(\mathbb{V} \parallel \phi), \\ 0, & \text{if } \psi^{\mathbb{V}} \notin \mathcal{A}(\mathbb{V} \parallel \phi). \end{cases} \quad (1.1)$$

Here $\sharp(\psi^{\mathbb{V}})$ stands for the number of particles in $\psi^{\mathbb{V}}$: $\sharp(\psi^{\mathbb{V}}) := \#\{x \in \mathbb{V} : \phi(x) = 1\}$. Next, $\mathbf{Z}(\mathbb{V} \parallel \phi)$ is the *partition function* in \mathbb{V} with the boundary condition ϕ :

$$\mathbf{Z}(\mathbb{V} \parallel \phi) = \sum_{\psi^{\mathbb{V}} \in \mathcal{A}(\mathbb{V} \parallel \phi)} u^{\sharp(\psi^{\mathbb{V}})}. \quad (1.2)$$

Parameter $u > 0$ is called *fugacity*, or *activity* (of an occupied site).

A probability measure μ on $(\mathcal{X}, \mathfrak{B}(\mathcal{X}))$ is called a D -HC Gibbs/DLR measure if (i) $\mu(\mathcal{A}) = 1$, (ii) \forall finite $\mathbb{V} \subset \mathbb{Z}^2$ and a function $f : \phi \in \mathcal{X} \mapsto f(\phi) \in \mathbb{C}$ depending only on the restriction $\phi \upharpoonright_{\mathbb{V}}$, the integral $\mu(f) = \int_{\mathcal{X}} f(\phi) d\mu(\phi)$ has the form

$$\mu(f) = \int_{\mathcal{X}} \int_{\{0, 1\}^{\mathbb{V}}} f(\psi^{\mathbb{V}} \vee \phi \upharpoonright_{\mathbb{Z}^2 \setminus \mathbb{V}}) d\mu_{\mathbb{V}}(\psi^{\mathbb{V}} \parallel \phi) d\mu(\phi). \quad (1.3)$$

One can say that under such measure μ , the probability of a configuration $\psi^\mathbb{V}$ in a finite ‘volume’ $\mathbb{V} \subset \mathbb{Z}^2$, conditional on a configuration $\phi \upharpoonright_{\mathbb{Z}^2 \setminus \mathbb{V}}$, coincides with $\mu_\mathbb{V}(\psi^\mathbb{V} \parallel \phi)$, for μ -a.a. $\phi \in \{0, 1\}^{\mathbb{Z}^2}$.

In the literature, equality (1.3) is referred to as the DLR (Dobrushin-Lanford-Ruelle) equation for a measure μ (it represents a system of equations labeled by \mathbb{V} and f).

The HC Gibbs measures form a *Choquet simplex* (in the weak-convergence topology on the set of probability measures on $(\mathcal{X}, \mathfrak{B}(\mathcal{X}))$), which we denote by $\mathcal{G} = \mathcal{G}(D, u)$. We are interested in *extreme Gibbs measures*, i.e., extreme points of \mathcal{G} . In Physics the extreme Gibbs measures are interpreted as *pure phases*. The collection of the extreme Gibbs measures (EGMs) is denoted by $\mathcal{E} = \mathcal{E}(D, u)$ and its cardinality is denoted by $\#\mathcal{E}$. Any HC DLR-measure μ is the barycenter for some unit mass distribution over \mathcal{E} . Cf. [18].

The current paper consists of 8 Sections. In Section 2 we state our main results: see Theorem S, Theorems 1 - 3 and Lemma I. Section 3 derives the proof of these assertions from existing results and methods. In particular, Section 3.3 contains the definition of a contour and the Peierls bound (see Lemma II). In Section 4 we provide some additional statements; cf. Theorem 4. We also discuss the issue of dominance in Section 4.2. Sections 5, 6 establish connections with algebraic number theory, namely, with *norm equations* in the ring $\mathbb{Z}[\sqrt[6]{-1}]$. More precisely, uniqueness and non-uniqueness in problem (2.1) is related to cosets in $\mathbb{Z}[\sqrt[6]{-1}]$ by the group of units. In particular, in Section 5.2 we prove an important property of (eventual) minimality along a coset. Next, in Section 6 we discuss simplest examples of infinite sequences of values D of Classes A and B, respectively. The proof of Theorem 3 (in a more detailed form - Theorems 5-10) is carried out in Section 7. Section 8 contains the proof of Theorem S claiming that all instances of sliding are identified in Table 2; see Section 2.2.

2 Periodic ground states in \mathbb{Z}^2 . Sliding. Main results

2.1 Periodic ground states and an optimization problem for sub-lattices.

The Pirogov-Sinai (PS) theory is based on two (mutually related) key properties: (I) a finite number of periodic ground states (PGSs) and (II) a *Peierls bound*: a lower estimate for an energy increment in a local perturbation of a PGS. An admissible configuration φ is called a HC *ground state* if one cannot remove finitely many occupied sites from φ and replace them by a larger number of particles without breaking D -admissibility. In other words, one cannot find a finite subset $\mathbb{V} \subset \mathbb{Z}^2$ and a configuration $\psi^\mathbb{V} \in \mathcal{A}(\mathbb{V} \parallel \varphi)$ compatible with φ such that $\#\psi^\mathbb{V} > \#\varphi \upharpoonright_\mathbb{V}$. Next, we say that a configuration ϕ is periodic if there exist two linearly independent vectors e_1, e_2 such that $\phi(x) = \phi(x + e_1) = \phi(x + e_2)$. The parallelogram with vertices $0, e_1, e_2, e_1 + e_2$ is a *fundamental parallelogram* (FP) for ϕ . We always assume that $e_{1,2}$ are chosen so that the shorter diagonal of the FP divides it into two triangles without obtuse angles; one of these triangles, with a vertex at the origin, is referred to as a *fundamental triangle* (FT). We say that a sub-lattice is isosceles or non-isosceles if the FT is isosceles or not.

Let $\mathcal{P} = \mathcal{P}(D)$ denote the set of PGSs for a given attainable D ; the cardinality of

\mathcal{P} is denoted by $\#\mathcal{P}$. Our first result (Lemma I in Section 2.3) is that, in absence of sliding, the set \mathcal{P} is finite and all PGSs are produced from maximally-dense admissible sub-lattices by means of \mathbb{Z}^2 -shifts, the rotation by $\pi/2$ and the reflection about the x-axis in \mathbb{R}^2 . We will use the term \mathbb{Z}^2 -congruence for each of these transformations. Since each maximally-dense sub-lattice is generated by a FP/FT of a minimal area we refer to it as an (admissible) min-area sub-lattice.

A natural way to identify a min-area FP for a given D is to solve the following discrete optimization problem:

$$\begin{aligned} & \text{minimize the area of a } \mathbb{Z}^2\text{-triangle} \\ & \text{with one vertex at the origin,} \\ & \text{with side-lengths } \ell_i \geq D \text{ and angles } \alpha_i \leq \pi/2. \end{aligned} \tag{2.1}$$

The term \mathbb{Z}^2 -triangle means a triangle with vertices in \mathbb{Z}^2 . The approach with minimizing the area of \mathbb{Z}^2 -triangles is natural because the (formal) amount of triangles in a Delaunay triangulation corresponding to an admissible configuration is always twice the (formal) number of particles in it. An additional constraint in (2.1) is that the optimization is performed over non-obtuse triangles only. The justification of this constraint is the subject of Section 3.1.

In what follows, $S = S(D)$ refers to the doubled minimal area in (2.1); it is instructive to note that $S(D) \in \mathbb{N}$. (Here and below, \mathbb{N} stands for the set of positive integers.) Also, for all values ℓ_i under consideration we have $\ell_i^2 = m^2 + n^2 \in \mathbb{N}$, with integer m, n . Problem (2.1) always has a solution but a minimizing \mathbb{Z}^2 -triangle may be non-unique (in one sense or another). Any minimizing triangle is referred to as an *M-triangle*. A notable part of this work attempts at clarifying algebraic aspects of non-uniqueness in (2.1). From now on we suppose that the triple of side-lengths $\ell_i, i = 0, 1, 2$, obeys

$$D \leq \ell_0 \leq \ell_1 \leq \ell_2, \tag{2.2}$$

and α_i stands for the opposite angles: $\pi/2 \geq \alpha_0 \geq \alpha_1 \geq \alpha_2$.

Of course, one cannot inscribe an equilateral triangle in \mathbb{Z}^2 . However, a pair of integers $a = \ell_1^2 - \ell_0^2$ and $b = \ell_2^2 - \ell_1^2$, called a *signature* of a \mathbb{Z}^2 -triangle, characterizes the closeness of the triangle to an equilateral one.

We say that a given value D (or D^2) is of Class S if there exist two M-triangles with a common side but different third vertices belonging to the same half-plane with respect to the common side. Assuming that a dense-packing configuration consists of M-triangles only, it is not hard to see that for all D belonging to Class S the HC model exhibits sliding. Theorem S proves that all sliding values of D belong to Class S, and there are only 39 of them.

We say that the non-sliding value D (or D^2) is of Class A if the M-triangle in (2.1), (2.2) is unique modulo \mathbb{Z}^2 -congruences. That is, all M-triangles have the same triple (ℓ_0, ℓ_1, ℓ_2) and are \mathbb{Z}^2 -congruent. We show that Class A contains infinitely many values of D (or D^2). An initial list of Class A values of D^2 is given in Table 3, together with the corresponding values of $S(D)$ and $\#\mathcal{E}(D)$.

For example, for $D^2 = 328$, the doubled area of an M-triangle is $S = 292$, with $\ell_0^2 = 328$, $\ell_1^2 = 338$, $\ell_2^2 = 346$. An example of such an M-triangle has vertices at sites

$(0, 0)$, $(13, 13)$ and $(-5, 18)$. As a result (see Theorem 1), the number of PGSs and EGMs equals $1168 = 4S$. (Here the factor 4 indicates four min-area sub-lattices for $D^2 = 328$.)

All values of D not belonging to Classes A and S necessarily exhibit non-uniqueness of a solution to (2.1), (2.2). One form of such non-uniqueness is where the corresponding triple (ℓ_0, ℓ_1, ℓ_2) is unique but the M-triangles form more than one \mathbb{Z}^2 -congruence class. In other words, the minimizing triangle for a given D (or D^2) is unique up to an \mathbb{R}^2 -congruence but has more than one \mathbb{Z}^2 -implementation. In this case we say that a value D (or D^2) belongs to Class B0 and speak of different \mathbb{Z}^2 -implementations for a given minimizing triple (or minimizing type) (ℓ_0, ℓ_1, ℓ_2) . An initial example of Class B0 is $D^2 = 425$; see Table 4. Here the M-triangle has the doubled area $S = 750$. The squared side-lengths in an M-triangle are $\ell_0^2 = \ell_1^2 = 425$, $\ell_2^2 = 450$ (so it is isosceles). However, such a triangle can be \mathbb{Z}^2 -implemented in two ways: (i) with vertices at $(0, 0)$, $(15, 15)$ and $(-5, 20)$, and (ii) with vertices at $(0, 0)$, $(21, 3)$ and $(8, 19)$. These \mathbb{Z}^2 -implementations are \mathbb{R}^2 - but not \mathbb{Z}^2 -congruent. Therefore, they will generate not \mathbb{Z}^2 -congruent min-area sub-lattices.

In fact, each equivalence class includes 1, 2 or 4 \mathbb{Z}^2 -congruent min-area sub-lattices, depending on whether the M-triangle is isosceles straight, isosceles non-straight or non-isosceles. (An isosceles straight triangle occurs only for $D^2 \leq 20$.) This explains why the number of PGSs for $D^2 = 328$ is $4S$ while for $D^2 = 425$ it is $2S$.

We establish that Class B0 includes infinitely many values of D . Moreover, the degree of degeneracy (the number of different \mathbb{Z}^2 -implementations) can be arbitrarily large. We present an initial list of Class B0 values D in Table 4, together with the specified values of $S(D)$ and $\sharp \mathcal{P}(D)$.

Another form of non-uniqueness is where the triple (ℓ_0, ℓ_1, ℓ_2) for an M-triangle is non-unique. Here we say that a value D (or D^2) belongs to Class B1 if (I) it generates at least 2 different minimizing triples (ℓ_1, ℓ_2, ℓ_3) in problem (2.1), (2.2) and (II) each triple has a single implementation modulo \mathbb{Z}^2 -congruences.

An example of Class B1 is $D^2 = 65$; again see Table 4. Here we have two minimizing triples (ℓ_0, ℓ_1, ℓ_2) : (a) with $\ell_0^2 = \ell_1^2 = 65$, $\ell_2^2 = 80$ and (b) with $\ell_0^2 = \ell_1^2 = 68$, $\ell_2^2 = 72$; both isosceles and of the doubled area $S = 120$. The M-triangles of type (a) are obviously not \mathbb{R}^2 -congruent to those of type (b). But each of triples (a), (b) has a unique \mathbb{Z}^2 -implementation (again, up to \mathbb{Z}^2 -congruences). The vertices can be selected as $(0, 0)$, $(8, 4)$ and $(-1, 8)$ for (a) and $(0, 0)$, $(8, 2)$ and $(2, 8)$ for (b).

We give an initial list of Class B1 values D in Table 4, together with the specified values of $S(D)$ and $\sharp \mathcal{P}(D)$.

In addition, if, for a given D , condition (I) holds true while condition (II) is not true then this D (or D^2) belongs to Class B2; as before it also occurs for infinitely many values of D . That is, for a given value D^2 of Class B2 we have (i) at least two non- \mathbb{R}^2 -congruent minimizing triangles, and (ii) at least one of them has at least two non- \mathbb{Z}^2 -congruent implementations. The first example of Class B2 is $D^2 = 15005$. Here we have three minimizing triples (ℓ_0, ℓ_1, ℓ_2) : (a) with $\ell_0^2 = 15005$, $\ell_1^2 = 15076$, $\ell_2^2 = 15133$, (b) with $\ell_0^2 = 15028$, $\ell_1^2 = 15041$, $\ell_2^2 = 15145$ and (c) with $\ell_0^2 = 15013$, $\ell_1^2 = 15061$, $\ell_2^2 = 15140$; all of them are non-isosceles and of the doubled area $S = 13052$. The M-triangles of types (a), (b) and (c) are obviously pair-wise not \mathbb{R}^2 -congruent. Moreover, each of triples (a) and (c) has a unique \mathbb{Z}^2 -implementation (again, up to \mathbb{Z}^2 -congruences). The vertices for triple (a) can be selected as $(0, 0)$, $(91, 82)$ and $(-26, 120)$. The vertices for triple

(c) can be selected as $(0, 0)$, $(118, 33)$ and $(30, 119)$. On the contrary, triple (b) has two implementations: the vertices can be selected as $(0, 0)$, $(108, 58)$ and $(4, 123)$ for one of them and $(0, 0)$, $(122, 12)$, and $(51, 112)$ for the other one.

In what follows, we collectively refer to the set of the values D with non-uniqueness and non-sliding as Class B. By definition, B0, B1 and B2 form a partition of Class B. Moreover, all attainable values of D^2 are partitioned into Class S, Class A and Class B.

Remark 2.1. For the HC model in \mathbb{A}_2 only the non-uniqueness type B0 is possible; cf. [32]. Also note that, contrary to [32], for lattice \mathbb{Z}^2 we do not partition Class A into Classes A0 and A1 as an acute triangle cannot be non-inclined with respect to \mathbb{Z}^2 . \blacktriangle

Observe that an M-triangle corresponding to a given D can also be minimal for smaller attainable exclusion distances. Moreover, for each \mathbb{Z}^2 -triangle which is minimal for some D there exists a minimal attainable exclusion distance, denoted by D^* , for which this triangle is still minimal. Consequently, this triangle is an M-triangle for a range of values of D starting with D^* and ending with the shortest side-length in the triangle. This observation allows us to speak about M-triangles without specifying the corresponding D (or D^2) unless it is required by the context. Cf. Section 5.

Every min-area sub-lattice φ gives rise to a collection of PGSs obtained by \mathbb{Z}^2 -shifts of φ ; the number of such PGSs is equal to $S(D)$. Consequently, a given congruence class of sub-lattices produces $m \cdot S(D)$ PGSs where $m = 1, 2, 4$ as stated in paragraph (ii) in Section 1.1. Thus, we can speak of PGS equivalence classes where every PGS is obtained from another PGS by means of a \mathbb{Z}^2 -shift, rotation by $k\pi/2$ and reflections about coordinate axes and bisectrices. This defines \mathbb{Z}^2 -congruences (or \mathbb{Z}^2 -symmetries) within a PGS equivalence class.

In the rest of this section we discuss the relationship between PGSs and EGMs. We say that a PGS $\varphi \in \mathcal{P}$ generates an EGM $\mu_\varphi \in \mathcal{E}$ if

$$\mu_\varphi = \lim_{\mathbb{V} \nearrow \mathbb{Z}^2} \mu_{\mathbb{V}}(\cdot \parallel \varphi) \quad (2.3)$$

(see (1.1)–(1.3)).

Note that the PGS equivalence class is unique iff D is of Class A. Our Theorem 1 (see Section 2.3) states that in this case the structure of the set \mathcal{E} of the extreme Gibbs measures for large u is relatively simple: each EGM $\mu \in \mathcal{E}$ is generated from a PGS $\varphi \in \mathcal{P}$ and each PGS $\varphi \in \mathcal{P}$ generates an EGM $\mu = \mu_\varphi$.

On the opposite end, for values D of Class B not all PGS classes will generate EGMs, only dominant ones possessing broader varieties of local excitations of a larger statistical weight. (For definitions and details see [49] where the term stable is used in place of dominant.) Our Theorem 2 (see Section 2.3) contains the corresponding results. Due to the underlying symmetries, if a PGS φ from a dominant PGS equivalence class generates an EGM μ_φ then every PGS from this class generates a corresponding EGM. The identification of dominant PGSs is a non-trivial task, see the discussion in Section 4.2.

To summarize, we may say that $\sharp\mathcal{P}(D)$ is a sum, over all PGS equivalence classes, of the numbers of PGSs in each class (which may be different for different classes). Accordingly, for u large enough $\sharp\mathcal{E}(D)$ is the sum over all dominant PGS equivalence classes of the number of PGSs in each class. Note that for such u non-periodic EGMs do not occur (see [14]).

2.2 Sliding as a pattern of non-uniqueness in Eqn (2.1).

We say that a given value D exhibits *sliding* if exist two or more M-triangles with (i) a common side called a *sliding base*, with two common vertices, and (ii) distinct third vertices lying in the same half-plane relative to the shared side. In what follows we refer to the sliding base as OW and the third vertices as A, B, \dots . Cf. Figures 1C and 6.

Thus, sliding can be viewed as a specific form of non-uniqueness in problem (2.1). It leads to a multitude of periodic and non-periodic ground states characterized by layered or staggered patterns. The point is that under sliding there are countably many periodic and continuum of non-periodic ground states. In fact, here both assumptions I and II of the PS theory are violated (a finite collection of PGSs and the Peierls bound).

The cases of sliding are listed in Table 2 below. The data format in Table 2 is

$$D^2 = m^2 + n^2 \quad W \quad [A, B, \dots] \quad S(D)$$

where $W = (w_1, w_2)$ and $A = (a_1, a_2)$, $B = (b_1, b_2)$, \dots . We would like to note that in Table 2 we omitted values of D^2 for which the M-triangles and areas $S(D)$ are re-produced for a larger value of D^2 viz., $D^2 = 1513$ and $D^2 = 1514$ have the same $W = (0, -39)$ and the same $A = (34, -19)$, $B = (34, -20)$ and $S(D) = 1326$ as for $D^2 = 1517$. In other words, we only list the values D^2 that are maximal for given M-triangles.

Examples of bases OW and vertices A, B, C, \dots are shown in Figure 6.

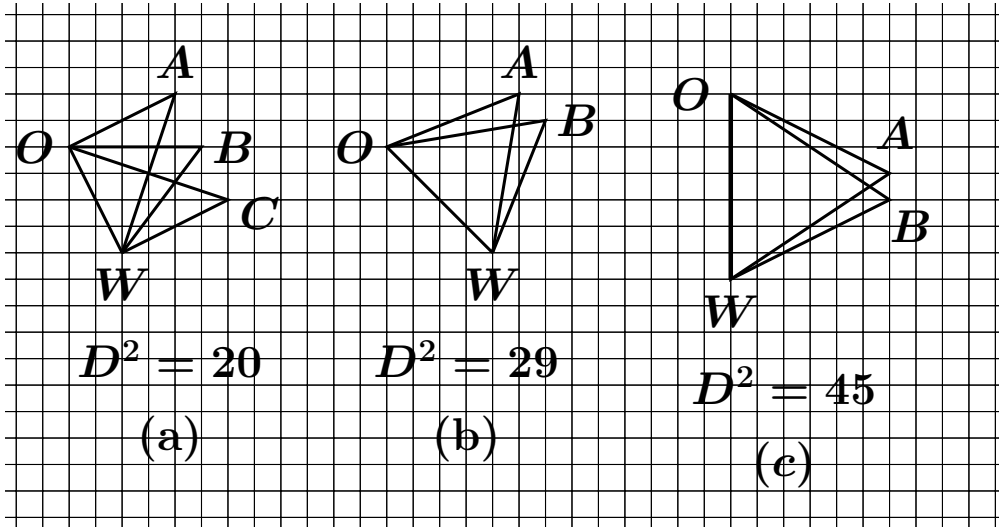


Figure 6: Sliding for $D^2 = 20$, $D^2 = 29$ and $D^2 = 45$. Note the rectangular $OACW$ (a) and circular trapezes $OABW$ (b,c).

The list of sliding values D in Table 2 is produced by `MinimalTriangles.java` and `ZSliding.java`.

Paper [28] confirms our conjecture that the sliding occurs only for a finite number of values D^2 i.e., the Class S is finite. That is, there exists a constant $d^* \in (0, \infty)$ such that sliding does not occur for $D^2 \geq d^*$. An improvement of the result of [28] is the following theorem.

Theorem S. *Table 2 contains all instances of sliding, i.e., exhausts Class S.*

$D^2 = m^2 + n^2$	W	$[A, B, \dots]$	$S(D)$
$4 = 2^2 + 0^2$	(0, -2)	[(2, 0), (2, -1), (2, -2)]	4
$8 = 2^2 + 2^2$	(2, -2)	[(2, 2), (3, 1), (4, 0)]	8
$9 = 3^2 + 0^2$	(0, -3)	[(3, 0), (3, -1), (3, -2), (3, -3)]	9
$18 = 3^2 + 3^2$	(3, -3)	[(3, 3), (4, 2), (5, 1), (6, 0)]	18
$20 = 4^2 + 2^2$	(2, -4)	[(4, 2), (5, 0), (6, -2)]	20
$29 = 5^2 + 2^2$	(4, -4)	[(5, 2), (6, 1)]	28
$45 = 6^2 + 3^2$	(0, -7)	[(6, -3)(6, -4)]	42
$72 = 6^2 + 6^2$	(6, -6)	[(6, 5), (7, 4), (8, 3), (9, 2), (10, 1), (11, 0)]	66
$80 = 8^2 + 4^2$	(0, -9)	[(4, 8), (5, 8)]	72
$90 = 9^2 + 3^2$	(7, -7)	[(9, 3), (10, 2)]	84
$106 = 9^2 + 5^2$	(0, -11)	[(9, -5), (9, -6)]	99
$121 = 11^2 + 0^2$	(0, -11)	[(10, -5), (10, -6)]	110
$157 = 11^2 + 6^2$	(0, -13)	[(11, -6), (11, -7)]	143
$160 = 12^2 + 4^2$	(9, -9)	[(12, 4), (13, 3)]	144
$218 = 13^2 + 7^2$	(0, -15)	[(13, -7), (13, -8)]	195
$281 = 16^2 + 5^2$	(12, -12)	[(16, 5), (17, 4)]	252
$392 = 14^2 + 14^2$	(14, -14)	[(19, 6), (20, 5)]	350
$521 = 20^2 + 11^2$	(0, -23)	[(20, 12), (20, 11)]	460
$698 = 23^2 + 13^2$	(0, -27)	[(23, -13), (23, -14)]	621
$821 = 25^2 + 14^2$	(0, -29)	[(25, -14), (25, -15)]	725
$1042 = 31^2 + 9^2$	(23, -23)	[(31, 9)(32, 8)]	920
$1325 = 35^2 + 10^2 = 34^2 + 13^2$ $= 29^2 + 22^2$	(26, -26)	[(35, 10), (36, 9)]	1170
$1348 = 32^2 + 18^2$	(0, -37)	[(32, -18), (32, -19)]	1184
$1517 = 34^2 + 19^2 = 29^2 + 26^2$	(0, -39)	[(34, -19), (34, -20)]	1326
$1565 = 38^2 + 11^2 = 37^2 + 14^2$	(28, -28)	[(38, 11), (39, 10)]	1372
$2005 = 41^2 + 18^2 = 39^2 + 22^2$	(0, -45)	[(39, -22), (39, -23)]	1755
$2792 = 46^2 + 22^2$	(0, -53)	[(46, -26), (46, -27)]	2438
$3034 = 55^2 + 3^2 = 53^2 + 15^2$	(39, -39)	[(53, 15), (54, 14)]	2652
$3709 = 53^2 + 30^2$	(0, -61)	[(53, -30), (53, -31)]	3233
$4453 = 63^2 + 22^2 = 58^2 + 33^2$	(0, -67)	[(58, -33), (58, -34)]	3886
$4756 = 66^2 + 20^2 = 60^2 + 34^2$	(0, -69)	[(60, -34), (60, -35)]	4140
$6865 = 76^2 + 33^2 = 72^2 + 41^2$	(0, -83)	[(72, -41), (72, -42)]	5976
$11449 = 107^2 + 0^2$	(0, -107)	[(93, -53), (93, -54)]	9951
$12740 = 112^2 + 14^2 = 98^2 + 56^2$	(0, -113)	[(98, -56), (98, -57)]	11074
$13225 = 115^2 + 0^2 = 92^2 + 69^2$	(0, -115)	[(100, -57), (100, -58)]	11500
$15488 = 88^2 + 88^2$	(88, -88)	[(120, 33), (121, 32)]	13464
$22784 = 128^2 + 80^2$	(0, -151)	[(131, -75), (131, -76)]	19781
$29890 = 161^2 + 63^2 = 147^2 + 91^2$	(0, -173)	[(150, -86), (150, -87)]	25950
$37970 = 179^2 + 77^2 = 169^2 + 97^2$	(0, -195)	[(169, -97), (169, -98)]	32955

Table 2: The values of D^2 with sliding.

The proof of Theorem S is presented in Section 8. A part of the proof is computer-assisted. The analytical upper bound upon constant d^* emerging from [28] was too high for performing an exhaustive enumeration of all cases of sliding for $D^2 < d^*$. We therefore needed (i) a better bound on d^* and (ii) an efficient algorithm of analysis of values $D^2 < d^*$. Cf. Section 8.

2.3 Main results

In this section we state Lemma I and Theorems 1 - 3. The proofs of Theorems 1, 2 are given in Section 3. The proof of Theorem 3 can be recovered from the material presented in Sections 5-7. In fact, Section 5.1 contains a finer version of this theorem (see Theorem 5-10).

A justification of problem (2.1) is provided in Lemma I (where we use an observation from [7]).

Lemma I. (i) *For any attainable D , every PGS is obtained as a tessellation by M-triangles and their \mathbb{Z}^2 -shifts.*

(ii) *Furthermore, if D is non-sliding then every PGS is obtained from a max-dense sub-lattice by means of \mathbb{Z}^2 -congruences. Consequently, for any non-sliding D the PGS set $\mathcal{P}(D)$ is finite.*

Let us repeat: a value D (or D^2) is of Class A if D produces a unique triple (ℓ_0, ℓ_1, ℓ_2) , unique \mathbb{Z}^2 -congruence class and no sliding. On the other hand, a non-sliding D (or D^2) is of Class B if value D features several equivalence classes in (2.1).

Theorem 1. (Main result, I) *Assume an attainable value D is of Class A. Then:*

(i) *The cardinality $\#\mathcal{P}(D)$ equals $mS(D)$ where $m = 1, 2$ or 4 . More precisely, (a) $m = 1$ for $D^2 = 1, 2$, (b) $m = 2$ if $D^2 > 2$ and the M-triangle is isosceles, (c) $m = 4$ if the M-triangle is non-isosceles. The PGSs are obtained from each other by \mathbb{Z}^2 -congruences.*

(ii) *There exists a value $u_*(D) \in (0, \infty)$ such that for $u \geq u_*(D)$ the following assertions hold true. Every EGM $\mu \in \mathcal{E}(D)$ is generated by a PGS $\varphi \in \mathcal{P}(D)$ in the sense of (2.3): $\mu = \lim_{\mathbb{V} \nearrow \mathbb{Z}^2} \mu_{\mathbb{V}}(\cdot || \varphi) (= \mu_{\varphi})$. The measures μ_{φ} are mutually disjoint ($\mu_{\varphi'} \perp \mu_{\varphi''}$ for $\varphi' \neq \varphi''$) and inherit the symmetry properties of their respective PGSs. Consequently, $\#\mathcal{E}(D) = \#\mathcal{P}(D)$.*

Table 3 indicates the number of extreme Gibbs measures for values D from Class A. See also Figures 3, 4. Values D in Tables 3, 4 are produced by `MinimalTriangles.java`.

Theorem 2. (Main result, II) *Suppose D is attainable, non-sliding and of Class B. Then the number of PGSs in a given congruence class is $2S(D)$ if the respective M-triangle is isosceles and $4S(D)$ if it is non-isosceles. The total number of PGSs equals the sum of the cardinalities of the equivalence classes.*

*Furthermore, there exist congruence classes (one or several) called **dominant** such that for $u \geq u_*(D) \in (0, \infty)$: (i) every PGS φ from a dominant class generates an EGM $\mu = \mu_{\varphi}$ with the same symmetries via the limit (2.3), (ii) all EGMs $\mu \in \mathcal{E}$ are obtained in such a way from the PGSs belonging to dominant classes. The EGMs μ_{φ} are disjoint for different PGSs φ .*

D^2	S	I/N	$\#\mathcal{E}$	D^2	S	I/N	$\#\mathcal{E}$	D^2	S	I/N	$\#\mathcal{E}$	D^2	S	I/N	$\#\mathcal{E}$
1	1	I	1	64	56	I	112	164	146	N	584	233	208	I	416
2	2	I	2	68	60	I	120	170	150	I	300	241	209	I	418
5	5	I	10	74	68	N	272	178	157	N	627	245	217	I	434
10	10	I	20	85	75	I	150	180	162	N	648	256	224	I	448
13	12	I	24	89	80	I	160	181	166	N	664	260	228	N	912
17	15	I	30	97	86	N	344	193	168	I	336	265	236	N	944
25	23	N	92	100	90	I	180	194	172	N	688	272	240	I	480
26	24	I	48	109	101	N	404	197	176	N	704	277	247	N	988
34	30	I	60	113	102	N	408	200	180	I	360	290	254	N	1016
37	34	N	136	117	105	N	420	202	181	N	724	293	258	N	1032
40	38	N	152	128	112	I	224	205	184	N	736	296	268	N	1072
41	39	N	156	136	120	I	240	208	188	N	752	305	269	N	1076
50	45	I	90	137	124	N	496	212	194	N	776	306	270	I	540
52	48	I	96	145	127	N	508	221	195	I	390	320	280	I	560
53	52	N	204	148	134	N	536	225	198	N	792	328	292	N	1168
58	53	N	212	153	135	I	270	226	203	N	812	333	299	I	598

Table 3: An initial list of quadruples $(D^2, S, I/N, \#\mathcal{E})$ for Class A with $D^2 < 337$. Here S stands for the area and I/N for Isosceles/Non-isosceles property of an M-triangle in (2.1). Furthermore, $\#\mathcal{E}$ indicates the number of extreme Gibbs measures. As above, we only list the maximal value of D^2 consistent with a given M-triangle. E.g., the entry $(32, 30, I, 60)$ preceding $(34, 30, I, 60)$ is not listed.

D^2	S	B0/1	$\#\mathcal{P}$	D^2	S	B0/1	$\#\mathcal{P}$	D^2	S	B0/1	$\#\mathcal{P}$
65	60	B1	240	1600	1400	B0	5600	3413	2971	B1	23768
130	120	B1	480	1845	1605	B0	12840	3505	3061	B1	24488
324	288	B1	1728	2098	1837	B1	14696	3690	3210	B0	25680
425	375	B0	1500	2116	1840	B1	14720	3701	3225	B1	19350
485	430	B0	3440	2213	1930	B1	15440	3770	3285	B0	26280
562	493	B1	2598	2245	1960	B0	15680	3816	3318	B1	26544
725	635	B0	5080	2468	2150	B1	17200	3865	3359	B1	26872
832	728	B1	5824	2578	2247	B1	17976	4100	3572	B1	28576
986	870	B1	5220	2609	2277	B1	18216	4210	3673	B1	29384
1010	889	B1	7112	2650	2315	B0	18520	4232	3680	B1	29440
1124	986	B1	5916	2725	2370	B0	18960	4250	3695	B0	29560
1234	1075	B1	6450	2770	2419	B1	19352	4426	3860	B1	30880
1297	1135	B1	9080	2993	2613	B1	15678	4441	3875	B1	31000
1409	1236	B1	9888	3041	2654	B1	21232	4505	3919	B1	31352
1489	1307	B1	10456	3060	2670	B0	21360	4624	4012	B1	24072
1521	1329	B1	10456	3130	2717	B1	16302	4709	4102	B1	32816

Table 4: Initial values of Class B with $D^2 \leq 4709$. Here we feature a quadruple $(D^2, S, B0/1, \#\mathcal{P})$. (A higher degree of degeneracy emerges for larger values of D .) Again we pick the largest value of D^2 with a given S ; e.g. $S = 635$ figures for $D^2 = 724$ and $D^2 = 725$; the former value $D^2 = 724$ is omitted. In all entries, the number of non-congruent sub-lattices equals 2. Accordingly, the number of the PGs $\#\mathcal{P}$ equals $4S$ if both sub-lattices are isosceles, $6S$ if one sub-lattice is isosceles and the other not (this can occur in Case B1 but not B0), and $8S$ if both sub-lattices are non-isosceles.

As we said earlier, for a given D , the dominant classes could be determined by an additional analysis of local excitations. A general scheme, based on a number of assumptions, was proposed in [49]. In this paper we comment on the cases $D^2 = 65, 130, 324$ (an initial triple of values D from Class B); see Section 4.2, Figures 10-12. On a triangular lattice \mathbb{A}_2 , an analysis of dominance has been performed in [32] and on \mathbb{Z}^3 in [33].

The following Theorem guarantees that all Classes A, B0, B1, and B2 are infinite. It also provides a coarse description of the algebraic structure of these classes. Here we use the cyclotomic ring $\mathbb{Z}[\sqrt[6]{-1}]$ and its group of units $\mathbb{U}[\sqrt[6]{-1}]$.

Theorem 3. (Main result, III) *Each of Classes A, B0, B1, B2 contains infinitely many values D^2 . Each non-sliding value D^2 falls in one of these classes. All \mathbb{Z}^2 -triangles can be partitioned into double infinite sequences with the alternating signatures a, b and b, a for all triangles in the sequence. Moreover, inside each double sequence the number of non-M-triangles is finite. Algebraically, these sequences are identified with the cosets in ring $\mathbb{Z}[\sqrt[6]{-1}]$ by the unit group $\mathbb{U}[\sqrt[6]{-1}]$.*

Furthermore, the set of all double sequences, i.e. cosets, can be partitioned into maximal families such that for a given family there exists a \mathbb{Z} -indexation of every double sequence such that all M-triangles with the same index $j \in \mathbb{Z}$ have the same area. For a given index j let D_j^2 be the shortest squared side-length among all M-triangles in the family indexed by j . Then all these D_j^2 (of which there are infinitely many) belong to the same Class (A, B0, B1, or B2). Every such family is finite. Among these families there are families corresponding (in the above sense) to each of Classes A, B0, B1, and B2, and the size of the corresponding Class B families can be arbitrarily large.

Theorems 1-3 give a detailed description of the phase diagram of the hard-core model in \mathbb{Z}^2 for any attainable non-sliding D^2 and large enough u .

However, the phase diagram in the case of sliding remains an open question. Another question is an identification of dominant phases (Class B). Here we expect that in the hard-core model in \mathbb{Z}^2 there always exists a single dominant congruent class of PGSs.

3 The Peierls condition. Proof of the main results

We begin this section by developing a technical background needed for the proof of Lemma I; see Lemmas 3.1–3.6. Next, the same background is used in the proof of Lemma II establishing the Peierls bound. After that, Theorems 1 and 2 are deduced from the general PS theory.

Section 3.1 establishes some related definitions and known facts. In our own opinion, it is quite elementary although seems rather tedious. It should be an easier reading when one is familiar with the concept of the Delaunay triangulation. Cf. [11], Chapters 1–3.

3.1 Voronoi cells, C-triangles and saturated configurations.

A given D -admissible configuration $\phi \in \mathcal{A}(D)$ has a uniquely defined collection of *Voronoi cells* $\mathcal{V}(x, \phi)$ constructed for the occupied sites $x \in \phi$. If ϕ has no unbounded Voronoi cells then to each cell $\mathcal{V}(x, \phi)$ there is assigned a finite set of circles centered at the vertices of $\mathcal{V}(x, \phi)$ and passing through x . We call them *V-circles* in ϕ . Each $x \in \phi$ lies in at

least one of V-circles but no $x \in \phi$ falls inside a circle. The sites $y \in \phi$ lying in a given V-circle form the vertices of a *constituting polygon*. These polygons form a tessellation of \mathbb{R}^2 : they have disjoint interiors, and the union of their closures gives the entire plane. If a constituting polygon has ≥ 3 vertices, it can be divided (non-uniquely) into *constituting triangles* (in short: C-triangles); this produces the Delaunay triangulation of ϕ (and of \mathbb{R}^2).

A D -AC ϕ is called *saturated* if no occupied site can be added to it without breaking admissibility. A *saturation* of a given D -AC ϕ is a completion of ϕ (in some uniquely defined way) with the maximal possible amount of added occupied sites.

Clearly, every PGS configuration is saturated. Saturated configurations are convenient as a natural initial step in a procedure of ‘identifying’ PGSs within the set $\mathcal{A}(D)$ of admissible configurations. The use of saturated configurations also makes more transparent the derivation of the Peierls bound in Section 3.3.

The idea of a saturated configuration worked well in the study of dense-packed circle configurations in \mathbb{R}^2 ; cf. [7]. We attempt to emulate a similar approach in \mathbb{Z}^2 . It generates some technical complications but we manage to get through, via Lemmas 3.1–3.5.

Lemma 3.1. *A saturated configuration does not have V-circles of radius $\geq D + \sqrt{2}/2$.*

Proof. Suppose there exists a V-circle of radius $\geq D + \sqrt{2}/2$. The center of the V-circle may not lie in \mathbb{Z}^2 but is at distance $\leq \sqrt{2}/2$ from one of the \mathbb{Z}^2 -sites. Then an additional particle can be added at this site without breaking admissibility. This contradicts the saturation assumption. ■

We would like to note a difference between Lemma 3.1 and Lemma 2 from [7]. We have a lower bound $D + \sqrt{2}/2$ whereas in [7], Lemma 2, one has D . This creates a specific technical complication arising in \mathbb{Z}^2 compared with \mathbb{R}^2 .

Lemma 3.2. *Let Δ be a C-triangle in an D -AC ϕ and consider 3 pair-wise disjoint disks of radius $D/2$ centered at the vertices of Δ . Consider 3 sectors in these disks which are intersections of the disks with the angles of Δ and let $\mathbb{S}(\Delta)$ denote the union of these sectors. Then the area of $\mathbb{S}(\Delta)$, i.e., the sum of the areas of these 3 sectors, equals $\pi D^2/8$.*

Proof. To avoid confusion we stress that $\mathbb{S}(\Delta)$ not necessarily fits completely inside the corresponding Δ . Nevertheless, the collection of sets $\mathbb{S}(\Delta)$ where Δ runs over C-triangles of ϕ forms a partition of the union of the disks $\bigcup_{x \in \phi} \mathbb{D}(x, D/2)$ (modulo a set of measure 0). Here $\mathbb{D}(u, r)$ stands for the disk of radius $r > 0$ centered at $u \in \mathbb{R}^2$: $\mathbb{D}(u, r) = \{y \in \mathbb{R}^2 : \rho(u, y) \leq r\}$.

For each angle of size α in Δ the intersection with the corresponding disk is a full sector with the angular measure α and area $\alpha D^2/8$. The sum of the triangle angles is π . ■

Lemma 3.3. *The value $S(D)/2$ gives the minimal area for the lattice triangles in problem (2.1) with angles $\alpha_i \leq 2\pi/3$ instead of $\alpha_i \leq \pi/2$.*

Proof. Consider a lattice triangle Δ with an angle α and the opposite side a , where $\pi/2 < \alpha \leq 2\pi/3$. The union of Δ with its central-symmetric counterpart relative to the middle of a is a lattice parallelogram whose longer diagonal is a . As $\alpha \leq 2\pi/3$, then the

shorter diagonal b has length $\geq D$. Then b divides the parallelogram into two congruent non-obtuse admissible triangles Δ' , Δ'' . The area of the parallelogram is twice the area of Δ' as well as twice the area of Δ . By construction, it is $\geq S(D)$. ■

Note that if the circumradius about a C-triangle Δ is $\leq D$ (which is the case for continuous dense-packing) then all angles of this triangle are $\leq 2\pi/3$ and the maximal side-length is $\leq D\sqrt{3}$. Consequently, Lemma 3.3 is applicable: the area of Δ is $\geq S(D)/2$. However, due to Lemma 3.1, when working with saturated D -ACs, we need to deal with C-triangles where the circumradius is between D and $D + \sqrt{2}/2$ which may lead to the maximal side-length $> D\sqrt{3}$. Such a C-triangle can have area $< S(D)/2$. However, it turns out that in this case there will be an adjacent C-triangle (sharing a side) with a rather large area, so that the area of their union is $\geq S(D) + 1$. It may also happen that two or three C-triangles, of area $< S(D)/2$ each, share a common adjacent triangle; in this case there will again be a lower bound upon the area of their union. Such an observation allows us to circumspect these issues; cf. Lemmas 3.4.1–3.4.5. The culmination is Lemma 3.4.5: it asserts that triangles with obtuse angles $> 2\pi/3$ could be circumvented with the help of adjacent triangles of a large area.

Lemma 3.4.1. *Suppose that a C-triangle Δ has the circumradius $r = D + \delta$ where $0 \leq \delta \leq \sqrt{2}/2$. Then the minimal area of Δ is $> \frac{\sqrt{3}D^2}{4} - \frac{D\delta}{2\sqrt{3}}$. Also the longest side in the min-area triangle has length $< D\sqrt{3} + \frac{\delta}{\sqrt{3}}$.*

Proof. Suppose a C-triangle Δ with vertices A, B, C satisfies the assumptions of the lemma. Let the side-lengths be $AB = l_0$, $BC = l_1$, $CA = l_2$, with $D \leq l_0 \leq l_1 \leq l_2 \leq 2r$. If two side-lengths are $> D$, say $l_1, l_2 > D$, then the area of the Δ can be made smaller by moving vertex C along the circumcircle towards B , until the length of side BC becomes D . Indeed, in the process of motion l_0 remains fixed but the height from C to AB shortens. (The resulting triangle does not necessarily fit \mathbb{Z}^2 .) Thus, the area of Δ is lower-bounded by the area of the triangle with two side-lengths D and the third side-length $2D\sqrt{1 - \frac{D^2}{4r^2}}$. A direct calculation shows that for $D \geq 1$ and $\delta \in [0, \sqrt{2}/2)$ the bound $2D\sqrt{1 - \frac{D^2}{4r^2}} < D\sqrt{3} + \frac{\delta}{\sqrt{3}}$ holds true. (The right-hand side is simply the Taylor expansion in δ up to order 1.) The area of such a triangle equals $\frac{D^3}{2r}\sqrt{1 - \frac{D^2}{4r^2}}$. As above, we have the bound $\frac{D^3}{2r}\sqrt{1 - \frac{D^2}{4r^2}} > \frac{\sqrt{3}D^2}{4} - \frac{D\delta}{2\sqrt{3}}$. ■

Lemma 3.4.2. *Suppose that a C-triangle Δ with side-lengths l_0, l_1, l_2 has the circumradius $r = D + \delta$ where $0 \leq \delta \leq \sqrt{2}/2$. Consider the adjacent C-triangle Δ' that shares with Δ the longest side (of length l_2). Then the area of the union $\Delta \cup \Delta'$ is lower-bounded by the area of a trapeze inscribed in a circle of radius r , with three sides being of length D . Furthermore, the area of $\Delta \cup \Delta'$ is $\geq \frac{3\sqrt{3}D^2}{4} - \sqrt{3}\delta^2$.*

Proof. Again, we write $D \leq l_0 \leq l_1 \leq l_2 \leq 2r$. Two vertices of triangle Δ' are the end-points of the side of length l_2 and lie in the V-circle of radius r circumscribing Δ . The third vertex of Δ' cannot lie inside this V-circle but can be placed on the circle. It also should lie outside the circles of radius D centered at the end-points of the side of length l_2 . Under these restrictions, the minimal area of Δ' is no less than the area of a triangle inscribed in the V-circle which shares the side of length l_2 with Δ and has the other side of length D . (Cf. the proof of Lemma 3.4.1.) If we now minimize the area of Δ , we arrive at the pair Δ, Δ' forming a trapeze, as specified in the assertion of Lemma 3.4.2. (Again, the resulting triangle may not fit \mathbb{Z}^2 .)

The area of the trapeze in question equals

$$\frac{2D^3}{r} \left(\sqrt{1 - \frac{D^2}{4r^2}} \right)^3 = \frac{3\sqrt{3}D^2}{4} - \sqrt{3}\delta^2 + \frac{19\delta^3}{3\sqrt{3}D} - \frac{113\delta^4}{9\sqrt{3}D^2} + \dots$$

A tedious (but straightforward) calculation asserts that for $D \geq 1$ and $0 \leq \delta \leq \sqrt{2}/2$ this expression is $\geq \frac{3\sqrt{3}D^2}{4} - \sqrt{3}\delta^2$, as claimed in the lemma. ■

Lemma 3.4.3. *Suppose that a C-triangle Δ has the circumradius $r = D + \delta$ where $0 \leq \delta \leq \sqrt{2}/2$. Let Δ' be the adjacent C-triangle sharing the longest side with Δ (cf. Lemma 3.4.2).*

- (i) *Suppose that Δ' is adjacent to another C-triangle, Δ_1 , with circumradius $r_1 = D + \delta_1$ where $0 \leq \delta_1 \leq \sqrt{2}/2$. Then the area of Δ' is $\geq D^2\sqrt{11}/4$.*
- (ii) *Further, suppose Δ' is adjacent to other two C-triangles, Δ_1 and Δ_2 , with circumradii $r_1 = D + \delta_1$ and $r_2 = D + \delta_2$ where $0 \leq \delta_1, \delta_2 \leq \sqrt{2}/2$. Then the area of Δ' is $\geq D^23\sqrt{3}/4$.*

Proof. (i) Here the triangle Δ' has one side-length $\geq D$ and two others $\geq D\sqrt{3}$. (Because in each of its neighboring triangles, Δ and Δ_1 , the angles opposite to the shared sides are $> 2\pi/3$ by construction). The area of such a triangle is, clearly, $\geq D^2\sqrt{11}/4$.

(ii) In this case all side-lengths of Δ' are $\geq D\sqrt{3}$. Hence, the area is $\geq D^23\sqrt{3}/4$. ■

Lemma 3.4.4. *The minimal area $S(D)$ in problem (2.1) satisfies*

$$\frac{\sqrt{3}D^2}{2} < S(D) < \frac{\sqrt{3}D^2}{2} + \sqrt{2}D. \quad (3.1)$$

Consequently, for $D^2 \geq 19$, the following holds true. In the situation of Lemma 3.4.2 we have:

$$\frac{3\sqrt{3}D^2}{4} - \sqrt{3}\delta^2 \geq S(D) + 1.$$

Next, in case (i) of Lemma 3.4.3,

$$\frac{\sqrt{3}D^2}{4} - \frac{D\delta}{2\sqrt{3}} + D^2\sqrt{11}/4 \geq 3(S(D) + 1)/2.$$

Finally, in case (ii) of Lemma 3.4.3,

$$\frac{\sqrt{3}D^2}{4} - \frac{D\delta}{2\sqrt{3}} + 3\sqrt{3}D^2/4 \geq 4(S(D) + 1)/2.$$

Proof. First, let us prove the two-sided bound (3.1). Consider a bisector of the line segment connecting two lattice sites at distance D from each other. On this bisector take a point at distance $D\sqrt{3}/2$ from the segment. Consider an angle of measure $2\pi/3$ originating from this point satisfying the following conditions: the angle is symmetric with respect to the bisector and the angle does not contain original two sites at distance D from each other. Such an angle is uniquely defined and any lattice site inside it is at distance larger than D from both original sites.

The selected point at distance $D\frac{\sqrt{3}}{2}$ from the segment belongs to some unit square from the base lattice. Our angle of measure $2\pi/3$ contains at least one \mathbb{Z}^2 -point at distance at most $D\frac{\sqrt{3}}{2} + \sqrt{2}$ from the line connecting the two original sites. Taking this vertex and the two original sites we obtain the triangle with the double area smaller than $\frac{\sqrt{3}D^2}{2} + \sqrt{2}D$. The lower bound for $S(D)$ is obvious.

Now, in the situation of Lemma 3.4.2, we want to have

$$\frac{D^2}{4}3\sqrt{3} - \sqrt{3}\delta^2 \geq S(D) + 1.$$

This follows from

$$\frac{D^2}{4}3\sqrt{3} - \frac{\sqrt{3}}{2} \geq \frac{D^2}{2}\sqrt{3} + D\sqrt{2} + 1, \quad \text{i.e.,} \quad \frac{D^2}{4}\sqrt{3} \geq D\sqrt{2} + 1 + \frac{\sqrt{3}}{2},$$

which is true for $D \geq 4.3$, i.e. $D^2 \geq 19$.

In the situation of Lemma 3.4.3(i) and Lemma 3.4.3(ii) the argument follows the same line. ■

Lemma 3.4.5. *For all attainable values of D the following holds true. In the situation of Lemma 3.4.2 we have:*

$$\text{area}(\Delta \cup \Delta') \geq 2(S(D) + 1)/2.$$

Next, in case (i) of Lemma 3.4.3,

$$\text{area}(\Delta \cup \Delta' \cup \Delta_1) \geq 3(S(D) + 1)/2.$$

Finally, in case (ii) of Lemma 3.4.3,

$$\text{area}(\Delta \cup \Delta' \cup \Delta_1 \cup \Delta_2) \geq 4(S(D) + 1)/2.$$

Also, for each of the aforementioned triangle groups $\{\Delta, \Delta'\}$, $\{\Delta, \Delta', \Delta_1\}$ and $\{\Delta, \Delta', \Delta_1, \Delta_2\}$, consider the union of the disks of radius $D/2$ centered at the vertices of the group. Then the intersection of this union, respectively, with $\Delta \cup \Delta'$, $\Delta \cup \Delta' \cup \Delta_1$ and $\Delta \cup \Delta' \cup \Delta_1 \cup \Delta_2$ has the area $k\pi D^2/8$ where k is the number of triangles in the group.

Proof. For $D^2 \geq 19$ the assertion follows from Lemmas 3.4.2–3.4.4. For $1 \leq D^2 \leq 18$ the proof is done by a direct enumeration of obtuse lattice triangles with the longest side of length $< D\sqrt{3} + \sqrt{1/6}$. The latter value emerges from the bound $2D\sqrt{1 - \frac{D^2}{4r^2}} < D\sqrt{3} + 1/\sqrt{6}$; cf. Lemma 3.4.1. The last assertion of Lemma 3.4.5 is straightforward; cf. the proof of Lemma 3.2. \blacksquare

Lemma 3.4.5 allows us to introduce a *re-distributed area* assigned to a C-triangle which can be conveniently lower-bounded. Namely, for a C-triangle not mentioned in Lemma 3.4.5, the re-distributed area coincides with its proper area. Next, if a triangle falls into one of the groups mentioned in Lemma 3.4.5 (as Δ , Δ' , Δ_1 or Δ_2) then its re-distributed area is set to be the total area of the group ($\Delta \cup \Delta'$, $\Delta \cup \Delta' \cup \Delta_1$ or $\Delta \cup \Delta' \cup \Delta_1 \cup \Delta_2$) divided by the number of the members in the group. According to Lemma 3.4.5, the redistributed area of a triangle will be $> (S(D) + 1)/2$.

3.2 Maximum-density configurations. Proof of Lemma I.

A D -admissible configuration containing only C-triangles of area $S(D)/2$ (i.e., only M-triangles) is called *perfect*. Clearly, a perfect configuration is saturated. An example of a perfect configuration is a max-dense sub-lattice.

In general, we define the *density* of a D -AC ϕ as

$$\limsup_{L \rightarrow \infty} \frac{\sharp(L, \phi)}{L^2}. \quad (3.2)$$

Here $\sharp(L, \phi)$ denotes the amount of occupied sites $x \in \phi$ lying in $\mathbb{Q}_L(0, 0)$. In turn, $\mathbb{Q}_L(m, n) \subset \mathbb{R}^2$, $m, n, L \in \mathbb{Z}$, $L \geq 1$, stands for the square of an integer odd side-length $\tilde{L} = L + 1 - (L \bmod 2)$, centered at site $(m, n) \in \mathbb{Z}^2$:

$$\mathbb{Q}_L(m, n) = \begin{cases} (m - \frac{L}{2}, m + \frac{L}{2}) \times (n - \frac{L}{2}, n + \frac{L}{2}), & L \text{ odd,} \\ (m - \frac{L+1}{2}, m + \frac{L+1}{2}) \times (n - \frac{L+1}{2}, n + \frac{L+1}{2}), & L \text{ even.} \end{cases} \quad (3.3)$$

The intersection of $\mathbb{Q}_L(m, n) \cap \mathbb{Z}^2$ (with L^2 lattice sites) is also denoted by $\mathbb{Q}_L(m, n)$; the specific context determines the meaning of this notation in the sequel.

Lemma 3.5. *The maximal possible density of a D -AC is $1/S(D)$. This density is attained on any perfect configuration, in particular, on any max-dense sub-lattice.*

Proof. (See [7].) The density of any non-saturated admissible configuration is not larger than the density of its saturation. Therefore, it is enough to analyze the densities of saturated configurations.

To calculate $\sharp(L, \phi)$ for saturated $\phi \in \mathcal{A}$ we need to count all occupied sites in ϕ which belong to $\mathbb{Q}_L(0, 0)$. If $A_D(L, \phi)$ denotes the total area of disks of diameter D centered at these occupied sites then $A_D(L, \phi) = \sharp(L, \phi)\pi D^2/4$.

Consider the total area $A_T(L, \phi)$ of all C-triangles such that the triangle itself or a member of its group determined in Lemma 3.4.5 has a vertex at an occupied point inside $\mathbb{Q}_L(0, 0)$. Then $A_T(L, \phi) = L^2 + E_1(L, \phi)$, where $E_1(L, \phi) = O(L)$ (recall that

the configuration ϕ is saturated and apply Lemma 3.1). The total area $E_2(L, \phi)$ of the intersection of all these triangles with the disks of diameter D centered at triangle vertices located outside of $\mathbb{Q}_L(0, 0)$ is also a quantity of order $O(L)$.

Thus,

$$\frac{\#(L, \phi)\pi D^2/4}{L^2} = \frac{A_D(L, \phi)}{A_T(L, \phi) - E_1(L, \phi)} = \frac{A_D(L, \phi) + E_2(L, \phi)}{A_T(L, \phi)} + O(1/L).$$

According to Lemma 3.2, 3.3 and 3.4.5, the ratio $\frac{A_D(L, \phi) + E_2(L, \phi)}{A_T(L, \phi)}$ is not larger than $\frac{\pi D^2/4}{S(D)}$ and equals $\frac{\pi D^2/4}{S(D)}$ for any perfect configuration. ■

Observe that PGS φ is uniquely mapped into a configuration in a torus $\mathbb{T}_{kS(D)}$ of size $kS(D) \times kS(D)$ with an integer $k = k(\varphi)$. Here an $L \times L$ torus \mathbb{T}_L is understood as square $\mathbb{Q}_L(0, 0)$ (cf. (3.3)) with the identified opposite sides and with the toroidal Euclidean metric ρ_L^T :

$$\rho_L^T(x, y) = \min \left\{ \rho(x, y), \rho(x, y \pm v_i), i = 1, 2 \right\}, \quad x, y \in \mathbb{Q}_L(0, 0). \quad (3.4)$$

Here vectors $v_1 = (\tilde{L}, 0)$ and $v_2 = (0, \tilde{L})$ where, as before, $\tilde{L} = L + 1 - (L \bmod 2)$.

The image configuration in torus $\mathbb{T}_{kS(D)}$ has a maximal possible amount of occupied sites. Note that the opposite implication is not true. A configuration which for some integer N has the maximal possible amount of occupied sites inside \mathbb{T}_N does not necessarily generate a PGS unless N^2 is divisible by $S(D)$.

Lemma 3.6. *For any attainable D , all PGSs are perfect configurations.*

Proof. For a PGS φ the density is a lim rather than a lim sup. This value must equal $1/S(D)$ as in the opposite case one can gain more occupied points by replacing the part of φ in a sufficiently large square with the part of a max-dense sub-lattice generated by M-triangles in a square of the same size.

Clearly, a PGS φ maps into the corresponding D -AC inside torus $\mathbb{T}_{k(\varphi)S(D)}$. If inside this torus there is at least one non- D -optimal triangle then the total number of occupied sites inside the torus is at most $\frac{k(\varphi)^2 S(D)^2}{S(D)} - 1$; consequently, the density is $< 1/S(D)$. ■

Proof of Lemma I. Lemma 3.6 implies assertion (i) in Lemma I. To deduce assertion (ii), observe that, in absence of sliding, any two M-triangles sharing a common side are centrally symmetric relative to the mid-point of the shared side. Thus, for any non-sliding D and any M-triangle Δ with a vertex at the origin, the corresponding min-area sub-lattice is the only possible perfect configuration containing Δ . The \mathbb{Z}^2 -congruences produce, from any max-dense sub-lattice, 1 or 3 additional sub-lattices, depending on whether Δ is isosceles or not. ■

We would like to note that here and below the absence of sliding is used in a particular manner (specified in the proof of Lemma 3.6): it implies that if in an D -AC ϕ there are two adjacent M-triangles sharing a common side then they are centrally symmetric.

3.3 The Peierls bound.

As was said, an application of the PS theory needs a Peierls bound. We again begin with some auxiliary notions and statements. From now on we assume that the value of D is non-sliding.

Lemma 3.7. *Consider a max-dense sub-lattice φ . Then for any $k \in \mathbb{N}$ and any lattice site $(m, n) \in \mathbb{Z}^2$, the square $\mathbb{Q}_{kS(D)}(m, n)$ contains $k^2 S(D)$ occupied sites from φ .*

Proof. The restriction of φ to $\mathbb{Q}_{kS(D)}(m, n)$ actually is a D -AC lying inside the corresponding torus $\mathbb{T}_{kS(D)}$. This torus is partitioned into $k^2 S(D)$ fundamental parallelograms of the sub-lattice. ■

Given an attainable D and a site $(m, n) \in \mathbb{Z}^2$, the $S(D) \times S(D)$ square $\mathbb{Q}_{S(D)}(mS(D), nS(D))$ (see (3.3)) is called a *template*. Given a D -AC $\phi \in \mathcal{A}(D)$ and PGS $\varphi \in \mathcal{P}(D)$, a template $\mathbb{Q}_{S(D)}(mS(D), nS(D))$ is said to be φ -correct in ϕ if φ and ϕ coincide inside $\mathbb{Q}_{3S(D)}(mS(D), nS(D))$. A template is called *incorrect* (in ϕ) if it is not φ -correct for some $\varphi \in \mathcal{P}(D)$.

A *contour* in a D -admissible configuration ϕ is a connected component Γ of incorrect templates in ϕ , where the connectedness is understood in the \mathbb{R}^2 sense. Cf. [42]. In particular, a contour has an exterior, $\text{Ext } \Gamma$, and an interior, $\text{Int } \Gamma$, which can be further divided into components $\text{Int}_\varphi(\Gamma)$.

Contour-related pictures are featured in Figures 7–9.

Let ϕ^* be a saturation of a given D -AC ϕ . If an added occupied site $x \in \phi^* \setminus \phi$ lies in a template then, clearly, this template is incorrect (more precisely, non- φ -correct in φ for each $\varphi \in \mathcal{P}$). We say that such a template is an *s-defect* (in ϕ). Another possibility for a defect is where, in the saturation ϕ^* , a template has a non-empty intersection with one of C-triangles that is not an M-triangle. We call it a *t-defect* (again in ϕ). Finally, an incorrect (but actually perfect) template can be simply a neighbor of an s- or a t-defect. We call it an *n-defect* (still in ϕ).

We would like to note that C-triangles with obtuse angles $> 2\pi/3$ (considered in Lemmas 3.4.1–3.4.5) lead to t-defects by definition.

Lemma 3.8. (A Peierls bound for defects.) *Consider a D -AC $\phi \in \mathcal{A}$ and assume that for configuration ϕ there exists a contour Γ containing m incorrect templates enclosed by n adjacent φ -correct templates (for the same or different values of φ). Additionally, assume that $m = i + j + k$ where i, j, k give the amount of s-, t- and n-defects, respectively. Then the amount of occupied sites inside Γ is at most*

$$(m + n)S(D) - i - \max\left(1, \frac{j}{8S(D)}\right). \quad (3.5)$$

Proof. As the contribution i given by s-defects is straightforward, we consider the saturation ϕ^* and its t-defects only. We confine the entire connected component of templates to a sufficiently large square $\mathbb{Q}_{kS(D)}(0, 0)$ by filling all additional $k^2 - m - n$ templates with the appropriate PGS. Here the appropriate means that for each added φ -correct template all neighboring templates (which by construction are correct) have the same value of φ . Afterwards we wrap $\mathbb{Q}_{kS(D)}(0, 0)$ into the $kS(D) \times kS(D)$ torus $\mathbb{T}_{kS(D)}$ and still obtain a D -admissible configuration in $\mathbb{T}_{kS(D)}$.

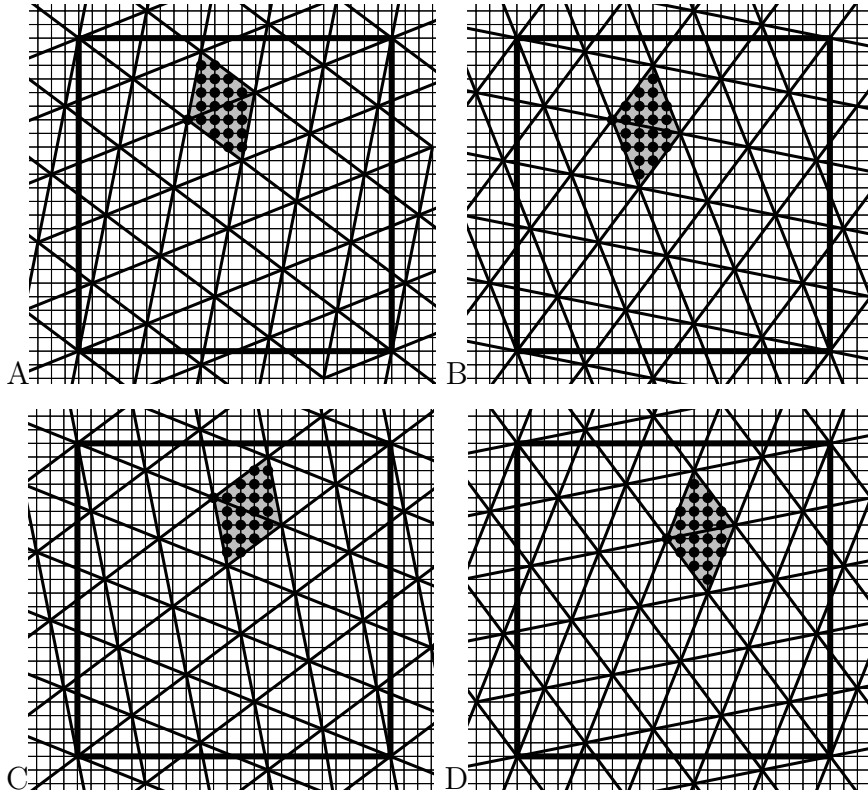


Figure 7: Templates (encircled with thick lines) and FPs (gray parallelograms) for $D^2 = 25$, with $S = 23$. Here each template (treated as a torus) has $23 \times 23 = 529$ lattice sites and 23 FPs, and each FP covers 23 lattice sites (represented by thick black dots). Since the FTs are not isosceles, there are 4 types of min-area sub-lattices and 92 PGSs.

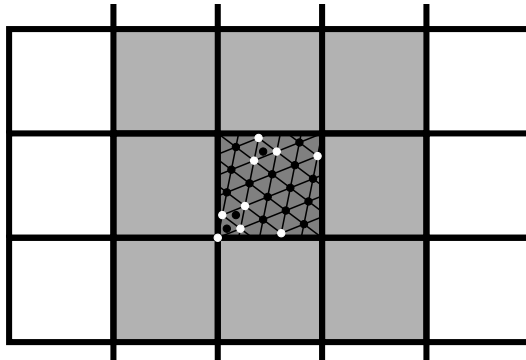


Figure 8: A snapshot of templates for $D^2 = 25$ with $S(D) = 23$. All squares are 23×23 and represent templates for this value of D . The white squares indicate φ -correct templates in a given D -AC ϕ while gray and light-gray squares indicate non- φ -correct ones. The original lattice \mathbb{Z}^2 is not shown due to its small scale. The PGS φ is represented by the mesh over the central (gray) square. The black dots indicate the occupied \mathbb{Z}^2 -sites over the central template square. The white dots indicate vacant sites in φ in the central square. All light-gray and white common squares indicated in the diagram are assumed to preserve the structure of the PGS φ unperturbed. However, the 8 light-gray templates around the central square are declared φ -non-correct by adjacency.

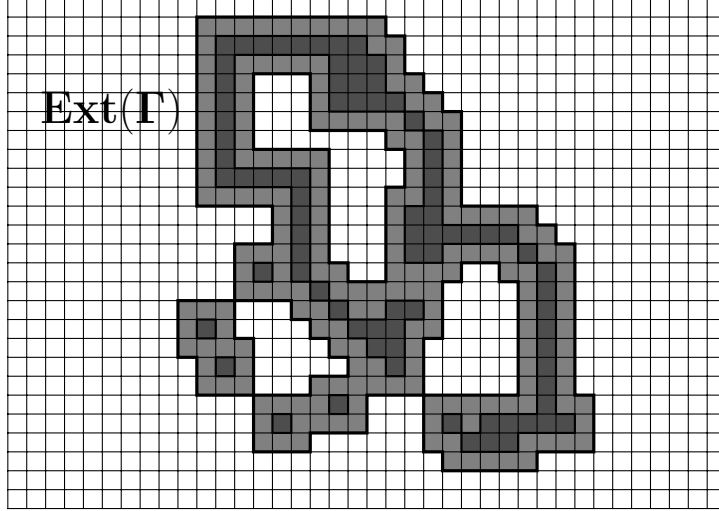


Figure 9: A contour support (the union of gray and dark gray common squares). Here the internal area $\text{Int}(\Gamma)$ includes three components $\text{Int}_{\varphi_i}(\Gamma)$, $i = 1, 2, 3$. The boundary layers are shown as the union of gray squares. For a φ -contour, the configuration over every white common square forming the external area $\text{Ext}(\Gamma)$ is supposed to be the restriction of φ .

Due to Lemma 3.2, for any saturated configuration in a torus the total amount of corresponding C-triangles inside this torus is twice the amount of the occupied sites in the configuration. In particular, the total amount of C-triangles is always even. Also the existence of at least one non- D -optimal C-triangle inside the torus reduces the maximal amount of occupied sites by at least one.

Observe that, according to Lemma 3.4.5, the re-distributed area of any C-triangle that is not an M-triangle is at least $(S(D) + \delta(D))/2$, where $\delta(D) \geq 1$. Further, a C-triangle that is not an M-triangle can be shared by at most 4 templates. Therefore, j templates with t-defects contain at least $j/4$ C-triangles that are not M-triangles. Thus, one half of the maximal possible amount of C-triangles inside $T_{kS(D)}$ is $k^2 S(D) - \max\left(1, \frac{j}{8S(D)}\right)$.

The term $(m + n)S(D)$ corresponds to the absence of defects and is calculated according to Lemma 3.6. ■

Informally, Lemma 3.8 states that the increment of ‘energy’ (i.e., decrease in the number of particles) caused by a deviation from a PGS is lower-bounded proportionally to the ‘size’ of the deviation. This is the gist of Peierls bounds used in the Pirogov–Sinai theory and its applications.

Lemma 3.9. *Let $\varphi', \varphi'' \in \mathcal{P}(D)$ be two distinct PGSs. Let Γ be a connected component of φ' -correct templates enclosed by a connected component of φ'' -correct templates. Then any extension of this restricted configuration to a D -AC $\phi \in \mathcal{A}(D)$ in \mathbb{Z}^2 contains a closed chain of adjacent non-minimal C-triangles enclosing Γ .*

Proof. Due to the absence of sliding, M-triangles from different classes cannot share a side in a D -AC. ■

Lemma II. (A Peierls estimate for contours) *Consider a finite contour containing m incorrect templates. Then the amount of occupied sites inside this contour is at most*

$$mS(D) - \max\left(1, \frac{m}{72S(D)}\right). \quad (3.6)$$

Proof of Lemma II. The lemma is a direct consequence of Lemmas 3.8 and 3.9 with an additional factor $1/9$ accounting for the possibility for each s- or t-defect to be surrounded by 8 n-defects. ■

Lemma II completes the verification of assumptions of the PS theory for HC models in \mathbb{Z}^2 .

Remark 3.1. The Peierls bound for the HC model on \mathbb{A}_2 is considerably simpler and is stated in terms of Voronoi cells. ▲

3.4 The proof of Theorems 1, 2.

With Lemmas I, II at hand, the proof of Theorems 1, 2 is obtained by a direct application of the PS-theory. Cf. [42, 49, 14] and [44].

We refer the reader to [32] for the scheme of such an application.

4 Additional results. The issue of dominance

4.1 More on extreme Gibbs measures.

As an annex to Theorem 1, based on straightforward applications of the approach from [49], we offer three more statements in Theorem 3. Consider a sequence of $nS(D) \times nS(D)$ tori $\mathbb{T}^{(n)} = \mathbb{T}_{nS(D)}$. Let $\mathcal{A}(D, \mathbb{T}^{(n)})$ denote the set of D -admissible configurations in $\mathbb{T}^{(n)}$:

$$\mathcal{A}(D, \mathbb{T}^{(n)}) = \left\{ \psi : \mathbb{Q}_{2nS(D)}(0, 0) \rightarrow \{0, 1\}, \right. \\ \left. \psi(x)\psi(y) = 0 \quad \forall x, y \in \mathbb{Q}_{nS(D)}(0, 0) \quad \text{with} \quad \rho_{nS(D)}^{\mathbb{T}}(x, y) < D \right\}. \quad (4.1)$$

Let $\mu_n^{\text{per}} = \mu_{\mathbb{T}^{(n)}}$ denote the probability measure on $\mathcal{A}(D, \mathbb{T}^{(n)})$ with

$$\mu_{\mathbb{T}^{(n)}}(\psi) = \frac{u^{\sharp\psi}}{\mathbf{Z}(\mathbb{T}^{(n)})}, \quad \psi \in \mathcal{A}(D, \mathbb{T}^{(n)}), \quad (4.2)$$

where the partition function $\mathbf{Z}(\mathbb{T}^{(n)}) = \sum_{\psi \in \mathcal{A}(\mathbb{T}^{(n)})} u^{\sharp\psi}$. Then $\mu_{\mathbb{T}^{(n)}}$ can be treated as a measure on $\mathcal{A}(D, \mathbb{Z}^2)$ concentrated on $\mathcal{A}(D, \mathbb{T}^{(n)})$.

Theorem 4. *Under assumptions of Theorem 1 or Theorem 2, the following properties (i), (ii) are satisfied:*

- (i) *For every extreme measure $\mu_\varphi \in \mathcal{E}(D) \exists$ a set $\mathcal{J} = \mathcal{J}(\varphi) \subset \mathcal{A}(D)$ with $\varphi \in \mathcal{J}$ and $\mu_\varphi(\mathcal{J}) = 1$ such that the set of φ -incorrect templates in any $\phi \in \mathcal{J}$ has no connected components of infinite diameters in \mathbb{R}^2 . Consequently, (a) $\forall \phi \in \mathcal{J}$ the set of φ -correct templates in ϕ has an infinite connected component, and (b) φ is the only D -AC with this property.*

- (ii) Measures μ_φ have an exponential decay of spatial correlations: $\forall l > 1$, finite sets $\mathbb{V}_{1,2} \subset \mathbb{Z}^2$ with $\rho(\mathbb{V}_1, \mathbb{V}_2) \geq l$ and $\forall D$ -ACs $\psi^{(\mathbb{V}_i)} \in \mathcal{A}(D, \mathbb{V}_i)$, $i = 1, 2$,

$$|\mu_\varphi(\psi^{(\mathbb{V}_1)} \vee \psi^{(\mathbb{V}_2)}) - \mu_\varphi(\psi^{(\mathbb{V}_2)})\mu_\varphi(\psi^{(\mathbb{V}_1)})| \leq \exp(-Cl)\mu_\varphi(\psi^{(\mathbb{V}_2)})\mu_\varphi(\psi^{(\mathbb{V}_1)}) \quad (4.3)$$

Here $C = C(D) > 0$ is a constant and $\mu(\psi^{(\mathbb{V}_1)} \vee \psi^{(\mathbb{V}_2)})$ and $\mu(\psi^{(\mathbb{V}_i)})$ stand for the μ_φ -probabilities of the cylinder events that $\phi \upharpoonright_{\mathbb{V}_1 \cup \mathbb{V}_2} = \psi^{(\mathbb{V}_1)} \vee \psi^{(\mathbb{V}_2)}$ and $\phi \upharpoonright_{\mathbb{V}_i} = \psi^{(\mathbb{V}_i)}$, respectively.

Furthermore, assume that all extreme measures μ_φ are generated by PGSs φ belonging to a single equivalence class. (In particular, this covers the case of Theorem 1.) Then the following property is satisfied.

- (iii) The weak limit $\mu^{\text{per}} = \lim_{n \rightarrow \infty} \mu_{\mathbb{T}^{(n)}}$ exists and determines a probability measure on \mathcal{X} which is the averaged sum: $\mu^{\text{per}} = \frac{1}{\#\mathcal{E}(D)} \sum_{\mu_\varphi \in \mathcal{E}(D)} \mu_\varphi$. In particular, μ^{per} is shift-invariant.

Proof. Assertion (i) is a standard corollary of the Pirogov–Sinai theory [42, 44, 49, 6]: it implies that (1) the μ_φ -probability that a given site $x \in \mathbb{Z}^2$ is encircled by infinitely many contours equals 0 and (2) the μ_φ -probability that there is an infinite contour equals 0 as well.

(ii) This statement follows from standard polymer expansions for probabilities $\mu(\psi^{(\mathbb{V}_1)} \vee \psi^{(\mathbb{V}_2)})$ and $\mu(\psi^{(\mathbb{V}_i)})$; cf. [49]. The polymers are determined as collections of overlapping contours, and the statistical weight of a polymer decays exponentially with the polymer size.

(iii) Observe that, under the stated assumption, \forall PGSs $\varphi_1, \varphi_2 \in \mathcal{P}(D)$ such that $\mu_{\varphi_1}, \mu_{\varphi_2} \in \mathcal{E}(D)$, there exists a 1-1 map $\Phi_{\varphi_1, \varphi_2} : \mathbb{Z}^2 \rightarrow \mathbb{Z}^2$ (a \mathbb{Z}^2 -congruence) taking $\varphi_1 \rightarrow \varphi_2$ such that μ_{φ_1} is taken to μ_{φ_2} by the induced map $\mathcal{A}(D) \rightarrow \mathcal{A}(D)$. On the other hand, \forall PGSs $\varphi_1, \varphi_2 \in \mathcal{P}(D)$ as above, the measure $\mu_{\mathbb{T}^{(n)}}$ is invariant under the map induced by $\Phi_{\varphi_1, \varphi_2}$ restricted to $\mathbb{T}^{(n)}$. Hence, any limit point for the sequence $\mu_{\mathbb{T}^{(n)}}$ is a uniform mixture of measures μ_φ . Hence, the limiting measure μ^{per} is a uniform mixture, as claimed. \blacksquare

Remark 4.1. A more detailed analysis of dependence of Gibbs measures μ upon boundary conditions requires a deeper technical involvement and will be given elsewhere. The same can be said about a similar question on the HC model in \mathbb{A}_2 and \mathbb{H}_2 . Cf. [32]. \blacktriangle

4.2 A discussion of dominance.

This section contains some discussions and comments but no formally proven results. First, as was said earlier, we conjecture that, under the assumptions of Theorem 2, there is only one dominant class. The reason is that co-existence of several dominant classes requires countably many ‘balance identities’ of a number-theoretical nature, in each order of an emerging perturbation series. In other words, it would require some (rather strong) form of equivalence between contributions from local excitations of a given weight coming from two or more distinct classes. It seems unlikely since the definition of

an equivalence PGS class probably captures all involved forms of symmetry in the hard-core model on \mathbb{Z}^2 . The identification of the dominant PGS class is an algorithmically finite procedure. According to [49], one needs to iteratively calculate truncated statistical weights of contours and the corresponding approximations to the free energies of the emerging truncated contour models. The procedure stops as soon as it detects a single class having the lowest free energy. The amount of calculations required by the direct approach is not accessible to modern computers. In cases where the above program was carried out to the end, one needed a number of tricks (both analytical and computational), as can be seen in [32].

As an illustration, we briefly discuss the cases $D^2 = 65$, $D^2 = 130$ and $D^2 = 324$: these are the lowest values of D from Class B. The algebraic nature of these values is commented upon in Section 6–8; here we focus on the structure of local excitations.

The numerical values presented below have been calculated by `CountTuples.java`.

For $D^2 = 65 = 8^2 + 1^2 = 7^2 + 4^2$, we have $S(D) = 60$. There are two minimizing triangle types. The corresponding side-length triples from (2.2) have $\ell_0^2 = \ell_1^2 = 65$, $\ell_2^2 = 80$ and $\ell_0^2 = \ell_1^2 = 68$, $\ell_2^2 = 72$. It is convenient to say that one type gives a [65|65|80]-triangle and the other a [68|68|72]-triangle. (This notation and terminology will be further elaborated in Sections 6, 7.) A [68|68|72]-triangle is also an M-triangle for a Class A value $D^2 = 68$ (cf. Table 3).

Both [65|65|80]- and [68|68|72]-types admit a single congruence class or a single implementation. (In Section 7.2 we speak of Class B1 in more general terms and provide details of a number-theoretical background.) For type [65|65|80], a representative is an M-triangle with vertices $\{(0, 0), (8, 4), (-1, 8)\}$, while for type [68|68|72] the vertices are $\{(0, 0), (8, 2), (2, 8)\}$. Recall, an M-triangle gives rise to a class of PGSs obtained as \mathbb{Z}^2 -shifts and reflections of the corresponding min-area sub-lattice.

As was said earlier, the dominance of a particular PGS class is established by comparing the number of local excitations for both minimizing types. (Actually, what we compare is the naturally emerging densities of excitations.) It is convenient to categorize the local excitations into ‘strains’ bearing a distinctive geometric character. The initial excitation strain is where we simply remove one particle from a PGS; this yields an excitation of (relative) weight u^{-1} . However, all PGSs are ‘equal in rights’ with respect to this strain of excitations as the particle density in all PGSs is the same. In other words, there is no discrimination between the PGSs in the perturbation order u^{-1} . A similar conclusion can be reached when one considers removing a pair of particles from a PGS which produces a strain of excitations of weight u^{-2} .

Next, we can remove three particles at vertices of a fundamental parallelogram Π in a max-dense sub-lattice and add one particle inside Π maintaining admissibility. We call this strain a single or 1-site insertion. This produces another strain of local excitations of weight u^{-2} (3 occupied sites removed, 1 added). Another strain of excitations of weight u^{-2} is a double or 2-site insertion where we add 2 particles in an FP Π and remove 4 occupied sites at the vertices of the Π . Next, we can attempt to add 3 particles and remove 5, then add 4 and remove 6, and so on. The PGSs must be compared by counting all strains of excitations per an FP; the ones with a larger total count will be dominant.

To complete the argument, we must check that there is no other possibilities to produce a local excitation of weight u^{-2} (which is the most difficult part) and prove that other strains of excitations (of higher weights) can be made ‘insignificant’ if u is large enough

(which is usually not a difficult part). Such a program has been carried through for a triangular lattice \mathbb{A}_2 in [32] with the help of an analytical construction and a computer-assisted argument. For the lattice \mathbb{Z}^2 it is a work in progress which will be published separately: here we only attempt to explain the place of the dominance argument in the whole study and comment on key points of the forthcoming argument.

The count of excitations of weight u^{-2} yields these results: there are 40 single insertions per an FP for both types. Next, there are 109 double insertions per an FP for type [65|65|80] and 126 for type [68|68|72]. Further, there are 104 triple insertions and no quadruple ones for type [65|65|80] whereas type [68|68|72] offers 140 triple insertions and 10. Finally, no insertions of 5 or more particles of weight u^{-2} exist for either type. The overall score is 253 for [65|65|80] and 316 for [68|68|72]. The tentative conclusion is that type [68|68|72], with an M-triangle with vertices $\{(0, 0), (8, 2), (2, 8)\}$, is dominant. Consequently, for u large enough, we expect that the number of the extreme Gibbs measures for $D^2 = 65$ is 120, and they all are generated by the PGSs coming from [68|68|72]-triangles. Cf. Figure 10.

Now, consider the value $D^2 = 130 = 11^2 + 3^2 = 9^2 + 7^2$, with $S(D) = 120$. Here we again have two minimizing types. They are represented by M-triangles with squared side-lengths (I) $\ell_0^2 = \ell_1^2 = 130$, $\ell_2^2 = 160$ and (II) $\ell_0^2 = \ell_1^2 = 136$, $\ell_2^2 = 144$, respectively, both isosceles. We again refer to them as [130|130|160]- and [136|136|144]-types or triangles. It turns out that a [136|136|144]-triangle also serves as the M-triangle for the value $D^2 = 136$, which is of Class A.

As above, both types admit a single implementation. For type [130|130|160], a representative is an M-triangle with vertices $\{(0, 0), (12, 4), (3, 11)\}$, while for type [136|136|144] the vertices are $\{(0, 0), (12, 0), (6, 10)\}$. In fact, it is easy to see that the picture of M-triangles (or min-area sub-lattices) for $D^2 = 130$ is obtained from that for $D^2 = 65$ by applying the linear transformation $\mathbf{T} : \mathbb{Z}^2 \rightarrow \mathbb{Z}^2$ effectuated by the matrix $\mathbf{T} = \begin{pmatrix} 1 & -1 \\ 1 & 1 \end{pmatrix}$ of determinant 2. In other words, the case $D^2 = 130$ is obtained from $D^2 = 65$ by scaling the side-length by a factor $\sqrt{2}$ and rotating by $\pm\pi/4$. However, it does not guarantee that all excitations are mapped to each other; in fact we will see that it is not the case, although type [136|136|144] again will look dominant.

Indeed, type [130|130|160] generates 72 single insertions, 303 double insertions, 284 triple insertions and no quadruple insertions per an FP, 659 in total. Further, for type [136|136|144], the corresponding numbers are 72, 356, 532 and 50, all-in-all 1010. As above, none of the types produces admissible insertions PGS of 5 or more particles of weight u^{-2} . Then, for u large enough, the number of the EGMs is 240, and they are generated by the PGSs of type [136|136|144]. Cf. Figure 11.

The next case is $D^2 = 324$, with $S = 288$. In Section 6 we show that this case gives rise to an infinite sequence of values of D^2 of Class B1. Here we have two minimizing types, [324|337|337] (isosceles), and [325|333|340] (non-isosceles). For congruence class representatives, one can take M-triangles with vertices $\{(0, 0), (18, 0), (9, 16)\}$ for type [324|337|337] and $\{(0, 0), (18, 3), (6, 17)\}$ for [325|333|340]. Here [325|333|340]-triangles give rise to 1152 PGSs, twice as much as [324|337|337]-ones. Cf. Figure 12. The total count of excitations of weight u^{-2} yields 3797 per an FP for type [324|337|337] and 2684 for [325|333|340]. As a result, [324|337|337]-triangles are expected to win, and the number of EGMs for u large will be 576, all of them being generated by the respective PGSs.

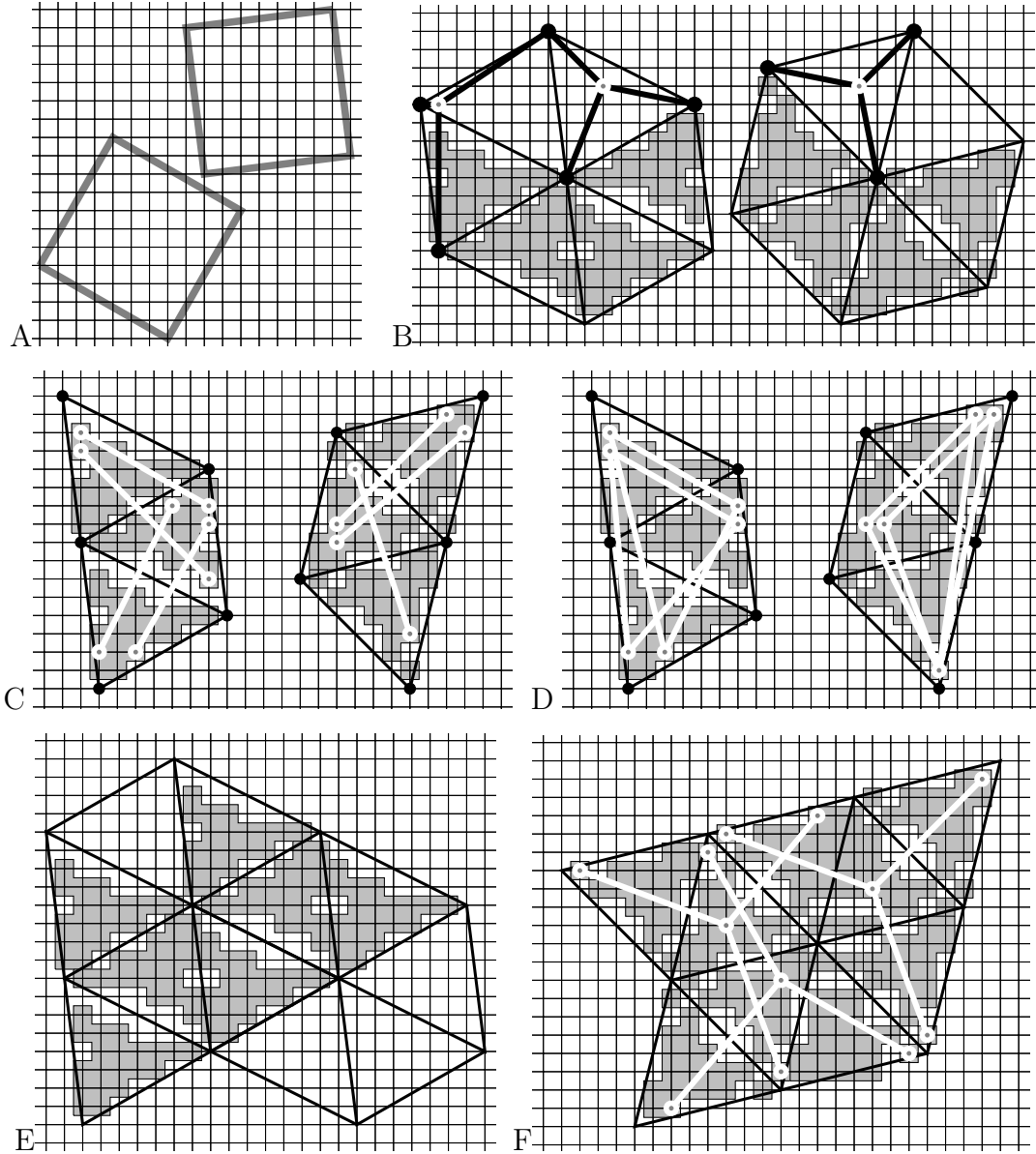


Figure 10: Excitation counts for $D^2 = 65$, with $S = 60$. The crucial excitations are those of weight u^{-2} . Frame A shows the 65×65 squares, for $65 = 8^2 + 1^2$ and $65 = 7^2 + 4^2$. In frame B we show the M-triangles of type $[65|65|80]$ (left) and $[68|68|72]$ (right) and their FPs. The gray regions indicate the single-insertion positions repelling 3 sites in a PGS (black circles); the white marks and black segments outline examples of such excitations. The total number of single insertions per an FP equals 40 for both types. Frame C shows double insertions (pairs of white marks connected with white lines) repelling 4 sites (the vertices of an FP). The total number of double insertions per an FP equals 109 and 126 for types $[65|65|80]$ and $[68|68|72]$, respectively. Frame D shows triple insertions (white marks and triangles) repelling 5 sites (the vertices of 3 adjacent M-triangles forming a trapezoid). The total number of triple insertions per an FP equals 104 for type $[65|65|80]$ and 140 for $[68|68|72]$. In frames E,F we attempt at quadruple insertions repelling 6 sites (they should be the vertices of 6 adjacent M-triangles forming a triangle of a double size). Their number of such insertions is 0 and 10 per an FP, respectively. In both cases there is no u^{-2} -excitations with 5 or more insertions. Total total of excitations of weight u^{-2} amounts to 253 for $[65|65|80]$ and 316 for $[68|68|72]$; the latter is expected to be the dominant one. So, for $D^2 = 65$ the number of extreme Gibbs measures for $u \geq u_*$ equals 120, and they are generated by min-area sub-lattices of type $[68|68|72]$.

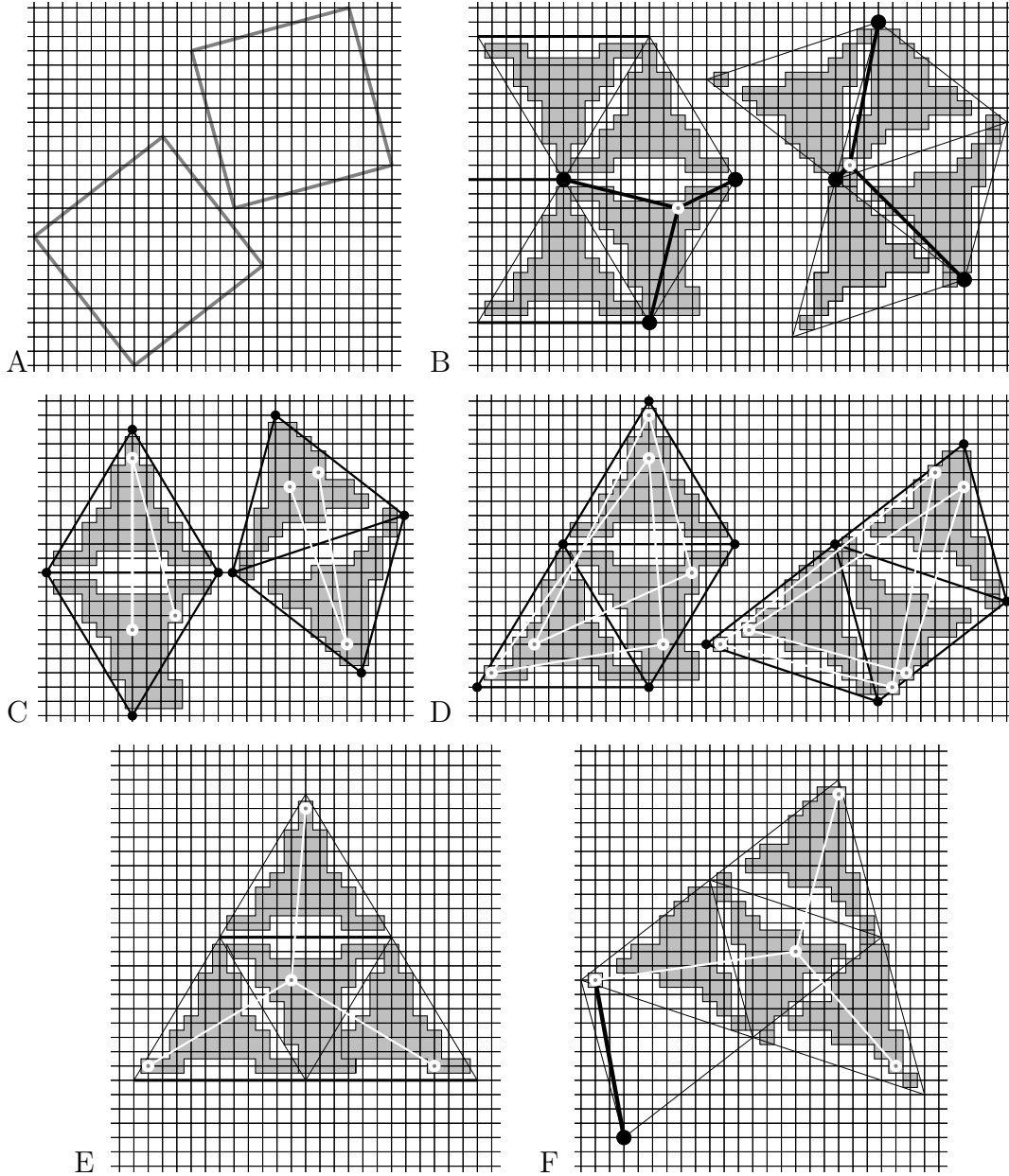


Figure 11: Excitation counts for $D^2 = 130$, with $S = 120$. As before, we look for excitations of weight u^{-2} . Frame A shows the 130×130 squares, for $130 = 11^2 + 3^2$ and $130 = 9^2 + 7^2$. In frame B we show the M-triangles $[136|136|144]$ (left) and $[130|130|160]$ (right) and their fundamental parallelograms; we also display 1-site insertions. Here again, the gray regions indicate the single-site insertions excluding 3 vertices in a PGS; the white marks and black lines show examples of such excitations. The total number of single insertions in an FP equals 72 for both type. Frame C shows double insertions (pairs of white marks connected with lines) repelling 4 sites (as above, – vertices of an FP). The total number of double insertions within an FP equals 356 and 303 for $[136|136|144]$ - and $[130|130|160]$ -types, respectively. Frame D shows triple insertions (white marks forming triangles) which repel 5 sites placed on a trapezium. The total number of such excitations per an FP equals 532 and 284, respectively. On frames E,F we comment on quadruple insertions that repel 6 vertices; their numbers are 50 per an FP and 0, respectively. Indeed, an attempt to construct a 4-site excitation in a $[130|130|160]$ -type PGS in frame F leads to a repulsion of 7 vertices, hence to the weight u^{-3} . As with $D^2 = 65$, neither type for $D^2 = 130$ yields an admissible u^{-2} -excitation with ≥ 5 insertions. The overall count of u^{-2} -excitations per an FP yields 1010 for type $[136|136|144]$ and 659 for $[130|130|160]$. Consequently, type I is dominant, and, for $u \geq u_*$, the number of extreme Gibbs measures for $D^2 = 130$ equals 240, and they are generated by the generated by the min-area sub-lattice of type $[136|136|144]$.

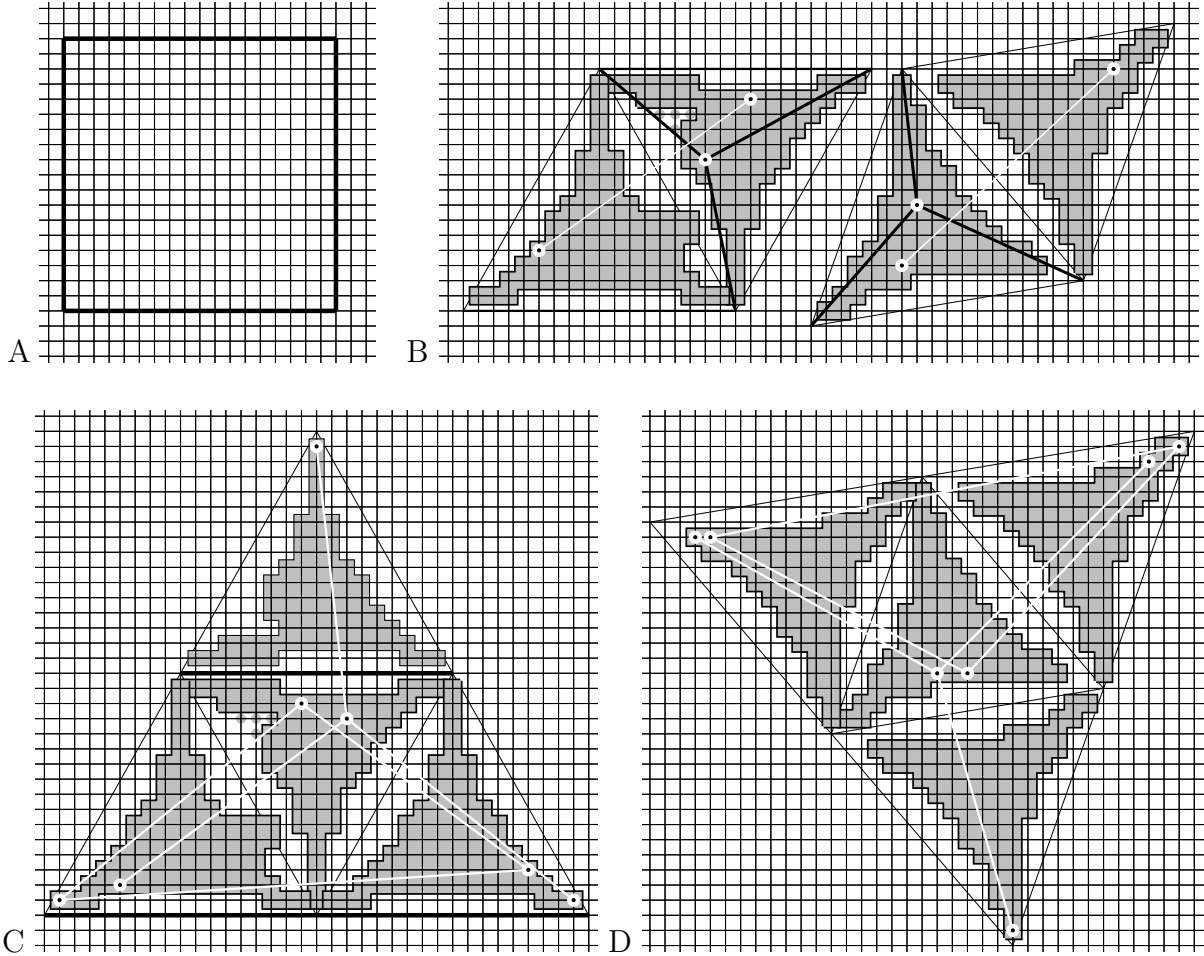


Figure 12: Excitation count, of weight u^{-2} , for $D^2 = 324 = 18^2$, with $S = 288$. Frame A shows a 324×324 square. Frame B indicates M-triangles $[324|337|337]$ (left, isosceles) and $[325|333|340]$ (right, non-isosceles). The gray areas again indicate the sites in an M-triangle which repel 3 vertices: examples are highlighted with thick black lines. The total number of 1-site insertions within an FP equals 144 for both types. Next, the white lines indicate double-insertions repelling four vertices of an FP; their numbers are 393 for $[324|337|337]$ and 408 for $[325|333|340]$. In frame C we show 3- and 4-site insertions for the type $[324|337|337]$ sub-lattice. There are 2510 triple and 750 quadruple insertions per an FP. Frame D addresses the similar issues for type $[325|333|340]$. Here we have 1982 triple and 150 quadruple insertions per an FP. As in the previous cases, there are no excitations of weight u^{-2} with at least five insertions. As a result, the total number of u^{-2} -excitations in a PGS equals 3797 for $[324|337|337]$ and 2684 for $[325|333|340]$. Consequently, the isosceles type is dominant. For $u \geq u_*$, the number of the extreme Gibbs measures for $D^2 = 324$ equals 576, and they are generated by a type $[324|337|337]$ min-area sub-lattice.

5 Minimal triangles and norm equations in $\mathbb{Z}[\sqrt[6]{-1}]$

In Sections 5 and 6 we focus upon number-theoretical aspects of the present work. To start with, in Section 5.1 we identify \mathbb{Z}^2 -triangles with the elements of ring $\mathbb{Z}[\sqrt[6]{-1}]$ and group them into double-infinite sequences corresponding to cosets by the unit group in the ring $\mathbb{Z}[\sqrt[6]{-1}]$; this is done via the solution cosets to the norm equations in $\mathbb{Z}[\sqrt[6]{-1}]$. At the end of Section 5.1 we state the relevant results, Theorems 5–10, which establish connections between solutions of the norm equation and classes of values D . We then

prove an eventual minimality property for \mathbb{Z}^2 -triangles emerging from a coset; cf. Lemma 5.1 in Section 5.2. Next, in Section 6 we give examples of sequences of values D from various classes. Section 7 contains the proof of Theorems 5–10.

We believe that the number-theoretical material regarding ring $\mathbb{Z}[\sqrt[6]{-1}]$ collected and used in Sections 5–7 is well-known to adepts of the algebraic number theory. In fact, a considerable part of this material can be derived directly from the basics contained in standard textbooks [5, 43], let alone such more advanced sources as [20, 38], to name a few. As a brief introduction, one can refer the reader to papers [12, 24, 31]. Nevertheless, we failed to find a single reference where all facts that we need for our analysis are discussed in full detail.

5.1 Triangles in \mathbb{Z}^2 as elements of ring $\mathbb{Z}[\sqrt[6]{-1}]$.

Consider a triangle with side-lengths ℓ_i^2 , $i = 1, 2, 3$ (cf. (2.2)). It is convenient to introduce the notation $[\ell_1^2|\ell_2^2|\ell_3^2]$ where $\ell_1^2 \leq \ell_2^2 \leq \ell_3^2$ for the set of \mathbb{Z}^2 triangles with given squared lengths of sides. Clearly, all triangles in the set $[\ell_1^2|\ell_2^2|\ell_3^2]$ are congruent but not necessarily \mathbb{Z}^2 -congruent.

Let us repeat the definition from Section 2.1: a pair of integers $a = \ell_2^2 - \ell_1^2$ and $b = \ell_3^2 - \ell_3^2$ is called a *signature* (of a triangle). All triangles with a given signature form a collection which we denote by $[\circ|\circ+a|\circ+a+b]$ assuming that a and b are fixed while the shortest squared side-length in the triangle varies.

Given non-negative a and b with $0 < a + b$, the collection $[\circ|\circ+a|\circ+a+b]$ may be empty. Later in this section we demonstrate that such collections (if they are not empty) can be partitioned into infinite sequences. Accordingly, we use a sequence notation, e.g. d_j , for running values of \circ . Without loss of generality we assume that d_j is indefinitely increasing. The existence of an infinite sequence d_j is the key fact behind the construction of infinite sequences of values D_j of Classes A and B. The second crucial fact is that all triangles in the the triangle sequence $[d_j|d_j+a|d_j+a+b]$ become M-triangles starting from some finite index j^* . The proof is given in the next section. The emerging theory clarifies the meaning of parameters a, b : they characterize closeness of the triangle to the equilateral one.

Triangles from collection $[\circ|\circ+a|\circ+a+b]$ are constructed in terms of coordinates of their vertices. First, consider a single \mathbb{Z}^2 -triangle with vertices

$$(0, 0), (m, n), (k, l) \tag{5.1}$$

referred to as triangle $\{m, n, k, l\}$. (This includes degenerate triangles which have all 3 vertices lying in a single line.) Its squared side-lengths are

$$d = (m - k)^2 + (n - l)^2, \quad e = k^2 + l^2, \quad f = m^2 + n^2. \tag{5.2.1}$$

The squared doubled area of triangle $\{m, n, k, l\}$ is

$$s^2 = (nk - ml)^2 \tag{5.2.2}$$

and the squared half-sum of its squared side-lengths

$$t^2 = (m^2 + n^2 + k^2 + l^2 - mk - nl)^2. \tag{5.2.3}$$

Assuming for definiteness that $d \leq e \leq f$, we observe that the signature is given by

$$a^2 = (e - d)^2 = (2mk + 2nl - m^2 - n^2)^2, \quad b^2 = (f - e)^2 = (m^2 + n^2 - k^2 - l^2)^2. \quad (5.2.4)$$

The quantity

$$r = a^2 + b^2 + ab \quad (5.2.5)$$

is called the *norm* of triangle $\{m, n, k, l\}$ for the reason explained later. It plays a central role in our algebraic considerations.

It is evident that triangle $\{m, -n, k, -l\}$ is the image of $\{m, n, k, l\}$ under reflection about the horizontal axis in \mathbb{Z}^2 . Triangle $\{k, l, m, n\}$ corresponds to swapping two triangle vertices (which geometrically but not algebraically leaves the triangle intact), and triangle $\{k, -l, m, -n\}$ is the image of the swapped triangle under reflection about the horizontal axis in \mathbb{Z}^2 .

The central idea of forthcoming considerations is that triangles $\{m, n, k, l\}$ can be mapped into a well-known algebraic structure. Let $\zeta = \frac{\sqrt{-1} + \sqrt{3}}{2}$ be the primary 12-th root of unity. From now on we use a standard notation ζ instead of $\sqrt[6]{-1}$. It is convenient for us to fix the basis $\{\zeta^{10}, \zeta^1, \zeta^2, \zeta^5\}$ in the corresponding cyclotomic field $\mathbb{Q}[\zeta]$:

$$\zeta^{10} = \frac{1 - \sqrt{-3}}{2}, \quad \zeta^1 = \frac{\sqrt{-1} + \sqrt{3}}{2}, \quad \zeta^2 = \frac{1 + \sqrt{-3}}{2}, \quad \zeta^5 = \frac{\sqrt{-1} - \sqrt{3}}{2} \quad (5.3)$$

The reason is that in a complex plane the angles between ζ^{10} and ζ^1 and angles between ζ^2 and ζ^5 are $\pi/2$ while the angles between ζ^2 and angles between ζ^{10} and ζ^1 and ζ^5 are $2\pi/3$, i.e. pairs of square lattices and pairs of triangular lattices are naturally fitting this basis. The triangle $\{m, n, k, l\}$ can be identified with an algebraic integer

$$\alpha = m\zeta^{10} + n\zeta^1 + k\zeta^2 + l\zeta^5 \quad (5.4)$$

in $\mathbb{Z}[\zeta]$. The choice of the basis (5.3) allows us to easily translate between manipulations with algebraic integers and those with triangles.

As the first example we investigate how the torsion group generated by $\zeta^1 = \{0, 1, 0, 0\}$ acts on $\alpha = \{m, n, k, l\}$. Observe that

$$\zeta^0 = \zeta^2 + \zeta^{10}, \quad \zeta^3 = \zeta^1 + \zeta^5, \quad \zeta^4 = -\zeta^{10}, \quad \zeta^6 = -\zeta^2 - \zeta^{10}, \quad (5.5.1)$$

$$\zeta^7 = -\zeta^1, \quad \zeta^8 = -\zeta^2, \quad \zeta^9 = -\zeta^1 - \zeta^5, \quad \zeta^{11} = -\zeta^5. \quad (5.5.2)$$

Accordingly,

$$\{m, n, k, l\}\zeta^1 = \{-l, k, n - l, k - m\}, \quad (5.6.1)$$

i.e. multiplication by ζ^1 rotates the triangle by $-\pi/2$ and then shifts the image of the vertex (k, l) to the origin. Next,

$$\{m, n, k, l\}\zeta^2 = \{m - k, n - l, m, k\}, \quad (5.6.2)$$

i.e. multiplication by ζ^2 rotates the triangle by π and then shifts the image of the vertex (m, n) to the origin. Further,

$$\{m, n, k, l\}\zeta^3 = \{-n, m, -l, k\}, \quad (5.6.3)$$

i.e. multiplication by ζ^3 rotates the triangle by $\pi/2$. Consequently, the multiplication by ζ^6 and ζ^9 corresponds to rotations by π and $3\pi/2$. Similarly, the multiplication by ζ^4 , ζ^7 or ζ^{10} rotates the triangle obtained after multiplication by ζ . In the same way, multiplication by ζ^5 , ζ^8 or ζ^{11} rotates the triangle obtained after multiplication by ζ^2 .

The triangle symmetries

$$\begin{aligned} \{m, n, k, l\} &\mapsto \{m, -n, k, -l\}, \\ \{m, n, k, l\} &\mapsto \{k, l, m, n\}, \\ \{m, n, k, l\} &\mapsto \{k, -l, m, -n\} \end{aligned} \quad (5.7)$$

correspond to algebraic conjugates of α . Combining (5.7) with multiplication by elements of the torsion group we obtain all 24 geometrical and all 48 algebraic congruent versions of a given triangle.

The norm $N(\alpha)$ of α is the product of all 4 conjugates of an algebraic integer α . It can be calculated by grouping conjugates in pairs:

$$\begin{aligned} N(\alpha) &= (\{m, n, k, l\}\{m, -n, k, -l\})(\{k, l, m, n\}\{k, -l, m, -n\}) \\ &= ((m^2\zeta^{-4} + k^2\zeta^4 + 2mk) - (n^2\zeta^2 + l^2\zeta^{-2} - 2nl)) \\ &\quad \times ((k^2\zeta^{-4} + m^2\zeta^4 + 2mk) - (l^2\zeta^2 + n^2\zeta^{-2} - 2nl)) \\ &= ((2mk + 2nl - m^2 - n^2) - (m^2 + n^2 - k^2 - l^2)\zeta^4) \\ &\quad \times ((2mk + 2nl - m^2 - n^2) - (m^2 + n^2 - k^2 - l^2)\zeta^{-4}) \\ &= (m^2 + n^2 - k^2 - l^2)^2 + (2mk + 2nl - m^2 - n^2)^2 \\ &\quad + (m^2 + n^2 - k^2 - l^2)(2mk + 2nl - m^2 - n^2). \end{aligned} \quad (5.8.1)$$

Different groupings of conjugates produce different representations for $N(\alpha)$:

$$\begin{aligned} N(\alpha) &= (\{m, n, k, l\}\{k, l, m, n\})(\{m, -n, k, -l\}\{k, -l, m, -n\}) \\ &= ((m^2 - n^2 + k^2 - l^2 - mk + nl) + (2mn + 2kl - ml - nk)\zeta^3) \\ &\quad \times ((m^2 - n^2 + k^2 - l^2 - mk + nl) - (2mn + 2kl - ml - nk)\zeta^3) \\ &= (m^2 - n^2 + k^2 - l^2 - mk + nl)^2 + (2mn + 2kl - ml - nk)^2 \end{aligned} \quad (5.8.2)$$

and

$$\begin{aligned} N(\alpha) &= (\{m, n, k, l\}\{k, -l, m, -n\})(\{k, l, m, n\}\{m, -n, k, -l\}) \\ &= ((m^2 + n^2 + k^2 + l^2 - mk - nl) - (ml - nk)(\zeta - \zeta^5)) \\ &\quad \times ((m^2 + n^2 + k^2 + l^2 - mk - nl) + (ml - nk)(\zeta - \zeta^5)) \\ &= (m^2 + n^2 + k^2 + l^2 - mk - nl)^2 - 3(ml - nk)^2. \end{aligned} \quad (5.8.3)$$

Comparing with the earlier definitions (5.8.1-3), we can see that

$$N(\alpha) = t^2 - 3s^2 = a^2 + b^2 + ab = r. \quad (5.9)$$

Similarly to a and b , the value r (which is always positive) can be considered as a measure of closeness of a \mathbb{Z}^2 -triangle to an equilateral one or, equivalently, a measure of closeness between a triangular sublattice of \mathbb{Z}^2 and a perfect triangular lattice.

A dual problem is closeness between a sub-lattice of a triangular lattice and a square lattice. In this case one needs to study triangles in a triangular lattice which are close to isosceles right ones. This duality is covered by expression (5.8.2) for the norm above. We interpret (m, k) and (n, l) (note the coordinate switch) as two sites of a unit triangular

lattice \mathbb{A}_2 (with the angle $2\pi/3$ between coordinate axes) which we call a *dual lattice*. Accordingly, we treat the triple

$$(0, 0), (m, k), (n, l) \quad (5.10)$$

as a triangle in the dual lattice. For this triangle the value

$$(m^2 + n^2 + k^2 + l^2 - mk - nl)^2 \quad (5.11.1)$$

is equal to the square of the sum of squared lengths of two of the triangle sides, while

$$3(ml - nk)^2 \quad (5.11.2)$$

equals the squared area of the triangle multiplied by 16. Moreover,

$$g^2 = (m^2 - n^2 + k^2 - l^2 - mk + nl)^2 \quad (5.11.3)$$

is equal to the square of the difference between squared lengths of two triangle sides while

$$h^2 = (2mn + 2kl - ml - nk)^2 \quad (5.11.4)$$

is equal to the square of the difference between the squared side length of the third side and the sum of squared side lengths of the first two sides. The quantities g^2 and h^2 in (5.11.3,4) again can be interpreted as a triangle signature. The sum $g^2 + h^2$ is the measure of closeness of a triangle to an equilateral right one.

The full group of units $\mathbb{U}[\zeta]$ of the cyclotomic field $\mathbb{Q}[\zeta]$ consists of elements

$$\zeta^i(1 + \zeta)^j, \quad i, j \in \mathbb{Z}, \quad (5.12.1)$$

or equivalently of elements

$$\zeta^i(2 + \sqrt{3})^j \quad \text{and} \quad \zeta^i(2 + \sqrt{3})^j(\zeta + \zeta^2), \quad i, j \in \mathbb{Z}.$$

Denoting by $\mathbb{U}^+[\zeta]$ the sub-group generated by ζ and $(2 + \sqrt{3})$ we obtain that

$$\mathbb{U}[\zeta] = \mathbb{U}^+[\zeta] \cup (\zeta + \zeta^2)\mathbb{U}^+[\zeta] \in \mathbb{Z}[\zeta]. \quad (5.12.2)$$

Note that for brevity we slightly deviate from traditional notations which reserve superscript $+$ for the sub-group of real units. Our notation is used for a larger (not real subgroup) which contains all real units together with their multiplications by the elements of the torsion sub-group. The relationship between $\mathbb{U}^+[\zeta]$ and $(\zeta + \zeta^2)\mathbb{U}^+[\zeta]$ can be understood from the identity

$$\begin{aligned} \tilde{\alpha} : &= \alpha(\zeta + \zeta^2) \\ &= (m\zeta^{10} + n\zeta^1 + k\zeta^2 + l\zeta^5)(\zeta + \zeta^2) \\ &= (m - k - l)\zeta^{10} + (n + k - l)\zeta^1 + (m + n - l)\zeta^2 + (-m + n + k)\zeta^5, \end{aligned} \quad (5.13.1)$$

i.e. multiplication by $(\zeta + \zeta^2)$ corresponds to the map

$$\{m, n, k, l\} \mapsto \{m - k - l, n + k - l, m + n - l, -m + n + k\}. \quad (5.13.2)$$

After the multiplication by $(\zeta + \zeta^2)$ the norm remains the same (as $(\zeta + \zeta^2)$ is a unit) but the signature changes. It is a direct calculation to verify that if the original triangle signature is a, b then the resulting signature is b, a .

Let

$$l_j = \frac{1}{2}((2 + \sqrt{3})^j + (2 - \sqrt{3})^j) \quad \text{and} \quad k_j = \frac{1}{2\sqrt{3}}((2 + \sqrt{3})^j - (2 - \sqrt{3})^j). \quad (5.14)$$

The multiplication of $\alpha = \{m, n, k, l\}$ by

$$(2 + \sqrt{3})^j = l_j + k_j\sqrt{3} = l_j(\zeta^2 - \zeta^4) + k_j(\zeta^1 - \zeta^5) \quad (5.15.1)$$

corresponds to the map

$$\begin{aligned} &\{m, n, k, l\} \\ &\mapsto \{l_j m + k_j(n - 2l), l_j n + k_j(2k - m), l_j k + k_j(2n - l), l_j l + k_j(k - 2m)\}. \end{aligned} \quad (5.15.2)$$

The image in (5.15.2) defines a triangle with the same signature as the original triangle. Indeed, the squared side-lengths of this triangle are

$$\begin{aligned} &(m^2 + n^2)l_j^2 + (m^2 + n^2 + 4k^2 + 4l^2 - 4mk - 4nl)k_j^2 - 4(ml - nk)k_j l_j, \\ &(k^2 + l^2)l_j^2 + (4m^2 + 4n^2 + k^2 + l^2 - 4mk - 4nl)k_j^2 - 4(ml - nk)k_j l_j, \\ &(m^2 + n^2 + k^2 + l^2 - 2mk - 2nl)l_j^2 \\ &\quad + (m^2 + n^2 + k^2 + l^2 + 2mk + 2nl)k_j^2 - 4(ml - nk)k_j l_j. \end{aligned} \quad (5.16)$$

Using the relation $l_j^2 = 3k_j^2 + 1$ (a Pell equation), it is not hard to verify that the difference between the first and second squared lengths in (5.16) is b whereas the difference between the second and third squared lengths is a .

Thus, any triangle $\{m, n, k, l\}$ with a given signature a, b is always a member of a coset of triangles $\{m, n, k, l\}\mathbb{U}^+[\zeta]$ (explicitly listed above), with the same signature and norm. Considering a coset (of $\mathbb{U}[\zeta]$ or $\mathbb{U}^+[\zeta]$) as a sequence labeled by $j \in \mathbb{Z}$ (up to multiplication by an element of the torsion group) we can see that the larger $|j|$ the closer the corresponding triangle is to the equilateral one. In particular, each coset contains only a finite number of obtuse triangles.

If we treat quadruples $\{m, n, k, l\}$ as a row vector in \mathbb{R}^4 then it is a straightforward calculation to verify that a multiplication by an algebraic number $\{m, n, k, l\}$ is equivalent to multiplication by the matrix

$$T = \begin{pmatrix} k & l & k - m & l - n \\ -l & k & n - l & k - m \\ m - k & n - l & m & n \\ l - n & m - k & -n & m \end{pmatrix}. \quad (5.17)$$

In particular, relationships (5.13.2) and (5.15.2) are the results of the multiplication by the corresponding matrices.

A natural approach to identifying all triangles with a given signature a, b consists in finding all solutions to the corresponding norm equation

$$N(\alpha) = r, \quad (5.18)$$

where $r = a^2 + b^2 + ab$. If solutions exist they can be further classified into Classes A, B0, B1 and B2 (see below) closely related to eponymous classes defined earlier for values D_n .

Being cyclotomic, the field $\mathbb{Q}[\zeta]$ possesses a unique factorization property for the corresponding algebraic integers in $\mathbb{Z}[\zeta]$. This implies the following algorithm of solving the norm equation. (I) First, analyze how rational primes are decomposed into algebraic primes. (II) After that decompose r into the product of rational primes and then decompose each rational prime into the product of algebraic primes. (III) Finally, partition the entire product of algebraic primes into 4 sub-products such that these sub-products give 4 conjugated algebraic integers from $\mathbb{Z}[\zeta]$. Each such partition corresponds to some solution coset $\{m, n, k, l\}\mathbb{U}[\zeta]$ to the norm equation, and all solutions to the norm equation can be found in this way. Given r , the above algorithm allows us to identify all the corresponding solution cosets and therefore calculate their total amount (which is always finite). It also clarifies that a larger amount of different prime factors in the prime decomposition of r leads to a larger number of solution cosets to the norm equation (5.18).

It is convenient to pick a unique representative of a solution coset $\{m, n, k, l\}\mathbb{U}[\zeta]$ which we call a *leader* or a *leading* triangle. We choose it to be a triangle with the minimal area within the coset. Moreover, among all 48 possible representations of such a triangle (12 members of the torsion group times 4 conjugations) we select the triangle, denoted by $\{m|n|k|l\}$, with $m, n \geq 0$ and $m^2 + n^2 \geq k^2 + l^2 \geq (m - k)^2 + (n - l)^2$. It is not hard to verify that the leading triangle is always unique. When we speak about a full coset, $\{m|n|k|l\}\mathbb{U}[\zeta]$ we usually assume that the triangle $\{m|n|k|l\}$ corresponds to $j = 0$. The notion of a leader allows us to use a ‘‘canonical’’ notation for different types of solution cosets: $\{m|n|k|l\}\mathbb{U}[\zeta]$, $\{m|n|k|l\}\mathbb{U}^+[\zeta]$, $\{m|n|k|l\}\mathbb{U}^+[\zeta](\zeta + \zeta^2)$, etc.

For the future reference we summarize that the coset leader $\{m|n|k|l\}$ uniquely defines

$$\begin{aligned} d &= (m - k)^2 + (n - l)^2, & e &= k^2 + l^2 & f &= m^2 + n^2, \\ a^2 &= (2mk + 2nl - m^2 - n^2)^2, & b^2 &= (m^2 + n^2 - k^2 - l^2)^2, \\ g^2 &= (m^2 - n^2 + k^2 - l^2 - mk + nl)^2, & h^2 &= (2mn + 2kl - ml - nk)^2, \\ s^2 &= (nk - ml)^2, & t^2 &= (m^2 + n^2 + k^2 + l^2 - mk - nl)^2 \end{aligned} \quad (5.19)$$

with

$$r = a^2 + b^2 + ab = g^2 + h^2 = t^2 - 3s^2. \quad (5.20)$$

A full coset $\{m|n|k|l\}\mathbb{U}[\zeta]$ is the union

$$\{m|n|k|l\}\mathbb{U}^+[\zeta] \cup \{m|n|k|l\}\mathbb{U}^+[\zeta](\zeta + \zeta^2). \quad (5.21)$$

Here

$$\begin{aligned} &\{m|n|k|l\}\mathbb{U}^+[\zeta] \\ &= \{l_j m + k_j(n - 2l), l_j n + k_j(2k - m), l_j k + k_j(2n - l), l_j l + k_j(k - 2m)\}, \\ &= \{l_j, k_j, l_j, -k_j\}T, \quad j \in \mathbb{Z}, \end{aligned} \quad (5.22)$$

is a coset with signature a, b while $\{m|n|k|l\}\mathbb{U}^+[\zeta](\zeta + \zeta^2)$ is a coset with signature b, a . The latter is obtained from the former via the map

$$\begin{aligned} &\{m, n, k, l\} \\ &\mapsto \{m - k - l, n + k - l, m + n - l, -m + n + k\} = \{0, 1, 1, 0\}T. \end{aligned} \quad (5.23)$$

It will be convenient to refer to $\{m|n|k|l\}\mathbb{U}^+[\zeta]$ and $\{m|n|k|l\}\mathbb{U}^+[\zeta](\zeta + \zeta^2)$ in (5.21) as the $\{m|n|k|l\}\mathbb{U}^+[\zeta]$ - and $\{m|n|k|l\}\mathbb{U}^+[\zeta](\zeta + \zeta^2)$ -halves of the full coset $\{m|n|k|l\}\mathbb{U}[\zeta]$, respectively.

As was mentioned earlier, an important property of a solution coset is the existence of a finite index $j^* = j^*(r)$ such that for any j with $|j| \geq j^* = j^*(r)$ the area s_j of the corresponding triangle is minimal among all acute \mathbb{Z}^2 -triangles having their squared side-lengths at least d_j . This assigns a quantitative meaning to the claim that the triangles in the coset become close to an equilateral one as $|j| \rightarrow \infty$. The proof of this property is presented in the next section (see Lemma 5.1).

We say that a full solution coset $\{m|n|k|l\}\mathbb{U}[\zeta]$ is of *Class A* if there is no other coset $\{m', n', k', l'\}\mathbb{U}[\zeta]$ with $s'_j = s_j$ for all $j \in \mathbb{Z}$. The meaning is that for each d_j with $|j| > j^*$, the minimal area of any acute \mathbb{Z}^2 -triangle with squared side-lengths $\geq d_j$ is equal to s_j , and it is achieved specifically on the corresponding triangle $\{m_j, n_j, k_j, l_j\}$ from the coset. (Here k_j and l_j should not be confused with the ones defined in (5.15.1).) Referring to the representation (5.21), we will say that $\{m|n|k|l\}\mathbb{U}^+[\zeta]$ and $\{m|n|k|l\}\mathbb{U}^+[\zeta](\zeta + \zeta^2)$ are solution cosets of Class A with constant signatures a, b and b, a , respectively.

Next, a family \mathfrak{B}_0 of solution cosets $\{m^{(i)}|n^{(i)}|k^{(i)}|l^{(i)}\}\mathbb{U}[\zeta]$ is said to be of *Class B0* if for each j the triangles labeled by j taken from any two cosets in the family are congruent to each other, and \mathfrak{B}_0 is the maximal one with this property. We will see later that it may happen only if the cosets in the family are obtained from each other via some \mathbb{R}^2 -rotation by an angle not multiple of $\pi/2$. For brevity, we often say that \mathfrak{B}_0 is a B0 family; a similar agreement is in place for families of Classes B1 and B2; see below.

We say that a family \mathfrak{B}_1 of solution cosets $\{m^{(i)}|n^{(i)}|k^{(i)}|l^{(i)}\}\mathbb{U}[\zeta]$ is a *Class B1* family if for each j the triangles labeled by j taken from any two cosets in the family are not congruent but have the same area, and the family is the maximal one with this property. This is related to \mathbb{R}^2 -rotations of the corresponding triangles in the dual lattice \mathbb{A}_2 .

Finally, a family \mathfrak{B}_2 of solution cosets $\{m^{(i)}|n^{(i)}|k^{(i)}|l^{(i)}\}\mathbb{U}[\zeta]$ is said to be of *Class B2* if, for any j , all triangles labeled by j in these cosets have the same area but some of them are congruent while some other are not, and the family is the maximal one with this property. This is related to superposition of rotations in both main and dual lattices.

The results of this section are given in Theorems 5 – 10 below. Here we suppose that the values $\varrho(\cdot)$ are non-negative integers.

Theorem 5. *A solution to the norm equation $N(\alpha) = r$ exists only for positive integers r with the prime decomposition*

$$r = 2^{2\varrho(2)} 3^{2\varrho(3)} \prod_i p_i^{\varrho(p_i)} \prod_j q_j^{2\varrho(q_j)} \prod_k w_k^{2\varrho(w_k)} \prod_l z_l^{2\varrho(z_l)}. \quad (5.24)$$

Here all $p_i \bmod 12 = 1$, $q_j \bmod 12 = 11$, $w_k \bmod 12 = 5$ and $z_l \bmod 12 = 7$.

The further relation between values of r of the form (5.24) and solution cosets to the norm equation is classified in Theorems 6–10.

Theorem 6. (Class A). *Assume that*

$$r = 2^{2\varrho(2)} 3^{2\varrho(3)} p^{\varrho(p)} w^{2\varrho(w)} z^{2\varrho(z)} \prod_j q_j^{2\varrho(q_j)}, \quad (5.25)$$

where $\varrho(p) + \varrho(w) + \varrho(z) \in \{0, 1\}$. Then the corresponding norm equation $N(\alpha) = r$ has at least one pair of solution cosets with constant signatures a, b and b, a such that $r = a^2 + b^2 + ab$:

$$\{m|n|k|l\}\mathbb{U}^+[\zeta] \quad \text{and} \quad \{m|n|k|l\}\mathbb{U}^+[\zeta](\zeta + \zeta^2), \quad (5.26)$$

and the union $\{m|n|k|l\}\mathbb{U}^+[\zeta] \cup \{m|n|k|l\}\mathbb{U}^+[\zeta](\zeta + \zeta^2)$ gives a full solution coset of Class A. Conversely, any Class A solution coset is obtained as a union of cosets (5.26) for a, b and b, a with $a^2 + b^2 + ab = r$ where r has the form (5.25).

Let $\sharp(r)$ denote the total number of pairs of solution cosets (5.26) of constant signatures a, b and b, a (that is, of full solution cosets). Then

$$\sharp(r) = 1 \quad \text{iff} \quad \varrho(p) + \varrho(w) + \varrho(z) + \sum_j \varrho(q_j) \leq 1.$$

If $\varrho(q_j) = 1$ for all j then

$$\sharp(r) = 2^{-1+\varrho(p)+\varrho(w)+\varrho(z)+\sum_j \varrho(q_j)}.$$

If all $\varrho(\cdot) = 0$ except for one q then

$$\sharp(r) = [\varrho(q)/2] + 1.$$

If $\varrho(p) + \varrho(w) + \varrho(z) = 1$ and the remaining $\varrho(q_j) = 0$ except for q_1 then

$$\sharp(r) = \varrho(q_1) + 1.$$

In a general case $\sharp(r)$ can be expressed via the collection of divisors of r in a fashion similar to Theorem 3, Chapter 1, §4 in [19].

Theorem 7. (Class B0). Assume that

$$r = 2^{2\varrho(2)} 3^{2\varrho(3)} p^{\varrho(p)} \prod_j q_j^{2\varrho(q_j)} \prod_k w_k^{2\varrho(w_k)} z^{2\varrho(z)}. \quad (5.27)$$

Here $\varrho(p), \varrho(z) \in \{0, 1\}$, $\varrho(p) + \varrho(z) \leq 1$, and $\varrho(p) + \varrho(z) + \sum_k \varrho(w_k) \geq 2$. Then the corresponding solution cosets are partitioned into one or several Class B0 families. Conversely, every B0 family corresponds to an r as in (5.27). Given an r of the form (5.27), the number $\sharp(r)$ of cosets in each emerging B0 family is the same. If additionally $\varrho(w_k) \leq 1$ for all k then

$$\sharp(r) = 2^{-1+\varrho(p)+\varrho(z)+\sum_k \varrho(w_k)}.$$

Increasing the value $\varrho(w_k) > 1$ increases $\sharp(r)$. In particular, if $\varrho(w_k) = 0$ for $k \neq 1$ then

$$\sharp(r) = \begin{cases} \varrho(w_1) + 1, & \text{if } \varrho(p) + \varrho(z) \neq 0, \\ [\varrho(w_1)/2] + 1, & \text{otherwise.} \end{cases}$$

Theorem 8. (Class B1). Assume that

$$r = 2^{2\varrho(2)} 3^{2\varrho(3)} \prod_i p_i^{\varrho(p_i)} \prod_j q_j^{2\varrho(q_j)} w^{2\varrho(w)} \prod_l z_l^{2\varrho(z_l)}, \quad (5.28)$$

where $\varrho(w), \varrho(p_i) \in \{0, 1\}$, and $\sum_i \varrho(p_i) + \sum_l \varrho(z_l) \geq 2$. Then the corresponding cosets are partitioned into one or several Class B1 families. The number $\sharp(r)$ of cosets in each emerging B1 family is the same. If additionally $\varrho(z_l) \leq 1$ then

$$\sharp(r) = 2^{-1+\varrho(w)+\sum_i \varrho(p_i)+\sum_l \varrho(z_l)}.$$

Increasing the value $\varrho(z_l) > 1$ increases $\sharp(r)$. In particular, if all $\varrho(p_i) = 0$ and $\varrho(z_l) = 0$ for $l \neq 1$ then

$$\sharp(r) = \begin{cases} \varrho(z_1) + 1, & \text{if } \varrho(w) \neq 0, \\ \lfloor \varrho(z_1)/2 \rfloor + 1, & \text{otherwise.} \end{cases}$$

Theorem 9. (Class B2). Assume that

$$r = 2^{2\varrho(2)} 3^{2\varrho(3)} \prod_i p_i^{\varrho(p_i)} \prod_j q_j^{2\varrho(q_j)} \prod_k w_k^{2\varrho(w_k)} \prod_l z_l^{2\varrho(z_l)},$$

where $\varrho(p_i) \in \{0, 1\}$, and $\sum_k \varrho(w_k) \geq 1$, $\sum_l \varrho(z_l) \geq 1$, $\sum_i \varrho(p_i) + \sum_k \varrho(w_k) \geq 2$, $\sum_i \varrho(p_i) + \sum_l \varrho(z_l) \geq 2$. Then the corresponding cosets are partitioned into one or several B2 families. The number $\flat(r)$ of cosets in each emerging B2 family is the same. If $\varrho(w_k) = 1$ for all k and $\varrho(z_l) = 1$ for all l then

$$\flat(r) = 2^{-2+\sum_i \varrho(p_i)+\sum_k \varrho(w_k)+\sum_l \varrho(z_l)}.$$

Increasing $\varrho(w_k) > 1$ and/or $\varrho(z_l) > 1$ increases $\flat(r)$.

Theorem 10. (Classes B1,2). Assume that

$$r = p^{\varrho(p)},$$

where $\varrho(p) > 2$. Then the whole set of solution cosets has cardinality

$$\sharp(r) = ((\varrho(p) + 2)(2\varrho(p)^2 + 8\varrho(p) + 15 + 9(-1)^{\varrho(p)})/48$$

and is partitioned into $\flat(r) = \lfloor \varrho(p)/2 \rfloor + 1$ families, where one family is of Class B1 and the remaining families are of Class B2.

The proof of Theorems 5 – 10 is given in Section 7: it is essentially an application of well-known facts from the algebraic number theory (see [5], [48], [30]) to the triangle representation developed above. A feature of the proof is that the statements of Theorems 5 – 10 are established via a common argument that goes in parallel for several or all of them.

5.2 Coset intersections and minimal triangles.

In Section 5.2 we prove eventual minimality of triangles in a solution coset. This finishes the proof of Theorem 3.

Lemma 5.1. Consider a coset $\{m|n|k|l\}\mathbb{U}[\zeta]$ with norm r , where

$$r = (m^2 - n^2 + k^2 - l^2 - mk + nl)^2 + (2mn + 2kl - ml - nk)^2.$$

Then there exists an integer j_* , with $0 \leq j_* \leq \log_{2+\sqrt{3}}(3200r^{3/2})$, such that for $|j| > j_*$ the members of the coset indexed by j are M -triangles (for all corresponding D^2).

Proof. Consider a non-obtuse triangle $[d + a|d + b|d + c]$ where $0 \leq a \leq b \leq c$ and $d \geq c - a - b$. Let $s = s(a, b, c)$ be the doubled area of this triangle. Then

$$4s^2 = 3d^2 + 2d(a + b + c) + (2ab + 2bc + 2ca - a^2 - b^2 - c^2).$$

In particular,

$$\frac{\partial(4s^2)}{\partial c} = 2d + 2(a + b) - 2c = 2(d - (c - a - b)) > 0,$$

and the area of the triangle is increasing in c . It is increasing in a and b for the same reason.

Consider another triangle $[d + a'|d + b'|d + c']$. Our aim is to compare the areas of these two triangles; without loss of generality we may assume that $a = 0$. Then

$$s(d, d + b, d + c) \leq s(d, d + c, d + c) < s(d, d, d + 4c) \leq s(d + a', d + b', d + 4c')$$

whenever $b \geq 0$, $c \geq \max(1, b)$, $a' \geq 0$, $b' \geq b$, $c' \geq c$ and $d > 4c$. The only non-trivial inequality here is in the middle:

$$4s(d, d + c, d + c)^2 = 3d^2 + 4dc < 3d^2 + 8dc - 16c^2 = 4s(d, d, d + 4c)^2$$

which follows from the acuteness requirement $d > 4c$ for a $[d|d|d + 4c]$ -triangle. Thus, given $b \geq 0$ and $c \geq \max(1, b)$, the area of a non-obtuse $[d' + a'|d' + b'|d' + c']$ -triangle may be smaller than that of a non-obtuse $[d|d + b|d + c]$ -triangle for at most $(4c)^3$ triples $a', b', c' \geq 0$. In fact, since no dependency of d upon a' , b' and c' is assumed, some of acute $[d' + a'|d' + b'|d' + c']$ -triangles may not exist, which makes the upper-bound $(4c)^3$ rather excessive.

For the rest of the argument we continue to assume that $a = 0$. Given $b \geq 0$ and $c \geq \max(1, b)$, we consider the corresponding norm equation $N(\{m, n, k, l\}) = r$ with

$$r = a^2 + b^2 + c^2 - ab - bc - ca.$$

As we are primarily interested in areas of triangles it is convenient to understand the norm equation in terms of variables $s^2 = (nk - ml)^2$, $t^2 = (m^2 + n^2 + k^2 + l^2 - mk - nl)^2$. Cf. (5.2.1,2). In these variables the norm equation is $t^2 - 3s^2 = r$, cf. (5.9). For each coset $\{m|n|k|l\}\mathbb{U}[\zeta]$ solving this equation we denote by (x, y) the corresponding leading solution (here $x = x(0, b, c)$, $y = y(0, b, c)$ and $y^2 - 3x^2 = r$). In these variables the triangle $\{m|n|k|l\}$ can be written as $[d|d + b|d + c]$ where $d = (2y - (b + c))/3$. The double area of this triangle is equal to x .

Denote by Δ an element of the triangle collection $[\circ| \circ + b| \circ + c]$. The double area of Δ is denoted by $s(\Delta)$ and equals to x . For a different collection $[\circ + a'| \circ + b'| \circ + c']$ with elements denoted by Δ' we would like to understand for which a', b', c' one may have $s(\Delta') < s(\Delta)$. We already know that there exist only finitely many triples (a', b', c') for which the double area $s(\Delta') < s(\Delta)$ for at least one value d (i.e. value of \circ). Next, for each such triangle $[d + a'|d + b'|d + c']$ there exists only a finite number of cosets solving the corresponding norm equation $t'^2 - 3s'^2 = r'$ where $r' = r'(a', b', c')$. Indeed, given a leading solution (x, y) of $t^2 - 3s^2 = r$ and a leading solution (x', y') of $t'^2 - 3s'^2 = r'$, we have

$$0 < x < \sqrt{r}, \quad 0 < y < 2\sqrt{r}, \quad \text{and} \quad 0 < x' < \sqrt{r'}, \quad 0 < y' < 2\sqrt{r'}$$

as the leader is the triangle with the smallest area. On the other hand,

$$0 \leq r = a^2 + b^2 + c^2 - ab - bc - ca \leq c^2,$$

and we are interested only in $0 \leq c' \leq 4c$ and, consequently, in $0 \leq r' \leq 16c^2$.

If $a' + b' + c' = a + b + c$ then $\text{Sign}(s(\Delta') - s(\Delta)) = \text{Sign}(r - r')$ since

$$4s(\Delta')^2 = \left(\sqrt{3}d + \frac{1}{\sqrt{3}}(a' + b' + c') \right)^2 - \frac{4}{3}r',$$

and

$$4s(\Delta)^2 = \left(\sqrt{3}d + \frac{1}{\sqrt{3}}(a + b + c) \right)^2 - \frac{4}{3}r.$$

In the opposite case $a' + b' + c' \neq a + b + c$ we have equality $s(\Delta') = s(\Delta)$ at $d = d^*$ where

$$2d^* = -\frac{1}{3}(a' + b' + c' + a + b + c) + \frac{4}{3} \frac{r' - r}{a' + b' + c' - a - b - c}.$$

Therefore, for

$$d > 16c^2 \geq |d^*|$$

the function $\text{Sign}(s(\Delta') - s(\Delta))$ is constant. If $a' + b' + c' > a + b + c$ then for d large enough

$$\left(\sqrt{3}d + \frac{1}{\sqrt{3}}(a' + b' + c') \right)^2 - \frac{4}{3}r' > \left(\sqrt{3}d + \frac{1}{\sqrt{3}}(a + b + c) \right)^2 - \frac{4}{3}r \quad (5.29)$$

and consequently $s(\Delta') > s(\Delta)$. Due to the previous argument, inequality (5.29) is true already for $d > 16c^2$. As we are interested only in the case when $s(\Delta') \leq s(\Delta)$, we assume from now on that

$$a' + b' + c' \leq a + b + c.$$

Specifically, we are looking for the situation where $3d'_i = 2y'_i - (a' + b' + c') = 2y_n - (a + b + c) = 3d_n$ and $x'_i = x_n$. In particular, in this case we have

$$0 \leq 2y_n - 2y'_i = (a + b + c) - (a' + b' + c') < 3c.$$

Thus, to finish the proof of lemma it is enough to verify that

$$2y_n - 2y'_i > 3c, \quad \text{whenever } i, n > \log_{2+\sqrt{3}}(3200c^3). \quad (5.30)$$

We start from the representation

$$\begin{aligned} 2y_n - 2y'_i &= 2yl_n + 6xk_n - 2y'l_i - 6x'k_i \\ &= \left((y - y'l_{i-n} - 3x'k_{i-n}) + \sqrt{3}(x - x'l_{i-n} - y'k_{i-n}) \right) (2 + \sqrt{3})^n \\ &\quad + \left((y - y'l_{i-n} + 3x'k_{i-n}) + \sqrt{3}(x - x'l_{i-n} + y'k_{i-n}) \right) (2 - \sqrt{3})^n, \end{aligned}$$

where k_j and l_j are given by (5.15.1). Next we observe that $l_{n+j} > (2 + \sqrt{3})^j l_n / 2$ and $k_{n+j} > (2 + \sqrt{3})^j k_n$ for $n, j > 0$. Therefore, if $(2 + \sqrt{3})^{i-n} > 4c$ then

$$2yl_n + 6xk_n - 2y'l_i - 6x'k_i < 4cl_n + 6ck_n - 2l_i - 6k_i < 0.$$

Similarly, if $(2 + \sqrt{3})^{n-i} > 19c$ then

$$2yl_n + 6xk_n - 2y'l_i - 6x'k_i > 2l_n + 6k_n - 16cl_i - 24ck_i > 3c.$$

Thus, we may safely assume that $(2 + \sqrt{3})^{n-i} < 19c$ and consequently $|l_{i-n}|, |k_{i-n}| < 10c$.

It is not hard to verify that for positive integer p and q , we have $|p \pm q\sqrt{3}| > 1/(4q)$. Then for $n > \log_{2+\sqrt{3}}(400c^2)$

$$\begin{aligned} & \left| (y - y'l_{i-n} + 3x'k_{i-n}) \right. \\ & \quad \left. + \sqrt{3}(x - x'l_{i-n} + y'k_{i-n}) \right| (2 - \sqrt{3})^n \leq 400c^2(2 - \sqrt{3})^n < 1, \end{aligned}$$

while for $n > \log_{2+\sqrt{3}}(3200c^3)$

$$\begin{aligned} & \left| (y - y'l_{i-n} - 3x'k_{i-n}) + \sqrt{3}(x - x'l_{i-n} - y'k_{i-n}) \right| (2 + \sqrt{3})^n \\ & > \frac{(2 + \sqrt{3})^n}{4(x - x'l_{i-n} - y'k_{i-n})} > \frac{(2 + \sqrt{3})^n}{800c^2} > 4c > 3c + 1. \end{aligned}$$

The straightforward estimate $c < \sqrt{r}$ completes the proof of Lemma 5.1. ■

6 Examples of Classes A, B0, B1 and B2

In this section we provide series of simplest examples related to Classes A and B0 - B2. The notations k_j and l_j refer to quantities defined in (5.15.1).

6.1. The coset $\{1|0|1|0\}U^+[\zeta](\zeta + \zeta^2) = \{0, 1, 1, 0\}U^+[\zeta]$ corresponding to $r = 1$ is of Class A; it contains all triangles from collection $[o|o|o+1]$, i.e, with signature 0, 1. These triangles have vertices

$$(0, 0), (2k_j - l_j, k_j), (k_j, 2k_j - l_j), \quad j \in \mathbb{N};$$

they provide the best \mathbb{Z}^2 -approximations to an equilateral triangle. These are M-triangles for the corresponding $D_j^2 = l_j^2 + 5k_j^2 - 4l_jk_j$ for all j and possibly for some smaller values \tilde{D} with $D_j^* \leq \tilde{D} < D_j$. (The latter possibility is admitted in all examples but not stressed every time again. The range $j \in \mathbb{N}$ is also purported throughout the whole section.)

In Examples **6.2**, **6.3** we construct families containing two cosets each. The families in Examples **6.4**, **6.5** have larger cardinalities.

6.2. The cosets $\{5|0|5|0\}U^+[\zeta]$ and $\{4|3|4|3\}U^+[\zeta]$ corresponding to $r = 5^4$ form a B0 family containing triangles from collection $[o|o+25|o+25]$. These triangles have vertices

$$(0, 0), (5l_j, 5k_j), (5l_j, -5k_j)$$

and

$$(0, 0), (4l_j - 3k_j, 3l_j + 4k_j), (4l_j + 3k_j, 3l_j - 4k_j),$$

respectively. These are M-triangles for $j \geq 3$ and $D_j^2 = 100k_j^2$.

6.3. The cosets $\{2|5|3|4\}\mathbb{U}^+[\zeta]$ and $\{5|3|4|1\}\mathbb{U}^+[\zeta]$ corresponding to $r = 13 \cdot 7^2$ form a B1 family containing triangles from collections $[\circ|\circ+23|\circ+4]$ and $[\circ|\circ+12|\circ+17]$. The vertices are

$$(0, 0), (2l_j - 3k_j, 5l_j + 4k_j), (3l_j + 6k_j, 4l_j - k_j)$$

and

$$(0, 0), (5l_j + k_j, 3l_j + 3k_j), (4l_j + 5k_j, l_j - 6k_j),$$

respectively. Here we obtain M-triangles for $j \geq 2$ and $D_j^2 = 2l_j^2 + 106k_j^2 + 28k_jl_j$.

6.4. The cosets $\{9|8|10|5\}\mathbb{U}^+[\zeta]$, $\{12|1|11|-2\}\mathbb{U}^+[\zeta]$, $\{7|11|7|6\}\mathbb{U}^+[\zeta]$ and $\{13|1|9|-2\}\mathbb{U}^+[\zeta]$ corresponding to $r = 13 \cdot 5^2 \cdot 7^2$ form a B2 family containing triangles from collections $[\circ|\circ+60|\circ+145]$, $[\circ|\circ+60|\circ+145]$, $[\circ|\circ+115|\circ+135]$ and $[\circ|\circ+115|\circ+135]$ respectively. These triangles have vertices

$$(0, 0), (9l_j - 2k_j, 8l_j + 11k_j), (10l_j + 11k_j, 5l_j - 8k_j),$$

$$(0, 0), (12l_j + 5k_j, l_j + 10k_j), (11l_j + 4k_j, -2l_j - 13k_j),$$

$$(0, 0), (7l_j - k_j, 11l_j + 7k_j), (7l_j + 16k_j, 6l_j - 7k_j),$$

and

$$(0, 0), (13l_j + 5k_j, l_j + 5k_j), (9l_j + 4k_j, -2l_j - 17k_j)$$

respectively. They are M-triangles for $j \geq 3$ and $D_j^2 = 10l_j^2 + 530k_j^2 + 140k_jl_j$.

6.5. The cosets $\{6|5|4|3\}\mathbb{U}^+[\zeta]$ and $\{2|7|2|6\}\mathbb{U}^+[\zeta]$ corresponding to $r = 13^3$ form a B1 family \mathfrak{B}_1 containing triangles from collections $[\circ|\circ+17|\circ+53]$ and $[\circ|\circ+39|\circ+52]$ respectively, while the cosets $\{8|1|5|-1\}\mathbb{U}^+[\zeta]$, $\{7|4|5|1\}\mathbb{U}^+[\zeta]$ and $\{3|7|4|5\}\mathbb{U}^+[\zeta]$ corresponding to the same $r = 13^3$ form a B2 family \mathfrak{B}_2 containing triangles from collections $[\circ|\circ+39|\circ+52]$, $[\circ|\circ+39|\circ+52]$ and $[\circ|\circ+17|\circ+53]$ respectively. The triangles in family \mathfrak{B}_1 have vertex triples

$$(0, 0), (6l_j - k_j, 5l_j + 2k_j), (4l_j + 7k_j, 3l_j - 8k_j),$$

and

$$(0, 0), (2l_j - 5k_j, 7l_j + 2k_j), (2l_j + 8k_j, 6l_j - 2k_j),$$

respectively. They are M-triangles for $j \geq 3$ and $D_j^2 = l_j^2 + 185k_j^2 + 8k_jl_j$. The triangles in family \mathfrak{B}_2 have vertices

$$(0, 0), (8l_j + 3k_j, l_j + 2k_j), (5l_j + 3k_j, -l_j - 11k_j),$$

$$(0, 0), (7l_j + 2k_j, 4l_j + 3k_j), (5l_j + 7k_j, l_j - 9k_j)$$

and

$$(0, 0), (3l_j - 3k_j, 7l_j + 5k_j), (4l_j + 9k_j, 5l_j - 2k_j),$$

respectively. They are M-triangles for $j \geq 3$ and $D_j^2 = 5l_j^2 + 193k_j^2 + 52k_jl_j$.

In all examples **6.1** - **6.5** the minimal value of j has been calculated numerically by `MinimalTriangles.java`.

7 Proof of Theorems 5-10

We start with a review of decomposition of rational primes into the product of algebraic primes in $\mathbb{Z}[\zeta]$ and the corresponding solutions to the norm equation. Then we proceed to the powers of rational primes and finally to the products of different rational primes, i.e. to the case of general r . In this section the notations k_j and l_j refer to quantities defined in (5.15.1).

7.1. For $r = 1$ the solutions to the corresponding norm equation $N(\alpha) = 1$ (Pell's equation) constitute the group of units $\mathbb{U}[\zeta] = \{1|0|1|0\}\mathbb{U}[\zeta]$. They represent the isosceles triangles in collections $[\circ|\circ|\circ+1]$ and $[\circ|\circ+1|\circ+1]$. Among them the triangles $\{1|0|1|0\}\mathbb{U}^+[\zeta]$, i.e., $\{l_j, k_j, l_j, -k_j\}$, form the collection $[\circ|\circ+1|\circ+1]$ whereas triangles $\{0, 1, 1, 0\}\mathbb{U}^+[\zeta]$, i.e., $\{k_j, l_j + 2k_j, l_j + 2k_j, k_j\}$, form the collection $[\circ|\circ|\circ+1]$. Obviously, the full solution coset $\{1|0|1|0\}\mathbb{U}[\zeta]$ is of Class A, and the corresponding $j^*(r) = 0$.

If r is a rational prime with $r \bmod 12 \in \{5, 7, 11\}$ then the corresponding norm equation does not have solutions as the decomposition $r = a^2 + b^2 + ab$ is impossible for $r \bmod 12 = 5, 11$, and the decomposition $r = a^2 + b^2$ is impossible for $r \bmod 12 = 7$. For $r = 2, 3$ the corresponding norm equation also does not have solutions for exactly the same reason.

The remaining rational primes are $r \bmod 12 = 1$. Each rational prime of this form has a unique decomposition (up to the multiplication by the unit from $\mathbb{U}[\zeta]$) into the product of 4 conjugated algebraic primes

$$r = \{m|n|k|l\}\{m, -n, k, -l\}\{k, l, m, n\}\{k, -l, m, -n\}, \quad (7.1)$$

which define a single full coset of $\mathbb{U}[\zeta]$. In other words, the integers m, n, k, l constituting the leader of the coset are uniquely defined by r . As before, the coset of $\mathbb{U}[\zeta]$ is partitioned into two cosets of $\mathbb{U}^+[\zeta]$ corresponding to two triangle collections.

Comparing the resulting coset with the original coset $\mathbb{U}[\zeta]$ one can see that the corresponding collections change from $[\circ|\circ|\circ+1]$ and $[\circ|\circ+1|\circ+1]$ to $[\circ|\circ+a|\circ+a+b]$ and $[\circ|\circ+b|\circ+a+b]$, respectively, where a, b are as in Eqn (5.19), (5.20).

The above argument verifies assertions of Theorems 5 and 6 for a rational prime r .

7.2. The next step is to consider r which is a square of a rational prime. Every rational prime w with $w \bmod 12 = 5$ admits a decomposition into the product of two self-conjugated algebraic primes: $w = \{m|n|m|n\}\{m, -n, m, -n\}$, and such a decomposition is unique. In addition, our definition of the leader implies that $0 < m < n$. Performing the multiplication we obtain $w = m^2 + n^2$ (a Gaussian representation). Consequently, for $r = w^2$ there exists a unique decomposition

$$w^2 = \{m|n|m|n\}^2\{m, -n, m, -n\}^2 \quad (7.2)$$

into the product of 4 conjugated algebraic integers, which generates a single full solution coset to the corresponding norm equation. Comparing this solution coset with the solution coset $\{1|0|1|0\}\mathbb{U}^+[\zeta]$ for $r = 1$, we observe that the isosceles triangles in the coset $\{m|n|m|n\}\mathbb{U}^+[\zeta]$ have the vertices $\{l_j m - k_j n, l_j n + k_j m, l_j m + k_j n, l_j n - k_j m\}$. They are obtained from the triangles $\{l_j, k_j, l_j, -k_j\}$ from the coset $\{1|0|1|0\}\mathbb{U}^+[\zeta]$ by the

magnifying rotation

$$T_{\square}(w) = \begin{pmatrix} m & n & 0 & 0 \\ -n & m & 0 & 0 \\ 0 & 0 & m & n \\ 0 & 0 & -n & m \end{pmatrix}. \quad (7.3)$$

which can be understood as the magnifying rotation $\begin{pmatrix} m & n \\ -n & m \end{pmatrix}$ in \mathbb{Z}^2 . Under $T_{\square}(w)$, the triangle collection is changing from $[\circ|\circ|\circ+1]$ to $[\circ|\circ|\circ+w]$. The same observation is true for the coset $\{1|0|1|0\}\mathbb{U}^+[\zeta](\zeta+\zeta^2) = \{0|1|1|0\}\mathbb{U}^+[\zeta]$ where under $T_{\square}(w)$ the triangle collection is changing from $[\circ|\circ+1|\circ+1]$ to $[\circ|\circ+w|\circ+w]$.

Further, every rational prime z with $z \bmod 12 = 7$ admits a decomposition into the product of two self-conjugated algebraic primes:

$$z = \{m|0|k|0\}\{k, 0, m, 0\},$$

and such a decomposition is unique. In addition, our definition of the leader implies that $0 < k < m$. Performing the multiplication we obtain $z = m^2 + k^2 - mk = (m - k)^2 + k^2 + (m - k)k$ (a Lösschian number). Consequently, for $r = z^2$ there exists a unique decomposition

$$z^2 = \{m|0|k|0\}^2\{k, 0, m, 0\}^2 \quad (7.4)$$

into the product of 4 conjugated algebraic integers, which generates a single full solution coset to the corresponding norm equation. The $\mathbb{U}[\zeta]^+$ -half of this coset (i.e. $\{m|0|k|0\}\mathbb{U}^+[\zeta]$) consist of the triangles

$$\{l_j m, k_j(2k - m), l_j k, -k_j(2m - k)\}$$

from collection $[\circ|\circ+2mk - m^2|\circ+2mk - k^2]$. This corresponds to the magnifying rotation

$$T_{\Delta}(z) = \begin{pmatrix} k & 0 & k - m & 0 \\ 0 & k & 0 & k - m \\ m - k & 0 & m & 0 \\ 0 & m - k & 0 & m \end{pmatrix} \quad (7.5)$$

which can be understood as the magnifying rotation $T_{\Delta}(z) = \begin{pmatrix} m & k - m \\ m - k & m \end{pmatrix}$ in the dual lattice \mathbb{A}_2 . The $\mathbb{U}[\zeta]^+(\zeta+\zeta^2)$ -half of the full coset (i.e. $\{m|0|k|0\}\mathbb{U}^+[\zeta](\zeta+\zeta^2) = \{m - k, k, m, k - m\}\mathbb{U}^+[\zeta]$) consists of the triangles from collection $[\circ|\circ+m^2 - k^2|\circ+2mk - k^2]$. The original cosets $\{1|0|1|0\}\mathbb{U}^+[\zeta]$ and $\{0|1|1|0\}\mathbb{U}^+[\zeta]$ have the corresponding values of a and b swapped, and the same property remains true for the resulting cosets (under the transformation $T_{\Delta}(z)$).

Next, every rational prime q with $q \bmod 12 = 11$ admits a decomposition into the product of two self-conjugated algebraic primes

$$q = \{m|n|m| - n\}\{m, -n, m, n\},$$

and this decomposition is unique. Performing the multiplication, we obtain $m^2 - 3n^2 = q$. Consequently, for $r = q^2$ there exists a unique decomposition

$$q^2 = \{m|n|m| - n\}^2\{m, -n, m, n\}^2 \quad (7.6)$$

into the product of 4 conjugated algebraic integers. This generates a single full solution coset $\{m|n|m|-n\}\mathbb{U}[\zeta]$ to the corresponding norm equation. The $\{m|n|m|-n\}\mathbb{U}^+[\zeta]$ -half of this coset consist of isosceles triangles

$$\{l_j m + k_j 3n, l_j n + k_j m, l_j m + k_j 3n, -l_j n - k_j m\}$$

from collection $[\circ|\circ|\circ+q]$. The $\{m|n|m|-n\}\mathbb{U}^+[\zeta](\zeta + \zeta^2)$ -half of this coset consists of isosceles triangles from collection $[\circ|\circ+q|\circ+q]$. This corresponds to the linear transformation

$$T_{\diamond}(q) = \begin{pmatrix} m & -n & 0 & -2n \\ n & m & 2n & 0 \\ 0 & 2n & m & n \\ -2n & 0 & -n & m \end{pmatrix} \quad (7.7)$$

which also can be understood as the linear transformation $T(q) = \begin{pmatrix} m & n \\ 3n & m \end{pmatrix}$ in the (t, s) lattice, i.e $\mathbb{Z}[\sqrt{3}]$ sub-ring of $\mathbb{Z}[\zeta]$.

The rational prime 2 is a product of two self-conjugated algebraic primes

$$2 = \{1|1|1|1\}\{1, -1, 1, -1\}$$

which are the same up to the multiplication by a unit $\{1, -1, 1, -1\} = \{1|1|1|1\}\zeta^9$. Consequently, for $r = 2^2$ there exists a unique decomposition

$$2^2 = \{1|1|1|1\}^2\{1, -1, 1, -1\}^2 \quad (7.8)$$

into the product of 4 conjugated algebraic integers, which generates a single full solution coset $\{1|1|1|1\}\mathbb{U}[\zeta]$ to the norm equation $N(\alpha) = 2^2$. This coset consist of isosceles triangles which are triangles from $\mathbb{U}[\zeta]$ transformed by the magnifying rotation

$$T_{\square}(2) = \begin{pmatrix} 1 & 1 & 0 & 0 \\ -1 & 1 & 0 & 0 \\ 0 & 0 & 1 & 1 \\ 0 & 0 & -1 & 1 \end{pmatrix}. \quad (7.9)$$

The resulting collections are $[\circ|\circ|\circ+2]$ and $[\circ|\circ+2|\circ+2]$ for each of the two halves of the full coset, respectively. E.g., the $\{1|1|1|1\}\mathbb{U}^+[\zeta]$ half is $\{l_j - k_j, l_j + k_j, l_j + k_j, l_j - k_j\}$.

The rational prime 3 is a product of two self-conjugated algebraic primes

$$3 = \{2|0|1|0\}\{1, 0, 2, 0\}$$

which are the same up to the multiplication by a unit $\{2|0|1|0\} = \{1, 0, 2, 0\}\zeta^{10}$. Consequently, for $r = 3^2$ there exists a unique decomposition

$$3^2 = \{2|0|1|0\}^2\{1, 0, 2, 0\}^2 \quad (7.10)$$

into the product of 4 conjugated algebraic integers. This again generates a single full solution coset $\{2|0|1|0\}\mathbb{U}[\zeta]$ to the norm equation $N(\alpha) = 3^2$. The resulting collections of isosceles triangles are $[\circ|\circ|\circ+3]$ and $[\circ|\circ+3|\circ+3]$ for each two halves of the full

coset, respectively. E.g., the $\{2|0|1|0\}\mathbb{U}^+[\zeta]$ half is $\{l_j 2, 0, l_j, k_j 3\}$ or, equivalently, $\{k_j 3, l_j, k_j 3, -l_j\}$. This correspond to the magnifying rotation

$$T_{\Delta}(3) = \begin{pmatrix} 1 & 0 & -1 & 0 \\ 0 & 1 & 0 & -1 \\ 1 & 0 & 2 & 0 \\ 0 & 1 & 0 & 2 \end{pmatrix} \quad (7.11)$$

in the dual lattice \mathbb{A}_2 .

By this moment we have verified the assertions of Theorems 5–8 for a value r that is a minimal power of a rational prime. The next portion of the argument deals with values r that are squares of the above.

7.3. For $r = w^4$ where $w \bmod 12 = 5$ there are 2 different possibilities to represent w^4 as the product of 4 conjugated algebraic integers. The first possibility contains all 4 conjugates of $\{m|n|m|n\}\{m, -n, m, -n\} = w$, which corresponds to $w^2 I$, where I is the identity matrix. The second possibility contains all 4 conjugates of $\{m|n|m|n\}^2 = \{m^2 - n^2, 2mn, m^2 - n^2, 2mn\}$, which corresponds to $T_{\square}(w)^2$. In the first case the resulting solution is the full coset $\{w|0|w|0\}\mathbb{U}[\zeta]$ containing w times magnified isosceles triangles $\{1|0|1|0\}\mathbb{U}^+[\zeta]$ and $\{0|1|1|0\}\mathbb{U}^+[\zeta]$ obtained earlier for $r = 1$. The corresponding triangle collections are $[\circ|\circ+w^2|\circ+w^2]$ and $[\circ|\circ|\circ+w^2]$ respectively. The second case results in the isosceles triangles obtained from triangles in $\{1|0|1|0\}\mathbb{U}[\zeta]$ by the magnifying rotation $T_{\square}(w)^2$. All details of this case can be recalculated from the case of $T_{\square}(w)$ via the map

$$m \mapsto m^2 - n^2, \quad n \mapsto 2mn. \quad (7.12)$$

It is clear that two full cosets (for two cases above) contain congruent (at given value of j) triangles rotated with respect to each other by $2 \arctan(n/m)$. This is a general mechanism behind a B0 family of solution cosets as stated in Theorem 7.

For $r = z^4$ where $z \bmod 12 = 7$ there are 2 different possibilities to represent z^4 as the product of 4 conjugated algebraic integers. The first possibility contains all 4 conjugates of $\{m|0|k|0\}\{k, 0, m, 0\} = z$, which corresponds to $z^2 I$. The second possibility contains all 4 conjugates of $\{m|0|k|0\}^2 = \{2mk - k^2, 0, 2mk - m^2, 0\}$, which corresponds to $T_{\Delta}(z)^2$. In the first case the resulting solution is the coset $\{z|0|z|0\}\mathbb{U}[\zeta]$ containing z times magnified isosceles triangles $\{1|0|1|0\}\mathbb{U}[\zeta]$ obtained earlier for $r = 1$. The corresponding triangle collections are $[\circ|\circ|\circ+z^2]$ and $[\circ|\circ+z^2|\circ+z^2]$. All details of the second case can be recalculated from the case of $T_{\Delta}(z)$ via the map

$$m \mapsto 2mk - k^2, \quad k \mapsto 2mk - m^2. \quad (7.13)$$

It is clear that two full cosets (for the two cases above) contain triangles of the same area (again for the same value of j). This is true because in both cases the area of the triangle is the solution to the same equation $t^2 - 3s^2 = 1$, and this solution is unique for a given j . This is a general mechanics behind a B1 family of solution cosets as stated in Theorem 8.

For $r = q^4$ where $q \bmod 12 = 11$ there are 2 different possibilities to represent q^4 as the product of 4 conjugated algebraic integers. The first possibility contains all 4 conjugates of $\{m|n|m| - n\}\{m, -n, m, n\} = p$, which corresponds to $q^2 I$. The second possibility

contains all 4 conjugates of $\{m|n|m|-n\}^2 = \{2m+3n, m+2n, 2m+3n, -m-2n\}$, which corresponds to $T_\diamond(q)^2$. In the first case the resulting solution is the full coset $\{q|0|q|0\}\mathbb{U}[\zeta]$ containing q times magnified isosceles triangles $\{1|0|1|0\}\mathbb{U}[\zeta]$ obtained earlier for $r = 1$. All details of the second case can be recalculated from the case of $T_\diamond(q)$ via the map

$$m \mapsto 2m + 3n, \quad n \mapsto m + 2n. \quad (7.14)$$

The triangle area (for a given value of j) is different for the two resulting full cosets of isosceles triangles though the triangle collection is the same for both full cosets. To be more specific, the $\mathbb{U}^+[\zeta]$ - and $\mathbb{U}^+[\zeta](\zeta + \zeta^2)$ -halves form collections $[\circ|\circ+q^2|\circ+q^2]$ and $[\circ|\circ|\circ+q^2]$ respectively. Note that triangles in each collections are mapped into itself under some \mathbb{Z}^2 -symmetry,

For $r = 2^4$ there is only one possibility to represent 2^4 as the product of 4 conjugated algebraic integers. This possibility contains all 4 conjugates of $\{1|1|1|1\}^2$ (which coincide with $\{1|1|1|1\}^2$ up to the multiplication by a unit). This is the case of $T_\square(2)^2$, and the resulting solution is the full coset $\{2|0|2|0\}\mathbb{U}[\zeta]$ containing triangles from collections $[\circ|\circ|\circ+4]$ and $[\circ|\circ+4|\circ+4]$.

For $r = 3^4$ there is only one possibility to represent 3^4 as the product of 4 conjugated algebraic integers. This possibility contains all 4 conjugates of $\{2|0|1|0\}$ (which coincide with $\{2|0|1|0\}^2$ up to the multiplication by a unit). This is the case of $T_\Delta(3)^2$, and the resulting solution is the full coset $\{3|0|3|0\}\mathbb{U}[\zeta]$ containing triangles from collections $[\circ|\circ|\circ+9]$ and $[\circ|\circ+9|\circ+9]$.

The case of $r = p^2$ where a rational prime p has $p \bmod 12 = 1$ is more diverse. In this case there are 4 distinct possibilities to represent r as a product of 4 conjugated algebraic integers. Starting from the decomposition

$$p = \{m|n|k|l\}\{m, -n, k, -l\}\{k, l, m, n\}\{k, -l, m, -n\}$$

we can form 4 products

$$\begin{aligned} & \{m|n|k|l\}\{m|n|k|l\}, \quad \{m, -n, k, -l\}\{m|n|k|l\}, \\ & \{k, l, m, n\}\{m|n|k|l\}, \quad \{k, -l, m, -n\}\{m|n|k|l\} \end{aligned} \quad (7.15)$$

coupling $\{m|n|k|l\}$ with any of its conjugates (including itself). The conclusion is that each couple together with its 3 conjugates constitutes the representation of r as the product of 4 conjugated algebraic integers. This corresponds to linear transformations $T_\square(p)T_\Delta(p)T_\diamond(p)/p$, $T_\Delta(p)$, $T_\square(p)$ and $T_\diamond(p)$ respectively and defines 4 distinct cosets of $\mathbb{U}[\zeta]$. Here

$$\begin{aligned} T_\square(p) &= \begin{pmatrix} g & h & 0 & 0 \\ -h & g & 0 & 0 \\ 0 & 0 & g & h \\ 0 & 0 & -h & g \end{pmatrix}, & T_\Delta(p) &= \begin{pmatrix} a & 0 & -b & 0 \\ 0 & a & 0 & -b \\ b & 0 & a & 0 \\ 0 & b & 0 & a \end{pmatrix}, \\ T_\diamond(p) &= \begin{pmatrix} t & s & 0 & -2s \\ -s & t & 2s & 0 \\ 0 & 2s & t & -s \\ -2s & 0 & s & t \end{pmatrix}, \end{aligned} \quad (7.16)$$

where g, h, a, b, s, t are expressed via m, n, k, l as in Eqns (5.19), (5.20). In particular, the coset corresponding to $T_{\square}(p)$ is p times scaled and rotated coset for $r = 1$. Cosets $T_{\square}(p)T_{\Delta}(p)T_{\diamond}(p)/p$ and $T_{\diamond}(p)$ have the same corresponding values of (t_j, s_j) but different signatures (a, b) and thus constitute a B1 family. The same is true for cosets $T_{\square}(p)$ and $T_{\Delta}(p)$.

This completes the part of the argument dealing with r that are the squares of the values discussed in **7.1** and **7.2**. This covers several cases in Theorems 5 – 8.

7.4. The situation becomes more involved when the corresponding power $\varrho(p) > 2$. The corresponding amount of different cosets

$$((\varrho(p) + 2)(2\varrho(p)^2 + 8\varrho(p) + 15 + 9(-1)^{\varrho(p)})/48 \quad (7.17)$$

is known as OEIS A053307 or spreading number $\alpha_3(\varrho(p))$ (see [17], [3], [39]). All these cosets can be partitioned into a single Class B1 family and remaining Class B2 families. We provide details for the cases $r = p^3$ and $r = p^4$ while the generalization to higher powers of p is straightforward. If $r = p^3$ and

$$p = \{m|n|k|l\}\{m, -n, k, -l\}\{k, l, m, n\}\{k, -l, m, -n\}$$

then the corresponding B1 family contains two cosets

$$\{m|n|k|l\}\{m|n|k|l\}\{m|n|k|l\}, \quad \{m|n|k|l\}\{k, -l, m, -n\}\{k, -l, m, -n\} \quad (7.18)$$

while the corresponding B2 family contains 3 cosets

$$\begin{aligned} \{m|n|k|l\}\{m, -n, k, -l\}\{m, -n, k, -l\}, \quad \{m|n|k|l\}\{k, l, m, n\}\{k, l, m, n\}, \\ \{m, -n, k, -l\}\{k, l, m, n\}\{k, -l, m, -n\}. \end{aligned} \quad (7.19)$$

The first and the third cosets from the B2 family contain congruent triangles (for the same j). This conclusion becomes transparent if we use the representation of conjugates of p via commuting linear transformations $T_{\bullet}(p)$:

$$\begin{aligned} \{m|n|k|l\} &\rightarrow \sqrt{1/p}T_{\square}^{1/2}(p)T_{\Delta}^{1/2}(p)T_{\diamond}^{1/2}(p), \\ \{m, -n, k, -l\} &\rightarrow \sqrt{p}T_{\square}^{-1/2}(p)T_{\Delta}^{1/2}(p)T_{\diamond}^{-1/2}(p), \\ \{k, l, m, n\} &\rightarrow \sqrt{p}T_{\square}^{1/2}(p)T_{\Delta}^{-1/2}(p)T_{\diamond}^{-1/2}(p), \\ \{k, -l, m, -n\} &\rightarrow \sqrt{p}T_{\square}^{-1/2}(p)T_{\Delta}^{-1/2}(p)T_{\diamond}^{1/2}(p). \end{aligned} \quad (7.20)$$

Similarly, if $r = p^4$ then the corresponding B1 family \mathfrak{B}_1 consists of 3 cosets

$$\begin{aligned} \{m|n|k|l\}\{m|n|k|l\}\{m|n|k|l\}\{m|n|k|l\}, \\ \{m|n|k|l\}\{m|n|k|l\}\{m|n|k|l\}\{k, -l, m, -n\}, \\ \{m|n|k|l\}\{m|n|k|l\}\{k, -l, m, -n\}\{k, -l, m, -n\}. \end{aligned} \quad (7.21)$$

The corresponding two B2 families $\mathfrak{B}_2^{(1)}$ and $\mathfrak{B}_2^{(2)}$ are

$$\begin{aligned} \{m|n|k|l\}\{m|n|k|l\}\{m|n|k|l\}\{m, -n, k, -l\}, \\ \{m|n|k|l\}\{m|n|k|l\}\{m|n|k|l\}\{k, l, m, n\}, \\ \{m|n|k|l\}\{m|n|k|l\}\{m, -n, k, -l\}\{k, -l, m, -n\}, \\ \{m|n|k|l\}\{m|n|k|l\}\{k, l, m, n\}\{k, -l, m, -n\} \end{aligned} \quad (7.22)$$

and

$$\begin{aligned}
& \{m|n|k|l\}\{m|n|k|l\}\{m, -n, k, -l\}\{m, -n, k, -l\}, \\
& \quad \{m|n|k|l\}\{m|n|k|l\}\{k, l, m, n\}\{k, l, m, n\}, \\
& \quad \{m|n|k|l\}\{m|n|k|l\}\{m, -n, k, -l\}\{k, l, m, n\}, \\
& \{m|n|k|l\}\{m, -n, k, -l\}\{k, l, m, n\}\{k, -l, m, -n\}.
\end{aligned} \tag{7.23}$$

Among them the cosets

$$\begin{aligned}
& \{m|n|k|l\}\{m|n|k|l\}\{m|n|k|l\}\{m, -n, k, -l\}, \\
& \quad \{m|n|k|l\}\{m|n|k|l\}\{m|n|k|l\}\{k, l, m, n\}
\end{aligned} \tag{7.24}$$

contain congruent triangles (labeled by the same j). Similarly, the cosets

$$\begin{aligned}
& \{m|n|k|l\}\{m|n|k|l\}\{m, -n, k, -l\}\{m, -n, k, -l\}, \\
& \{m|n|k|l\}\{m, -n, k, -l\}\{k, l, m, n\}\{k, -l, m, -n\}
\end{aligned} \tag{7.25}$$

also contain congruent triangles (again with the same label j). For larger values $\varrho(p)$ the corresponding B1 family contains $[\varrho(p)/2] + 1$ cosets

$$\begin{aligned}
& T_{\square}^{\varrho(p)/2}(p) T_{\Delta}^{\varrho(p)/2}(p) T_{\diamond}^{\varrho(p)/2}(p) p^{-\varrho(p)/2}, \\
& p T_{\square}^{(\varrho(p)-2)/2}(p) T_{\Delta}^{(\varrho(p)-2)/2}(p) T_{\diamond}^{\varrho(p)/2}(p) p^{-\varrho(p)/2}, \\
& p^2 T_{\square}^{(\varrho(p)-4)/2}(p) T_{\Delta}^{(\varrho(p)-4)/2}(p) T_{\diamond}^{\varrho(p)/2}(p) p^{-\varrho(p)/2}, \dots
\end{aligned} \tag{7.26}$$

which all have different signatures (as they correspond to different powers of T_{Δ}).

Adding the next power of p , i.e. considering $\varrho(p)+1$ instead of $\varrho(p)$ splits this B1 family into Class B1 and Class B2 families. The Class B1 family corresponds to multiplication by conjugates $T_{\square}^{1/2}(p)T_{\Delta}^{1/2}(p)T_{\diamond}^{1/2}(p)/\sqrt{p}$ and $T_{\square}^{-1/2}(p)T_{\Delta}^{-1/2}(p)T_{\diamond}^{1/2}(p)\sqrt{p}$. The Class B2 family corresponds to the multiplication by conjugates $T_{\square}^{1/2}(p)T_{\Delta}^{-1/2}(p)T_{\diamond}^{-1/2}(p)\sqrt{p}$ and $T_{\square}^{-1/2}(p)T_{\Delta}^{1/2}(p)T_{\diamond}^{-1/2}(p)\sqrt{p}$.

The arbitrary powers of prime factors 2, 3, q , w , z behave in a somewhat simpler fashion (we continue using letters w, z, q for primes having values 5, 7, 11, respectively, modulo 12). The factor $2^{2\varrho(2)}$ generates a single solution coset $T_{\square}(2)^{\varrho(2)}$ which is the $2^{\varrho(2)}$ -times magnification of the coset corresponding to $r = 1$. Similarly, the factor $3^{2\varrho(3)}$ generates a single coset $T_{\square}(3)^{\varrho(3)}$.

Each factor $w^{2\varrho(w)}$ generates $[\varrho(w)/2] + 1$ cosets

$$T_{\square}(w)^{\varrho(w)}, T_{\square}(w)^{\varrho(w)-2}w^2, T_{\square}(w)^{\varrho(w)-4}w^4, \dots, \tag{7.27}$$

which form a Class B0 family. We count here only non-negative powers of $T_{\square}(w)$ because all triangles in these cosets are \mathbb{Z}^2 -symmetric (and therefore isosceles).

Next, each factor $z^{2\varrho(z)}$ generates $[\varrho(z)/2] + 1$ cosets

$$T_{\Delta}(z)^{\varrho(z)}, T_{\Delta}(z)^{\varrho(z)-2}z^2, T_{\Delta}(z)^{\varrho(z)-4}z^4, \dots, \tag{7.28}$$

which form a Class B1 family. We count here only non-negative powers of $T_{\Delta}(z)$ because all triangles in these cosets are \mathbb{A}_2 -symmetric.

Further, each factor $q^{2\varrho(q)}$ generates $[\varrho(q)/2] + 1$ Class A cosets

$$T_{\Delta}(q)^{\varrho(q)}, T_{\Delta}(q)^{\varrho(q)-2}q^2, T_{\Delta}(q)^{\varrho(q)-4}q^4, \dots \tag{7.29}$$

They again consist of \mathbb{Z}^2 -symmetric triangles.

7.5. The arguments in **7.1** – **7.4** cover the situation where r is an arbitrary power of a single rational prime number. To complete the proof of Theorems 5 – 10 one needs to understand what happens when powers of different primes are combined with each other. Viz., consider $r = \prod_j q_j^2$ and assume that the corresponding statement of Theorem 6 is already verified for r (the initial case $r = 1$ is straightforward). Then $r = q^2 \prod_j q_j^2$ has a doubled number of solution cosets, and each of them is of Class A. This is true because every partitioning of $\prod_j q_j^2$ into the product of 4 conjugated algebraic integers can be combined with each of two partitioning of q into the product of 4 conjugated algebraic integers. In this way we are able to form every partitioning of $q^2 \prod_j q_j^2$ into the product of 4 conjugated algebraic integers. It is not hard to see that an additional factor p , w^2 or z^2 also doubles the amount of cosets, and all of them still are of Class A. In addition, the factor w^2 magnifies and rotates all triangles in each coset while the factor z^2 changes the signature of all triangles in each coset. The factor p performs 3 transformations $T_{\square}^{1/2}$, $T_{\triangle}^{1/2}$ and $T_{\diamond}^{1/2}$ simultaneously. Observe that the presence of any additional factor p , w^2 or z^2 breaks the \mathbb{Z}^2 -symmetry of the initial coset. This symmetry-breaking is responsible for the difference in the coset count between $r = q^{2\varrho(q)}$ and $r = * \cdot r$ where $*$ = p, w^2 or z^2 . A general case where each q_j enters the product at an arbitrary even power $2\varrho(q_j)$ is similar but the total number of cosets cannot be expressed as an elementary function of values $\varrho(q_j)$. This comes as a result of different symmetry properties of different cosets generated by single factor $q_j^{2\varrho(q_j)}$. Consequently, different pairs of cosets corresponding to $q_{j'}^{2\varrho(q_{j'})}$ and $q_{j''}^{2\varrho(q_{j''})}$ generate different amount of cosets corresponding to the product $q_{j'}^{2\varrho(q_{j'})} q_{j''}^{2\varrho(q_{j''})}$, and the resulting total amount turns out to be smaller than $[(\varrho(q_{j'})/2) + 1][(\varrho(q_{j''})/2) + 1]$.

Now we can take any r of the above type and start adding factors w_k^2 . The first of them, w_1^2 , doubles the number of cosets and converts each Class A coset into two cosets forming a Class B0 family. The first of the cosets in the pair corresponds to the magnifying rotation $T_{\square}(w_1)$ while the second one correspond to magnification $w_1^2 I$. Adding another factor w_2^2 doubles the number of cosets in each B0 family, and so on. A generalization to the case $\prod_k w_k^{2\varrho(w_k)}$ is straightforward but is affected by a similar inability to express the resulting amount of B0 families as an elementary function of $\varrho(w_k)$.

The statements of Theorem 8 regarding Class B1 families are verified in a similar way. The only difference is that B1 families are generated by two types of prime factors: p_i and $z_i^{2\varrho(z_i)}$. Recall that the factors $p_i^{\varrho(p_i)}$ with $\varrho(p_i) > 1$ also generate Class B1 families but they are accompanied by Class B2 families.

A simpler way to generate Class B2 families is to combine factors p_i and/or $w_k^{2\varrho(w_k)}$ with factors $z_i^{\varrho(z_i)}$. Observe that, due to \mathbb{Z}^2 -symmetry of triangles generated by a single w^2 factor, adding a single z^2 factor produces a single Class B1 family containing two cosets with different signatures. Nevertheless, an additional p or w_1^2 factor converts this family into two B2 families (due to the fact that $w^2 p$ or $w^2 w_1^2$ generate two cosets forming a B0 family). Any additional factor z_i^2 doubles the amount of cosets in each of two families. Finally, any additional factor w_k^2 doubles the amount of B2 families.

In view of earlier considerations, additional factors $2^{2\varrho(2)}$ and/or $3^{2\varrho(3)}$ change neither the amount of cosets nor the class type of the family nor the amount of cosets in a given family.

8 Proof of Theorem S

A characteristic pattern of sliding is that we have a \mathbb{Z}^2 -trapeze $OABW$ where both $\triangle OAW$ and $\triangle OBW$ are M-triangles, and side OW is the base of sliding, with $|OA| = |BW|$. Cf. Figures 1C and 6. (The property $|OA| = |BW|$ may require to re-label some vertices.) Let $z = |AB|$. Then we say that each of the M-triangles OAW and OBW has z -sliding (for a given D).

The following Lemmas 8.1 and 8.3 are essentially repetitions of Theorem 2 and Lemma 2.1 from [28].

Lemma 8.1. *For a D -admissible M-triangle \triangle with z -sliding the corresponding doubled area $A(\triangle)$ is bounded from below as follows*

$$A(\triangle) > \frac{1}{2}D\sqrt{(3D-1)(D+z)}. \quad (8.1)$$

Proof. The trapeze $OABW$ is a cyclic quadrilateral; therefore

$$|OB| \cdot |WA| = |AB| \cdot |OW| + |OA| \cdot |WB|. \quad (8.2)$$

As $|OA| = |WB|$ and $|OB| = |WA|$, we have

$$|WA|^2 = |AB| \cdot |OW| + |OA|^2. \quad (8.3)$$

Observe that $|OW|, |OA| \geq D$. Hence, $|WA|$ is minimal when $|AB| = z$ and $|OW| = |OA| = D$. In this case $|WA|^2 = D^2 + zD$ and

$$A(\triangle) \geq \frac{1}{2}D\sqrt{(3D-1)(D+z)}. \quad (8.4)$$

■

Lemma 8.2. *For $D > 30$ and $z^2 \geq 14$ there is no z -sliding.*

Proof. According to estimate (3.1) in Lemma 3.4.4 the doubled area of M-triangle $S(D) < \frac{\sqrt{3}D^2}{2} + \sqrt{2}D$. It is not hard to see that

$$\frac{\sqrt{3}D^2}{2} + \sqrt{2}D < \frac{1}{2}D\sqrt{(3D-1)(D+z)}$$

for $D > 30$ and $z^2 \geq 14$. Now one can apply Lemma 8.1. ■

For $x \in \mathbb{R}$ let $\{x\}$ be the fractional part of x , $\llbracket x \rrbracket$ an integer closest to x and

$$\{\!\!\{x\}\!\!\} = \min\left(\{x\}, 1 - \{x\}\right) = \left|x - \llbracket x \rrbracket\right|. \quad (8.5)$$

The most important idea in [28] is the way to construct admissible triangles with small enough area which is described in Lemma 8.3 below. For small z the corresponding estimate (8.7) is better than (3.1).

Lemma 8.3. *A \mathbb{Z}^2 -triangle Δ with vertices*

$$(0, 0), \quad (\llbracket x - \sqrt{3}y \rrbracket, \llbracket y + \sqrt{3}x \rrbracket), \quad (2x, 2y) \quad (8.6)$$

has all sides longer than D and a double area

$$A(\Delta) < \left(D + \frac{z}{10}\right) \left(\frac{\sqrt{3}}{2}D + \frac{z\sqrt{2} + z\sqrt{3}}{20}\right) < \frac{1}{2}D\sqrt{(3D-1)(D+z)} \quad (8.7)$$

as soon as

$$1 \leq z < 12, \quad D > 5, \quad \{\{x\sqrt{3}\}\}, \{\{y\sqrt{3}\}\} < \frac{z}{20}$$

and

$$D + \frac{z\sqrt{2}}{20} \leq \sqrt{4x^2 + 4y^2} \leq D + \frac{z}{10}. \quad (8.8)$$

Proof. Observe that under the assumptions on $\sqrt{4x^2 + 4y^2}$ in (8.8) the distance \bar{D} from the point $(x - \sqrt{3}y, y + \sqrt{3}x)$ to each of two sites $(0, 0)$ and $(2x, 2y)$ is upper-bounded by

$$D + \frac{z\sqrt{2}}{20} \leq \bar{D} \leq D + \frac{z}{10}, \quad (8.9)$$

as the corresponding triangle is equilateral. Owing to the assumptions on $\{\{\cdot\}\}$ in (8.8), the distance between site $(\llbracket x - \sqrt{3}y \rrbracket, \llbracket y + \sqrt{3}x \rrbracket)$ and point $(x - \sqrt{3}y, y + \sqrt{3}x)$ is at most $z\sqrt{2}/20$. Thus, by the triangle inequality all sides of Δ are longer than D .

To estimate the doubled area of Δ , observe that the base of Δ is shorter than $D + z/10$ while the corresponding height can be estimated as

$$\frac{\sqrt{3}}{2} \left(D + \frac{z}{10}\right) + \frac{z\sqrt{2}}{20} = \frac{\sqrt{3}}{2}D + \frac{z\sqrt{2} + z\sqrt{3}}{20}. \quad (8.10)$$

Therefore,

$$A(\Delta) \leq \left(D + \frac{z}{10}\right) \left(\frac{\sqrt{3}}{2}D + \frac{z\sqrt{2} + z\sqrt{3}}{20}\right). \quad (8.11)$$

A direct calculation verifies that the last inequality in (8.7) holds true for $1 < z < 12$ and $D > 5$. \blacksquare

Lemma 8.4. *Consider a countable set of integers*

$$\left\{x \in \mathbb{Z} : \{\{\sqrt{3}x\}\} < \frac{1}{20}\right\} \quad (8.12)$$

and numerate them as x_n in increasing order (so that $x_n < x_{n+1}$). Then for $n > 1$

$$x_{n+1} - x_n \in \{4, 11, 15\} \quad (8.13)$$

Proof. Consider the following fractional parts

$$\begin{aligned} \delta_{11} &= \{11\sqrt{3}\} \approx 0.05255888325764957, \\ \delta_4 &= \{4\sqrt{3}\} \approx 0.9282032302755088, \\ \delta_{15} &= \{15\sqrt{3}\} \approx 0.9807621135331566. \end{aligned}$$

If $0.95 < \{\sqrt{3}x_n\} < 1.9 - \delta_4$ then $x_{n+1} = x_n + 4$. If $1.9 - \delta_4 < \{\sqrt{3}x_n\} < 1$ or $0 < \{\sqrt{3}x_n\} < \delta_{11} - 0.05$ then $x_{n+1} = x_n + 15$. If $\delta_{11} - 0.05 < \{\sqrt{3}x_n\} < 0.05$ then $x_{n+1} = x_n + 11$. It is a direct calculation to verify that $\{\{\sqrt{3}x_n + j\}\} > 0.05$ for any other positive integer j smaller than 15. ■

Lemma 8.5. *Consider a countable set of integers*

$$\left\{ d = 4x^2 + 4y^2 : x, y \in \mathbb{Z}, \{\{\sqrt{3}x\}\}, \{\{\sqrt{3}y\}\} < \frac{1}{20} \right\} \quad (8.14)$$

and numerate them as d_n in increasing order, as above. Then for $d_n > 810000$

$$d_{n+1} - d_n \leq 477\sqrt[4]{d_n}. \quad (8.15)$$

Proof. Given an integer $d \geq 1$, find n_1 such that

$$4x_{n_1}^2 \leq d \leq 4x_{n_1+1}^2. \quad (8.16)$$

Then, according to Lemma 8.4,

$$4x_{n_1+1}^2 - 4x_{n_1}^2 < 120x_{n_1} + 900 < 60\sqrt{d} + 900 \leq 61\sqrt{d}, \quad (8.17)$$

where the last inequality is true for $d \geq 810000$. Now find n_2 such that

$$4x_{n_1}^2 + 4x_{n_2}^2 \leq d \leq 4x_{n_1}^2 + 4x_{n_2+1}^2. \quad (8.18)$$

Then

$$4x_{n_2+1}^2 - 4x_{n_2}^2 < 120x_{n_2} + 900 < 61\sqrt{4x_{n_1+1}^2 - 4x_{n_1}^2} < 61\sqrt{61\sqrt{d}} < 477\sqrt[4]{d}. \quad (8.19)$$

Taking $d = d_n$ finishes the proof. ■

Lemma 8.6. *For $1 \leq z < 12$ and any $D = \sqrt{d}$, there exists $\bar{d} \in \mathbb{N}$ such that*

$$\left(D + \frac{z\sqrt{2}}{20} \right)^2 \leq \bar{d} \leq \left(D + \frac{z}{10} \right)^2, \quad \bar{d} = 4x^2 + 4y^2, \quad \{\{\sqrt{3}x\}\}, \{\{\sqrt{3}y\}\} < \frac{1}{20} \leq \frac{z}{20}$$

as soon as $D > 66438468 z^{-2}$. Consequently there is no z -sliding for $D > 66438468 z^{-2}$.

Proof. Set $\hat{d} = (D + z\sqrt{2}/20)^2$. According to Lemma 8.3, there exists \bar{d} such that

$$\hat{d} \leq \bar{d} \leq \hat{d} + 477\sqrt[4]{\hat{d}}, \quad \bar{d} = 4x^2 + 4y^2, \quad \{\{\sqrt{3}x\}\}, \{\{\sqrt{3}y\}\} < \frac{1}{20}. \quad (8.20)$$

Therefore,

$$\bar{d} \leq \left(D + \frac{z\sqrt{2}}{20} \right)^2 + 477\sqrt{D + \frac{z\sqrt{2}}{20}} \leq \left(D + \frac{z}{10} \right)^2 \quad (8.21)$$

as soon as $D > 66438468 z^{-2}$. Indeed, in terms of $\bar{D} := D/477$ and $\bar{z} := z\sqrt{2}/(20 \cdot 477)$ we need

$$\begin{aligned}
& (\bar{D} + \sqrt{2}\bar{z})^2 - (\bar{D} + \bar{z})^2 - \sqrt{\frac{\bar{D}}{477} + \frac{\bar{z}}{477}} > 0, \\
& (2(\sqrt{2} - 1)\bar{D}\bar{z} + \bar{z}^2)^2 > \frac{\bar{D}}{477} + \frac{\bar{z}}{477}, \\
& \bar{z}^2 4(\sqrt{2} - 1)^2 \left(\bar{D} + \frac{\bar{z}}{2(\sqrt{2} - 1)} \right) 477 > 1, \\
& D > \frac{477^2 \cdot 200}{4(\sqrt{2} - 1)^2 z^2},
\end{aligned} \tag{8.22}$$

which holds for $D > 66438468 z^{-2} = 292 \cdot 477^2 z^{-2}$. \blacksquare

Lemma 8.7. *Suppose $z^2 = p^2 + q^2$ where integers $p, q \geq 1$ are mutually prime, and there is no z -sliding. Then there is no kz -sliding for any positive integer k .*

Proof. If there exists kz -sliding then the segment AB contains $k + 1$ lattice sites at distance z from each other. Among them any two consecutive sites generate z -sliding which is impossible. \blacksquare

Lemma 8.8. *Let $z^2 = p^2 + q^2$ and $\bar{z}^2 = \bar{p}^2 + \bar{q}^2$ where integers $p, q \geq 1$ are mutually prime and $\bar{p}, \bar{q} \geq 0$ are mutually prime, with $\bar{z}^2 \geq 1$. If all 4 vertices of a trapeze implementing a $z \cdot \bar{z}$ -sliding belong to the skewed sub-lattice $\mathbb{Z}^2 \begin{pmatrix} \bar{p} & \bar{q} \\ -\bar{q} & \bar{p} \end{pmatrix}$ then this trapeze is a \bar{z} times magnified version of a trapeze implementing z -sliding.*

Proof. If for the scaled down triangle there exists an admissible triangle with a smaller area then the same is true for the scaled up version of this admissible triangle. \blacksquare

Given integers z^2, \bar{z}^2, p, q and \bar{p}, \bar{q} as in Lemma 8.9, we define a (\bar{p}, \bar{q}) -constrained z -sliding as a z -sliding with additional requirement that all vertices of an implementing trapeze $OABW$ belong to $\mathbb{Z}^2 \begin{pmatrix} \bar{p} & \bar{q} \\ -\bar{q} & \bar{p} \end{pmatrix}$.

Lemma 8.9. *Let $z^2 = p^2 + q^2$ where integers $p, q \geq 1$ are mutually prime. If there is a z -sliding then it is a (p, q) -constrained z^2 -sliding.*

Proof. The lemma is a direct consequence of the observation that for lattice \mathbb{Z}^2 hosting a (p, q) -constrained z^2 -sliding its $\mathbb{Z}^2 \begin{pmatrix} p & q \\ -q & p \end{pmatrix}$ sub-lattice hosts a z -sliding. \blacksquare

Lemma 8.10. *Suppose $z^2 = p^2 + q^2$ where $p, q \geq 1$ are mutually prime integers. Consider an instance of (p, q) -constrained z^2 -sliding implemented by the trapeze with vertices*

$$(0, 0), \quad (\bar{x}, y), \quad (\bar{x} + z^2, y), \quad (x, 0), \tag{8.23}$$

where $x, \bar{x}, y \in \mathbb{N}$, $x \bmod z^2 = 0$ and $x - 2z^2 < 2\bar{x} < x - z^2$. Then

$$\sqrt{3\bar{x}} < y < \sqrt{3\bar{x}} + \frac{4}{\sqrt{3}}z^2 + 1 \tag{8.24}$$

and

$$\frac{\sqrt{3}}{2}x - \sqrt{3}z^2 < y < \frac{\sqrt{3}}{2}x + \frac{1}{\sqrt{3}}z^2 + 1. \quad (8.25)$$

Consequently, given \bar{x} or x , only 3 corresponding values of y are possible.

Proof. For any trapeze with vertices as in (8.23) which is a candidate for a (p, q) -constrained z^2 -sliding, either $d = x^2$ or $d = (x - \bar{x} - z^2)^2 + y^2$. If $(x - z^2)^2 \geq d$ then the admissible triangle with vertices

$$(0, 0), \quad (\bar{x}, y), \quad (x - z^2, 0) \quad (8.26)$$

has a smaller area. Therefore, $(x - z^2)^2 < (x - \bar{x} - z^2)^2 + y^2$, implying

$$y^2 > 2x\bar{x} - \bar{x}^2 - 2\bar{x}z^2 > 3\bar{x}^2 > 3\left(\frac{x}{2} - z^2\right)^2. \quad (8.27)$$

As p and q are mutually prime there exists $\bar{x} < \hat{x} < \bar{x} + z^2$ such that $(\hat{x}, y - 1)$ belongs to sub-lattice $\mathbb{Z}^2 \begin{pmatrix} p & q \\ -q & p \end{pmatrix}$. The condition that the triangle with vertices

$$(0, 0), \quad (\hat{x}, y - 1), \quad (x - z^2, 0) \quad (8.28)$$

is not admissible is $(\min(\hat{x}, x - \hat{x}))^2 + (y - 1)^2 < x^2$. Consequently,

$$(y - 1)^2 < \frac{3}{4}x^2 + xz^2 - z^4 < 3\bar{x}^2 + 8z^2\bar{x} + 4z^4. \quad (8.29)$$

■

Lemma 8.11. *All existing 39 instances of z -sliding are listed in Table 2.*

Proof. Due to Lemma 8.6, we only need to examine $D < \bar{D} = 66438468$ and due to Lemma 8.2 only with $z^2 < 14$. This investigation is done via a computer-assisted enumeration by `ZSliding.java`. Given integers $z^2 = p^2 + q^2$ and $d = D^2$ we need to (i) enumerate all d -admissible triangles which are *candidates* for z -sliding and (ii) perform an exhausting search for an *improvement*, i.e. a d -admissible triangle with smaller area.

To construct an efficient algorithm we consider an auxiliary unit square lattice $\mathbb{Z}_{p,q}^2$ and embed into it z^2 times magnified original unit lattice. For definiteness we assume that this embedding is given by sublattice $\mathbb{Z}_{p,q}^2 \begin{pmatrix} p & q \\ -q & p \end{pmatrix}$. Inside $\mathbb{Z}_{p,q}^2$ any z^2 times magnified trapeze $OABW$ that is a z -sliding candidate has an embedding with sides AB and OW being horizontal. Thus, placing the trapeze vertex O at the origin we only need to choose vertex W from the list of sites $(z^2, 0), (2z^2, 0), (3z^2, 0), \dots, ([\bar{D}/z^2]z^2, 0)$, which grows linearly in \bar{D} . With vertex W being selected, there are at most $3\lceil z^2/2 \rceil$ possible positions for vertex A satisfying $|OA| \leq |OB|, |AW|, |BW|$. The $3\lceil z^2/2 \rceil$ -upper bound is a consequence of Lemma 8.11; accordingly, we obtain $O(\bar{D})$ candidates for z -sliding to examine.

Now, for each of z -sliding candidates we need to find an improvement. The candidates without an improvement are the desired instances of z -sliding. Given a trapeze $OABW$ with $|OW| = X$, there are $O(X^2z^{-4})$ possibilities to select the second vertex of the

improvement and $O(1)$ possibilities to then select the third vertex. This amounts to $O(\overline{D}^2)$ iterations for each of $O(\overline{D})$ candidates. The total order of an $O(\overline{D}^3)$ enumeration is unreachable to modern computers. To this end, we use an empirical approach to achieve a reasonable calculation time. Namely, given $W = (X, 0)$, we perform the search for the second vertex of an improvement in the following order:

$$\begin{aligned} & (X - 1, 0), (X - 1, 1), \dots, (X - 1, X), \\ & (X - 2, 0), (X - 2, 1), \dots, (X - 2, X), \\ & \dots \end{aligned} \tag{8.30}$$

In the worst situation it still requires $O(X^2 z^{-4})$ iterations. Because of that we additionally limit the search for the second coordinate to only 10 attempts, i.e. we perform the following enumeration

$$\begin{aligned} & (X - 1, 0), (X - 1, 1), \dots, (X - 1, 10), \\ & (X - 2, 0), (X - 2, 1), \dots, (X - 2, 10), \\ & \dots \end{aligned} \tag{8.31}$$

Now it is $O(Xz^{-2})$ iterations summing up to a total $O(\overline{D}^2)$ iterations for the entire algorithm, which is still a considerable lot. Nevertheless, it appears that typically the improvement is found already among $(X - 1, \cdot)$, and the algorithm rarely goes to $(X - 1, \cdot)$ or further. Because of that the actual amount of iterations performed by the algorithm is of order $O(\overline{D})$, and on a mediocre personal computer the entire algorithm finishes in less than 5 hours.

Due to a non-exhaustive nature of our empirical search for an improvement, any identified instance of z -sliding needs to be additionally verified to be an actual instance of z -sliding. In practice, all 39 instances of sliding detected by the algorithm are those listed in Table 2.

We also stress that our algorithm performs a search only among integers $z^2 < 14$ which correspond to mutually prime integers p and q . The algorithm finds no sliding for (p, q) pairs different from $(1, 0)$ and $(1, 1)$. Due to Lemmas 8.7–8.9, the last step is to verify that, being scaled more than $\sqrt{2}$ times but less than 12 times, none of the 39 sliding instances generate an additional instance of z -sliding. This appears to be the case, which completes our computer-assisted proof. ■

Acknowledgement. IS and YS thank the Math Department, Penn State University, for hospitality and support. YS thanks St John’s College, Cambridge, for long-term support.

References

- [1] Akimenko, S.S., Gorbunov, V.A., Myshlyavtsev, A.V., Stishenko, P.V. The renormalization group study of hard-disk model on a triangular lattice. *Phys. Rev. E* **100** (2019), 022108.

- [2] Akimenko, S., Myshlyavtsev, A., Myshlyavtseva, M., Gorbunov, V., Podgornyi, S., Solovyeva, O. Triangles on triangular lattice: insights into self-assembly in two dimensions driven by shape complementarity. *Phys. Rev. E* **105** (2022), 044104.
- [3] Babcock, B., Van Tyle, A. Revisiting the Spreading and Covering Numbers, *Australian Journal of Combinatorics*, **56** (2013), 77-84.
- [4] Barbier, J., Krzakala, F., Zdeborova, L., Zhang, P. The hard-core model on random graphs revisited. *J. Phys.: Conf. Ser.* **473**, 012021 (2013).
- [5] Borevich, Z.I., Shafarevich, I.R. *Number theory*. Pure and Applied Mathematics, **20**. New York–Boston: Academic Press, 1966.
- [6] Bricmont, J., Slawny, J. Phase transitions in systems with a finite number of dominant ground states. *J. Stat. Physics*, **54**, (1989), 89-161.
- [7] Chang, H.-C., Wang, L.-C. A simple proof of Thue’s theorem on circle packing. arXiv:1407.2199, (2010).
- [8] Charbonneau, P., Kurchan, J., Parisi, G., Urbani, P., Zamponi, F. Glass and jamming transitions: from exact results to finite-dimensional descriptions. *Annual Rev. Cond. Mat. Phys.*, **8** (2016), 1-26.
- [9] Cohn, H., Kumar, A.D., Miller, S.D., Radchenko, D., Viazovska, M. The sphere packing problem in dimension 24. *Annals of Math.*, **185** (2017), 1017-1033.
- [10] Darjani, S., Koplik, J., Banerjee, S., Pauchard, V. Liquid-hexatic-solid phase transition of a hard-core lattice gas with with third neighbor exclusion. *J. Chem. Phys.* **151** (2019), 104702.
- [11] De Loera, J.A., Rambau, J., Santos, F. *Triangulations. Structures for algorithms and applications*. Heidelberg: Springer, 2010.
- [12] Dekker, T.J., Prime numbers in quadratic fields. *CWI Quarterly*, **7** (1994), 367–394; Primes in quadratic fields. arXiv: 1001.5214, (2010).
- [13] Dobrushin R.L. The problem of uniqueness of a Gibbsian random field and the problem of phase transitions. *Funct. Anal. Appl.* **4:4** (1968), 302–312.
- [14] Dobrushin, R.L., Shlosman S. The problem of translation invariance of Gibbs states at low temperatures. *Mathematical Physics Reviews* **5**, 53-195. Soviet Sci. Rev. Sect. C Math. Phys. Rev., 5, Harwood Academic Publ., Chur, 1985.
- [15] Fejes Tóth, L. Some packing and covering theorems. *Acta Sci. Math.*, **12A** (1950), 62-67.
- [16] Fernandes, H.C.M., Arenzon, J.J., Levin, Y. Monte carlo simulation of two-dimensional hard core lattice gases. *J. Chem. Phys.* **126** (2007), 114508.
- [17] Geramita, A., Gregory, D., Roberts, L. Monomial Ideals and Points in Projective Space, *J. Pure and Applied Algebra* **40** (1986), 33-62.

- [18] Georgii, H.-O. *Gibbs measures and phase transitions*. Berlin/New York: De Gryuter, 2011.
- [19] Grosswald, E. *Representation of integers as sum of Squares* New York: Springer, 1985.
- [20] Grosswald, E. *Topics from the theory of numbers* (2nd Edition). Cambridge: CUP, 2008.
- [21] Hadas, D., Peled, R. Columnar order in random packings of 2×2 squares on the square lattice. arXiv:2206.01276, (2022).
- [22] Hales, T.C. A proof of the Kepler conjecture. *Annals of Math.*, **162** (2005), 1065-1185.
- [23] Hsiang, W-Y. Simple proof of a theorem of Thue on the maximal density of circle packings in E^2 , *L'Enseignement Mathématique*, **38** (1992), 125-131.
- [24] Ionascu, E.J., Patterson, J. Primes of the form $\pm a^2 \pm qb^2$. arXiv: 1207.0172, (2013).
- [25] Jaleel, A.A., Mandal, D., Thomas, J.E., Rajesh, R. The freezing phase transition in hard core lattice gases on triangular lattice with exclusion up to seventh next-nearest neighbor. arXiv:2206.04985v1, (2022).
- [26] Jaleel, A.A., Thomas, J.E., Mandal, D., Sumedha, Rajesh, R. Rejection-free cluster Wang-Landau algorithm for hard-core lattice gases. *Phys. Rev. E* **104** (2021), 045310.
- [27] Jauslin, I., Lebowitz, J.L. High-fugacity expansion, Lee-Yang zeros and order-disorder transitions in hard-core lattice systems. *Comm. in Math. Phys.*, **364**:2 (2018), 655-682.
- [28] Krachun, D. Triangles on \mathbb{Z}^2 and sliding phenomenon. arXiv:1912.07566v1, (2019).
- [29] Krzakala, F., Montanari, F., Ricci-Tersenghi, F., Semerjian, G., Zdeborova, L. Gibbs states and the set of solutions of random constraint satisfaction problems. *Proc. Nat. Acad. Sci. USA*, **104**:25 (2007), 10318-10323.
- [30] Lang, S. *Cyclotomic Fields I and II*, 2-d Ed., NewYork: Spinger Science+Business, 1990.
- [31] Lenstra, H.W. Solving the Pell equation. In: *Algorithmic Number Theory*. MSRI Publications **44**. Cambridge: CUP, 2008.
- [32] Mazel, A., Stuhl, I., Suhov, Y. High-density hard-core model on triangular and hexagonal lattices. arXiv:1803.04041v2, (2020).
- [33] Mazel, A., Stuhl, I., Suhov, Y. Kepler's conjecture and phase transitions in the high-density hard-core model on \mathbb{Z}^3 . arXiv:2112.14250v2, (2023).
- [34] Mazel, A., Stuhl, I., Suhov, Y. The hard-core model on planar lattices: the disk-packing problem and high-density Gibbs distributions. arXiv:2011.14156, (2021).

- [35] Mazel, A., Stuhl, I., Suhov, Y. The hard-core model on \mathbb{Z}^3 and Kepler's conjecture arXiv:2304.08642, (2023).
- [36] Nath, T., Rajesh, R. Multiple phase transitions in extended hard-core lattice gas models in two dimensions. *Phys. Rev. E* **90** (2014), 012120.
- [37] Nath, T., Rajesh, R. The high density phase of the k -nn hard core lattice gas model. *J. Stat. Mech.* (2016), 073203.
- [38] Neukirch, J. *Algebraic Number Theory*. Grundlehren der mathematischen Wissenschaften. **322**. Berlin: Springer-Verlag, 1999.
- [39] The On-Line Encyclopedia of Integer Sequences, <http://oeis.org/> (2010), sequences A053307.
- [40] Parisi, G., Zamponi, F. Mean-field theory of hard-sphere glasses and jamming. *Rev. Mod. Phys.*, **82** (2010), 789–845.
- [41] Peled, R., Samotij, W. Odd cutsets and the hard-core model on \mathbb{Z}^2 . *Annales de l'IHP, Probabilites et Statistiques*, **50** (2014), 975-998.
- [42] Pirogov, S.A., Sinai, Ya.G. Phase diagrams of classical lattice systems. *Teor. Mat. Fiz.* **25** (1975), 1185-1192; **26** (1976), 61-76.
- [43] Sierpinski, W. *Elementary theory of numbers*. Amsterdam: North-Holland, 1988.
- [44] Sinai, Ya.G. *Theory of phase transitions. Rigorous results*. Oxford: Pergamon Press, 1982.
- [45] Suhov, Y. Absence of phase transitions in a lattice hard-core model. *Master Thesis, Moscow State University (Lomonosov)*; (1967).
- [46] Thewes, F.C., Fernandes, C.M. Phase transitions in hardcore lattice gases on the honeycomb lattice. *Phys. Rev. E* **101** (2020), 062138.
- [47] Viazovska, M. The sphere packing problem in dimension 8. *Annals of Math.*, **185** (2017), 991-1015.
- [48] Washington, L. *Introduction to Cyclotomic Fields*. (2nd Ed.) New York: Springer-Verlag, 1997.
- [49] Zahradnik, M. An alternate version of Pirogov-Sinai theory. *Comm. Math Phys.* **93** (1984) 559-581.